HIGHWAY RESEARCH RECORD

Number 471

Evaluation of Pavement Surface Properties and Vehicle Interaction

12 reports
prepared for the
52nd Annual Meeting

Subject Areas

25 Pavement Design
26 Pavement Performance

HIGHWAY RESEARCH BOARD
DIVISION OF ENGINEERING NATIONAL RESEARCH COUNCIL
NATIONAL ACADEMY OF SCIENCES—NATIONAL ACADEMY OF ENGINEERING

Washington, D.C. 1973

NOTICE

These papers report research work of the authors that was done at institutions named by the authors. The papers were offered to the Highway Research Board of the National Research Council for publication and are published here in the interest of the dissemination of information from research, one of the major functions of the Highway Research Board.

Before publication, each paper was reviewed by members of the HRB committee named as its sponsor and accepted as objective, useful, and suitable for publication by the National Research Council. The members of the review committee were chosen for recognized scholarly competence and with due consideration for the balance of disciplines appropriate to the subject concerned.

Responsibility for the publication of these reports rests with the sponsoring committee. However, the opinions and conclusions expressed in the reports are those of the individual authors and not necessarily those of the sponsoring committee, the Highway Research Board, or the National Research Council.

Each report is reviewed and processed according to the procedures established and monitored by the Report Review Committee of the National Academy of Sciences. Distribution of the report is approved by the President of the Academy upon satisfactory completion of the review process.

ISBN 0-309-02256-8
Library of Congress Catalog Card No. 73-22747
Price: $4.00

CONTENTS

FOREWORD

The papers in this RECORD relate to skid resistance, road roughness, braking, vehicle control, pavement performance and serviceability, design, and measurement systems for evaluating surface properties and vehicle interaction.

Burns and Peters conducted sideway force measurements to determine frictional characteristics of pavements in Arizona. They found seasonal variation in skid resistance that cannot be attributed to temperature alone. The differential wheelpath friction was investigated and may be large enough to affect vehicle control.

Ivey and Gallaway advocate the consideration of tire-pavement friction in the planning and design of a roadway so that adequate skid resistance is provided for particular vehicle maneuvers and various highway geometrics.

Traffic accidents can be reduced by decreasing the traveling speed. Weaver, Hankins, and Ivey developed guides for wet-weather speed zoning and give examples to illustrate the application of these principles.

Gillespie, Meyer, and Hegmon recognize the variation of highway skid resistance and the anomalies of skid testing and conclude that statistical analysis is essential for proper interpretation of test results.

In testing and evaluating pavement roughness, Rizenbergs, Burchett, and Davis devised an index based on the measurement of vertical accelerations of a test passenger during travel. The as-constructed condition of a roadway is a significant factor in the pavement riding quality throughout its lifetime.

Road roughness can adversely affect vehicle handling and may result in loss of control. This is shown by a simple mathematical model of a passenger car developed by Quinn and Hildebrand.

Road roughness also affects vehicle braking, causes errors in friction measurements, and may be a reason for poor correlation of skid test results according to Wambold, Brickman, Park, and Ingram.

Holbrook and Darlington recommended statistical methods to interpret the riding quality of a roadway from highway profile measurements.

A tentative model for concrete pavement thickness design for a wide range of truck volumes was developed by Brokaw. The model is based on an extensive survey of road roughness obtained by a road meter.

Swift developed instrumentation for measuring moving-load pavement deflections. The system is operable for vehicle speeds greater than 25 mph.

Road profile data from the surface dynamics profilometer are being interpreted through models developed by Walker and Hudson to evaluate pavement serviceability.

A continuous-time Markov process to predict pavement joint deterioration is discussed by Holbrook.

—Glenn G. Balmer

SURFACE FRICTION STUDY OF ARIZONA HIGHWAYS

John C. Burns and Rowan J. Peters, Materials Division, Arizona Highway Department

The specific aims of the program were to investigate the side-force method or cornering slip mode for the prediction of frictional characteristics of pavement surfaces in terms of pavement types, layout features, and traffic conditions. As part of the program, an evaluation of the adaptability of the Mu-meter as a standard highway friction-measuring trailer was conducted. In the evaluation items such as repeatability, speed, temperature, tire pressure, and the ability to correlate with other friction-measuring devices were of prime interest. The research indicated that the Mu-meter, when modified, is a highly acceptable, economical, and functional friction-measuring trailer capable of testing 250 lane-miles per working day.

•DURING August 1972, the Arizona Highway Department published its findings (1) of a research program to investigate the side-force method or cornering slip mode for the prediction of frictional characteristics of pavement surfaces. As part of the program, an evaluation of the adaptability of the Mu-meter as a standard highway friction-measuring trailer was conducted. This paper is a compendium of that report.

MU-METER

The Mu-meter is a continuous recording friction-measuring trailer (Fig. 1). It measures the side-force friction generated between the test surface and the 2 pneumatic tires that are set at a fixed toe-out angle of $7^1/_2$ deg to the line of drag (Fig. 2). Pulling the Mu-meter over a surface produces a frictional force that is sensed by a transducer located in the apex of the trailer's A frame. The resulting hydraulic pressure is transmitted through a flexible line on the recorder's Bourdon tube and recording mechanism. The recorder stylus makes a trace on the moving pressure-sensitive chart paper. The chart paper moves at a rate of 1 in. for every 450 ft of surface tested.

The Mu-meter was originally designed to measure the actual surface friction conditions of airport runways. The unit was a completely mechanical device that had to be manually put into the testing position before a test could be made and taken out of the test position before it was moved to another site. For highway work, this method was extremely time-consuming and unsatisfactory.

The Utah State Department of Highways had converted the Mu-meter to a more automatic system, and we expanded on those ideas to make the system fully automatic. A hydraulic system was added to the test unit that consisted of 2 hydraulic rams and a hydraulic control system for moving the test wheel in and out and moving the recording wheel up and down (Fig. 3). The hydraulic system worked extremely well and enabled tests to be made by the operator from the cab of the towing vehicle. Thus, testing could be accomplished without stopping.

To simulate wet pavement conditions, a watering system was added that enabled a uniform 0.018-in. layer of water to be placed in front of the test tires. A valve regulated the flow and ensured that the water layer remained consistent at all speeds. Tests indicated that the Mu-meter yielded the same results even when the water layer thickness was only 0.005 in. At the present time, however, the 0.018-in. water setting is being used for all testing and was the amount used for all tests and correlations presented in this report.

A special electrical monitoring system was integrated into the hydraulic and water systems. The system included a number of microswitches that enabled the driver to

Publication of this paper sponsored by Committee on Surface Properties-Vehicle Interaction.

Figure 1. Original (left) and modified (right) Mu-meter.

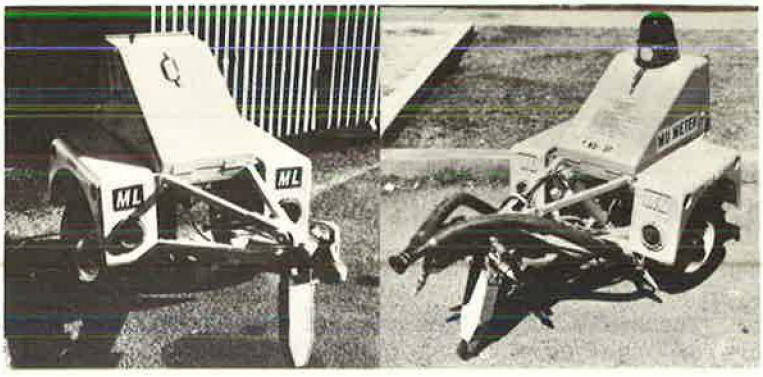

Figure 2. Schematic of Mu-meter.

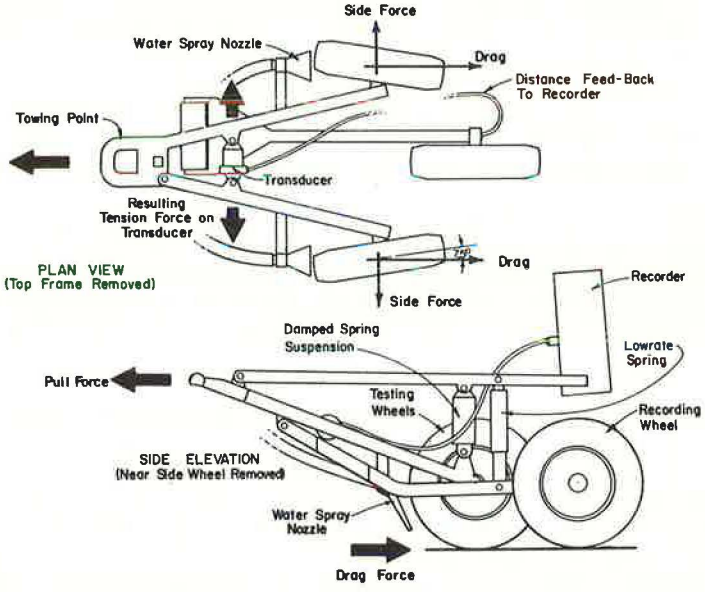

Figure 3. Cutaway view of skid test unit.

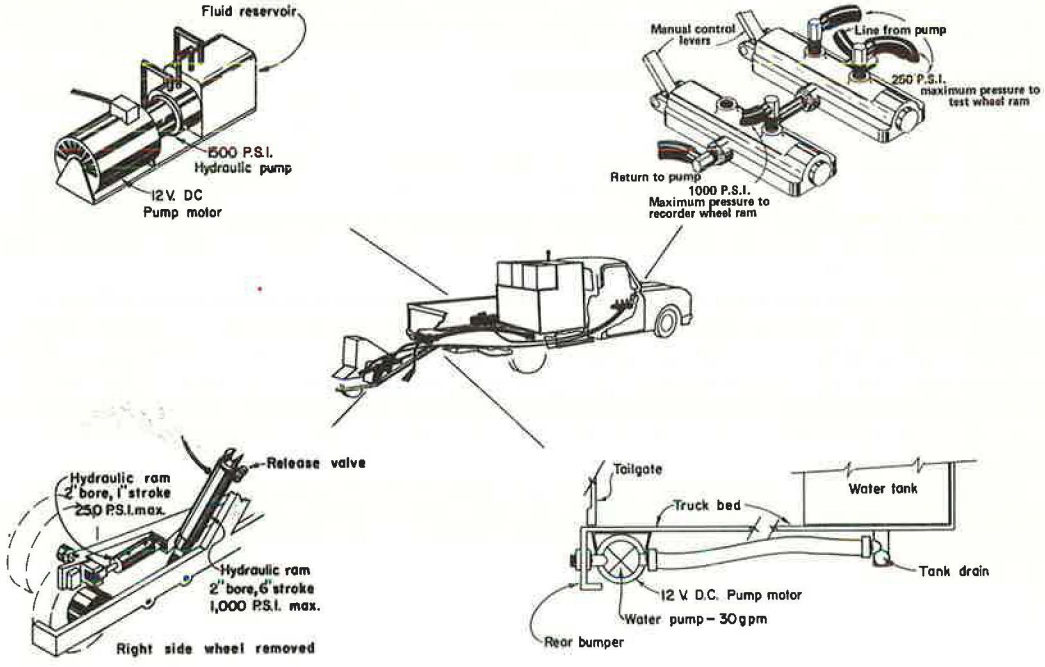

determine the condition of all systems through a series of lights on the control panel. The system was very efficient and easy to install.

The towing vehicle, which has now become a part of the skid test unit, is a 1-ton truck that carries a 300-gal water supply and all of the support equipment (Fig. 4).

The total cost to create an acceptable friction-measuring test unit was approximately $10,600 (Mu-meter, $5,585; truck, $2,700; and labor and parts, $2,300). The upkeep of the unit is also economical; a test tire ($24.00) will last for a complete inventory of the Arizona highway system. Compared to other available skid trailers, this unit will result in savings from $25,000 to $85,000.

The modified Mu-meter is highly maneuverable, and tests can be conducted without stopping or interfering with traffic flow. Approximately 250 lane-miles of highway can be tested in one 8-hour day. The normal test speed is 40 mph; higher speeds are possible between test sites. An automatic speed control on the truck ensures the desired test speed.

EVALUATION

Repeatability

In the evaluation of the Mu-meter, the variable repeatability was studied at 29 sites of varying surface and friction types.

The Mu-meter made a series of 6 passes over each site at speeds of 20 and 40 mph, 6 passes over selected sites at 10, 20, 30, 40, and 50 mph, and 12 passes over each site at 40 mph. Each site was 500 ft in length. There was no significant increase in the standard deviation as speed was increased from 10 to 50 mph on selected sites. However, the fluctuation about the average for individual tests increased significantly with increasing speed.

The Mu-meter reading for each pass was calculated by the operator by visually averaging the entire reading for the 500 ft of test area. The averages from these individual readings were used to calculate all of the standard deviations for a series of passes. Thus, the standard deviations include an error in the averaging of the actual recorded friction. This method was used, however, because it is the method that would normally be used in field testing and inventory work. Even with the included interpretation error, the standard deviation for 29 sites and 6 passes at each site was found to be 1.4 friction values at 40 mph, which is very good for a friction-measuring trailer. When all locations were averaged, the standard deviation was the same for 6 passes as it was for 12 passes at the same speed.

A question arose as to whether the standard deviation might be related to the friction value at a particular site. For this reason, the average Mu-meter reading for each site was compared to the standard deviation. It was concluded that the standard deviation was not significantly affected by the friction value of the pavement surface.

Tire Pressure

The results of numerous tests on the effect of tire pressure change on the measured surface friction indicated that there is an increase of 0.5 friction numbers with an increase of 1 lb of tire pressure.

Temperature

No relation was found between temperature and friction probably because of the nondestructive method of the Mu-meter test and the type of rubber used in its pneumatic tires.

Speed

A strong correlation was found between test speed and friction. Increasing speed reduces the coefficient of friction, as measured by the Mu-meter. Although the texture of the surface is reflected in the slope of the speed gradient, it can be assumed that there will be a decline of 4.0 friction numbers for every 10-mph increase in test speed.

From these correlations, a prediction can be made of what the friction value will be at higher speeds.

Geometry

The slope of the highway did not appear to affect the Mu-meter, but a sharp curve may cause the unit to record a lower friction than may actually exist, as is the case with other skid trailers. Fortunatoly, modern highway curves are not that sharp.

CORRELATIONS

The final test of the Mu-meter was its capability to correlate with 3 other types of friction-measuring devices: locked-wheel trailer (Fig. 5), stopping distance car (Fig. 6), and pendulum tester such as the British portable tester (Fig. 7).

The Mu-meter correlated extremely well with the first and second but only fairly well with the third (Fig. 8 and Tables 1 and 2). Because the British portable tester does not correlate well with other test devices, it is assumed that the lack of correlation was due to the inconsistency of the British portable tester and not the Mu-meter.

The results indicate that the Mu-meter correlates extremely well with another Mu-meter similarly modified, to standard skid trailers, and to the stopping distance car and that by simple equations the Mu-meter reading can be interchanged with the values recorded by other accepted friction-measuring equipment. The results also indicate that the Mu-meter correlates much better to other equipment when pavement is wet by its own watering system instead of by a water truck or sprinkling system. This may have been the cause of the lower correlations reported by Gallaway and Rose (2). Because of its generally greater friction range, the Mu-meter also appears to be more sensitive than the other units.

We hoped we could evaluate the minimum acceptable Mu-meter reading at 40 mph by calculating the corresponding Mu-meter reading for a recorded value of 35 for other skid trailers and a 46 for the skid car (3). There was a wide range in the calculated values because of the inconsistencies of the trailers. When all units were averaged, a corresponding Mu-meter value of 42 was calculated. When only the skid trailers were averaged, a value of 43 was calculated. For this reason and because the accident analysis indicated a braking point of approximately the same value, a wet Mu-meter reading of 43 at 40 mph appears to correlate best with other skid-trailer values of 35 at 40 mph. In the future, when units have been standardized, this value may be changed to conform with other devices.

GENERAL OBSERVATIONS

The Mu-meter, being completely mechanical, proved to be an extremely trouble-free testing unit. The only inoperative time was due to a broken hitch and an initially defective recorder, which was promptly replaced. The unit can function at speeds as high as 85 mph (limits of tow truck) and has suspension superior to most highway vehicles. It is a rugged unit and can be towed anywhere a truck can travel. In the 2 years we have had the unit, it has been out of operation for approximately 2 weeks.

SKID INVENTORY

During the program, a complete inventory of 3,439 miles of the state highway system was conducted. The inventory consisted of skid tests made at every other milepost. In the increasing milepost direction, tests were made at the even-numbered mileposts. In the decreasing milepost direction, tests were made at the odd-numbered mileposts. In this way, a test was made at least once at every milepost.

The surface friction inventory made by the Mu-meter will be used to locate low friction areas and monitor the yearly frictional changes of the entire highway system. Pavement problem areas can then be detected. Predictions can also be made as to when borderline cases will, if ever, fall to questionable friction levels so that they can be corrected before becoming hazardous.

Figure 4. Complete surface friction test unit.

Figure 5. Locked-wheel skid trailer.

Figure 6. Stopping distance car.

Figure 7. British portable tester.

Figure 8. Correlation between Mu-meter and other pavement friction testers.

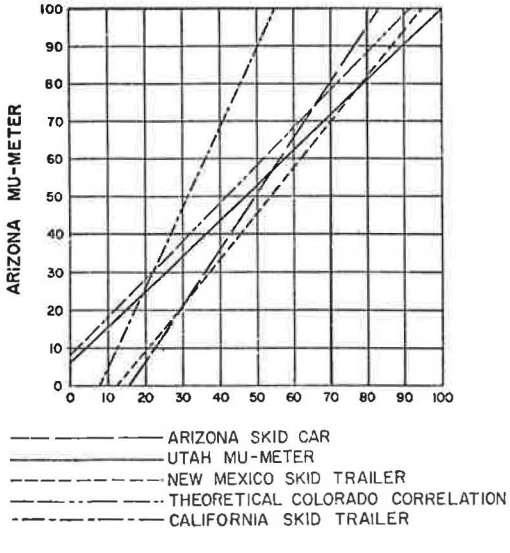

Table 1. Correlation values of Mu-meter and other pavement friction testers.

Variable[a]				
Y	X	Equation	Correlation Coefficient	Standard Error[b]
1	2	Y = 5.923 + 0.9430(X)	0.9820	3.45
1	3	Y = 8.180 + (X)[c]	—[c]	—[c]
1	4	Y = 14.939 + 1.2105(X)	0.9897	3.16
1	5	Y = 22.456 + 1.4755(X)	0.9800	2.72
1	6	Y = 17.829 + 2.1416(X)	0.9172	3.21

[a] 1 = Arizona Mu-meter; 2 = Utah Mu-meter; 3 = Colorado skid trailer; 4 = New Mexico skid trailer; 5 = Arizona skid car; and 6 = California skid trailer.
[b] All values are for X-variable except the first.
[c] Theoretical, based on Utah-Colorado correlation.

Table 2. Correlation values of Mu-meter, skid car, and British portable tester.

Variable[a]					
Y	X	Observations	Regression Equation	Correlation Coefficient	Standard Error
3	1	26	$Y = 8.349 + 0.8590(X)$	0.9383	4.44
7	1	25	$Y = -3.424 + 0.8030(X)$	0.8661	6.55
1	4	26	$Y = 13.138 + 2.2416(X) - 0.01886(X)^2$	0.8539	7.45
1	5	19	$Y = 26.208 + 4.1320(X) - 0.09857(X)^2$	0.8535	6.53
6	1	24	$Y = 21.169 + 0.4741(X)$	0.7946	5.23
8	1	24	$Y = 35.154 + 0.2717(X)$	0.6130	4.97
7	2	26	$Y = 15.219 + 0.6777(X)$	0.9802	2.72
3	2	27	$Y = 11.915 + 1.6450(X) - 0.01024(X)^2$	0.9438	4.46
2	4	30	$Y = -13.309 + 2.3952(X) - 0.01650(X)^2$	0.9394	6.93
2	5	18	$Y = 15.377 + 2.8023(X) - 0.02864(X)^2$	0.8760	9.28
6	2	24	$Y = 31.744 + 0.3789(X)$	0.8527	4.69
8	2	22	$Y = 40.866 + 0.2371(X)$	0.7652	4.09
3	4	24	$Y = 9.339 + 2.3903(X) - 0.02031(X)^2$	0.9506	4.24
3	2	27	$Y = 11.915 + 1.6450(X) - 0.01024(X)^2$	0.9438	4.46
3	1	26	$Y = 8.349 + 0.8590\ (X)$	0.9383	4.44
3	5	19	$Y = 27.850 + 3.7960(X) - 0.08719(X)^2$	0.9163	4.56
3	7	26	$Y = 22.001 + 0.8793(X)$	0.8894	6.14
6	3	23	$Y = 16.870 + 0.5499(X)$	0.8703	4.24
8	3	22	$Y = 35.621 + 0.2520(X)$	0.6656	3.17
3	4	24	$Y = 9.339 + 2.3903(X) - 0.02031(X)^2$	0.9506	4.24
4	5	18	$Y = 20.011 + 0.7971(X)$	0.9499	6.29
2	4	30	$Y = 13.309 + 2.3952(X) - 0.01650(X)^2$	0.9394	6.93
7	4	28	$Y = 24.426 + 0.5883(X)$	0.9212	5.16
1	4	26	$Y = 13.138 + 2.2416(X) - 0.1886(X)^2$	0.8539	7.45
6	4	25	$Y = 37.426 + 0.3521(X)$	0.7919	5.38
8	4	23	$Y = 42.561 + 0.2685(X)$	0.7896	3.95
4	5	18	$Y = 20.011 + 0.7971(X)$	0.9499	6.29
3	5	19	$Y = 27.850 + 3.7960(X) - 0.08719(X)^2$	0.9163	4.56
2	5	18	$Y = 15.377 + 2.8023(X) - 0.02864(X)^2$	0.8760	9.28
1	5	19	$Y = 26.208 + 4.1320(X) - 0.09857(X)^2$	0.8535	6.53
8	5	18	$Y = 47.224 + 0.2025(X)$	0.7076	4.85
7	5	19	$Y = 41.488 + 0.3741(X)$	0.6951	9.06
6	5	19	$Y = 46.947 + 0.2103(X)$	0.5376	7.73
6	7	24	$Y = 21.718 + 0.6025(X)$	0.8860	4.16
6	3	23	$Y = 16.870 + 0.5499(X)$	0.8703	4.24
6	2	24	$Y = 31.744 + 0.3789(X)$	0.8527	4.69
6	1	24	$Y = 21.169 + 0.4741(X)$	0.7946	5.23
6	4	25	$Y = 37.426 + 0.3521(X)$	0.7919	5.38
8	6	24	$Y = 26.816 + 0.4995(X)$	0.7729	3.51
6	5	19	$Y = 46.947 + 0.2103(X)$	0.5376	7.73
7	2	26	$Y = 15.219 + 0.6777(X)$	0.9802	2.72
7	4	28	$Y = 24.426 + 0.5883(X)$	0.9212	5.16
3	7	26	$Y = 22.001 + 0.8793(X)$	0.8894	6.14
6	7	24	$Y = 21.718 + 0.6025(X)$	0.8860	4.16
7	1	25	$Y = -3.424 + 0.8030(X)$	0.8661	6.55
8	7	23	$Y = 35.878 + 0.3570(X)$	0.7573	4.09
7	5	19	$Y = 41.488 + 0.3741(X)$	0.6951	9.06
8	4	23	$Y = 42.561 + 0.2685(X)$	0.7896	3.95
8	6	24	$Y = 26.816 + 0.4995(X)$	0.7729	3.51
8	2	22	$Y = 40.866 + 0.2371(X)$	0.7652	4.09
8	7	23	$Y = 35.878 + 0.3570(X)$	0.7573	4.09
8	5	18	$Y = 47.224 + 0.2025(X)$	0.7076	4.85
8	3	22	$Y = 35.621 + 0.2520(X)$	0.6656	3.17
8	1	24	$Y = 35.154 + 0.2717(X)$	0.6130	4.97

[a]1 = Mu-meter using own watering system at 20 mph; 2 = Mu-meter using own watering system at 40 mph; 3 = Mu-meter using external watering system at 20 mph; 4 = Mu-meter using external watering system at 40 mph; 5 = Mu-meter using external watering system at 60 mph; 6 = skid car using external watering system at 20 mph; 7 = skid car using external watering system at 40 mph; and 8 = British portable tester.

SEASONAL VARIATION

The research studies show that the coefficient of friction appears to have seasonal variations that follow similar patterns at any particular location in a given area. The average pattern for each direction of a highway in a 20-mile area is shown in Figure 9. The patterns and values are almost identical for each direction. A climatological investigation of these results was generated and included a comparison of (a) temperature versus friction and (b) days since the last 0.01 in. or more of rain versus friction. The results indicate that the variation is due to a combination of factors; however, temperature and days since last rain do not explain the phenomenon satisfactorily. Correlations were made with higher amounts of rainfall, but the correlation was lower than with the 0.01 in. of rain. Further examination of the data is necessary to determine the significance of all the variables affecting this variation.

The seasonal variation must be considered when skid data are analyzed because a pavement that may have a satisfactory friction level at one time of the year could have an unsatisfactory value at another time of the year. Present information indicates that the lowest friction level is reached during the summer months in Arizona, and the Arizona Highway Department plans to conduct its friction inventories during these months.

DIFFERENTIAL WHEELPATH FRICTION

During our testing, a condition was noted that we feel warrants special attention and further investigation. The condition occurs when the 2 wheelpaths in which a vehicle rides have a different coefficient of friction. We are aware that there is usually a small difference, but this is not the condition we are describing. The differential wheelpath friction we are considering is one in which a vehicle may be riding on 2 different surface types, 2 different ribbons of asphaltic concrete or concrete pavement, or on one wheelpath that is flushed or polished and one that is not. To our surprise, a very small difference in the wheelpath frictions will cause a car to spin out of control when braked. Examples of 2 conditions are shown in Figures 10 and 11.

In Figure 10, the wet stopping distance number at 40 mph (SDN_{40}) was 50 for the right wheelpath and 60 for the left wheelpath, a 17 percent difference. In the left picture, the car skidded at 30 mph and rotated 25 deg counterclockwise. In the middle picture, the car skidded at 40 mph and rotated 40 deg counterclockwise. In the right picture, the car skidded at 50 mph and rotated 95 deg counterclockwise. When the direction of skidding was reversed, the same values were recorded with the car turning clockwise. In Figure 11, the wheelpath had a wet SDN_{40} of 67 on the right and 41 on the left, a 39 percent difference. In the left picture, the car skidded at 40 mph and rotated 90 deg clockwise. In the right picture, the car skidded at 50 mph and rotated 270 deg clockwise. Again, when the direction of skidding was reversed the same values were recorded with the car rotating counterclockwise.

Figure 11 shows an extreme case that portrays what might happen if one wheelpath were flushing while the other were not. However, the first case is one that is fairly common and, although both wheelpaths have a satisfactory level of friction, a hazardous condition occurs because of their difference. As the speed increases, the effects increase dramatically. Under such conditions, the normal driver tends to remove his foot from the brake as he begins to rotate. When he does, his car is propelled in the direction the vehicle is turned, perhaps off the road or into the oncoming traffic lane.

Because construction practices at the present time can produce lanes containing 2 ribbons and because a friction inventory would not detect unsatisfactory friction differences in the wheelpaths (for only one wheelpath is tested), it is the opinion of the authors that an investigation should be conducted to determine whether both wheelpaths should be tested. In the case of skid trailers, the trend is to lock only one wheel; but, if both were locked and had independent recorders, such differential friction areas could be located and corrected. In such a case, some form of stabilizing unit would have to be added to the trailers. Further research is needed to determine an acceptable differential wheelpath friction level.

FRICTION ANALYSIS

As part of the study, an analysis of the percentage of the highway system in each friction range was made (Fig. 12). These and the following interpretations are made from the highway inventory previously mentioned. Only 2.8 percent of the Arizona highway system has a skid number below 40, and 50 percent is within the Mu-meter frictional range of 71 to 80. These results indicate that the skid resistance level of the Arizona highway system is good and that the present pavement designs and aggregate types are producing satisfactory skid-resistant surfaces.

ACCIDENT ANALYSIS

During the research study, the question arose, What is a satisfactory level of friction? To determine this, an accident analysis was made of the entire Arizona highway system and correlated to the skid inventory previously described. The results of this analysis were most revealing. The accident types were divided into 3 categories: dry pavement accidents, wet pavement accidents, and wet skidding accidents.

Most wet-weather accidents were in the low skid-resistance ranges. The analysis indicated that, although less than 3 percent of the total Arizona highway system had a coefficient of friction below 40, 29 percent of the wet-weather accidents occurred in those areas. When a friction level of below 50 is considered, it relates to less than 7 percent of the highway system but 43 percent of the wet-weather accidents.

A study of the amount of rainfall occurring on the days of the accidents was made, to determine whether there was a significant amount of rainfall necessary to create a hazardous condition. A 50-mile section of portland cement concrete freeway was selected, and the accidents were analyzed for a 3-year period of recorded information. The analysis was based on the relation between the total number of accidents occurring and various daily rainfalls. These accidents per amount of rainfall were compared to the percentage of the 3 years that the particular amount of rainfall was present. The accumulated percentages were calculated (Table 3) and then plotted.

The location where the curve reached a one-to-one slope was picked as the point where the accumulated percentage of accidents begin increasing faster than the accumulated percentage of days. This point was related to the accumulated percentage of accidents that were present at a particular amount of daily rainfall. The results revealed that the slope reached unity at approximately 26 percent of the accumulated accidents. This percentage relates to a rainfall of approximately 0.11 in./day. Simply, this means that 0.1 in. or more occurred only 23 percent of the time but was responsible for 74 percent of the accidents. The same relation holds true when only sections with a Mu-meter reading of 40 or below were considered. Apparently, although a small amount of water is necessary to reduce the friction level as recorded by the Mu-meter, at least 0.1 in./day is necessary to create a significant increase in the wet-weather accident rate.

CORRECTIVE MEASURES FOR SLICK PAVEMENTS

We found that the methods of correcting low friction pavements by the use of chip seals, slurry seals, and heater scarifying are very effective, and all have an adequate coefficient of friction after construction. However, as others have also noted, there is a question of how long each method can last prior to the reappearance of the original or a lower friction value. In our opinion, the slurry seal should only be used as an intermediate step in the correction of low friction pavements because it could flush and create an even worse condition after a short period of time. As for heater scarifying and chip seals, the predicted life may vary significantly with construction techniques. It is generally agreed, and our research confirmed, that an open-graded asphaltic concrete finishing course should be considered as a lasting remedial action.

FRICTIONAL EFFECTS OF ASPHALT REJUVENATING AGENTS

In the evaluation of asphalt rejuvenating agents, various surface types and amounts of applications were studied. The results from these tests are shown in Figure 13.

Figure 9. Seasonal variation on concrete pavement.

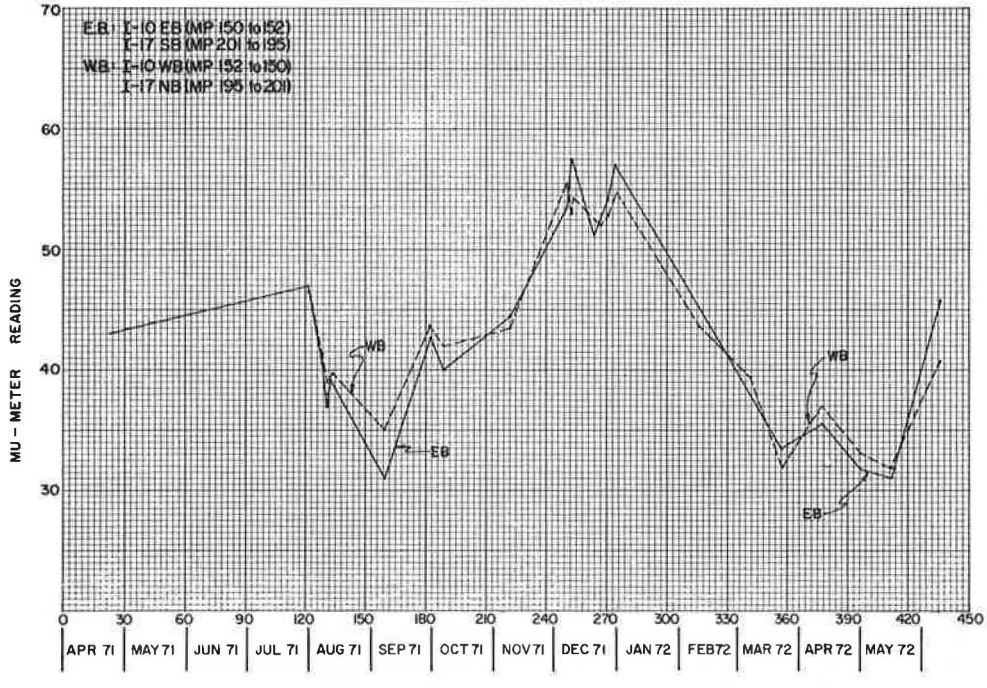

Figure 10. Differential wheelpath friction at SDN_{40} of 50 (right) and 60 (left).

Figure 11. Differential wheelpath friction at SDN_{40} of 67 (right) and 41 (left).

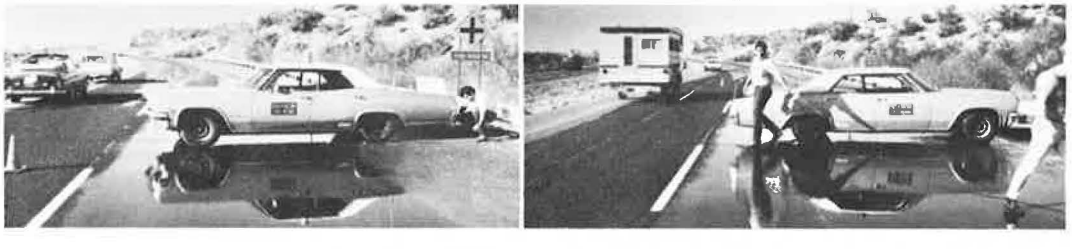

Figure 12. Interstate, state, and U.S. highway friction levels.

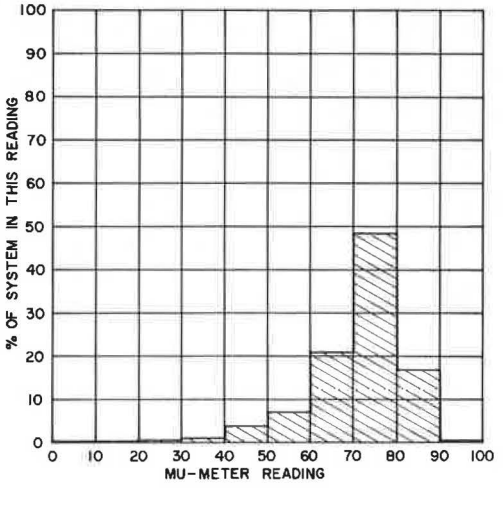

Table 3. Daily rainfall and accident rates from January 1968 to December 1970.

Rainfall (in./day)	Accidents			Days of Occurrence		
	Number	Percent	Accumulated Percent	Number	Percent	Accumulated Percent
<0.01	11	4.60	4.60	92	46.23	46.23
0.01	12	5.02	9.62	12	6.03	52.26
0.02	14	5.85	15.48	13	6.53	58.79
0.03	4	1.67	17.15	5	2.51	61.30
0.04	3	1.25	18.41	11	5.52	66.83
0.05	2	0.83	19.24	3	1.50	68.34
0.06	4	1.67	20.92	3	1.50	69.84
0.07	3	1.25	22.17	3	1.50	71.35
0.08	4	1.67	23.84	7	3.51	74.87
0.09	2	0.83	24.68	3	1.50	76.38
0.11[a]	2	0.83	25.52	2	1.00	77.38
0.12	3	1.25	26.77	4	2.01	79.39
0.13	9	3.76	30.54	2	1.00	80.40
0.14	4	1.67	32.21	3	1.50	81.90
0.15	2	0.83	33.05	1	0.50	82.41
0.16	9	3.76	36.82	3	1.50	83.91
0.17	11	4.60	41.42	2	1.00	84.92
0.18	4	1.67	43.09	1	0.50	85.42
0.19	5	2.09	45.18	1	0.50	85.92
0.20	8	3.34	48.53	5	2.51	88.44
0.21	1	0.41	48.95	1	0.50	88.94
0.26	5	2.09	51.04	3	1.50	90.45
0.27	2	0.83	51.88	1	0.50	90.95
0.28	4	1.67	53.55	1	0.50	91.45
0.29	3	1.25	54.81	1	0.50	91.95
0.34	20	8.36	63.17	2	1.00	92.96
0.36	4	1.67	64.85	1	0.50	93.46
0.37	3	1.25	66.10	1	0.50	93.96
0.38	8	3.34	69.45	1	0.50	94.47
0.43	8	3.34	72.80	1	0.50	94.97
0.45	2	0.83	73.64	1	0.50	95.47
0.52	10	4.18	77.82	3	1.50	96.98
0.59	3	1.25	79.07	1	0.50	97.48
0.64	8	3.34	82.42	1	0.50	97.98
0.74	14	5.85	88.28	1	0.50	98.49
0.77	13	5.43	93.72	1	0.50	98.99
1.33	4	1.67	95.39	1	0.50	99.49
2.43	11	4.60	100.00	1	0.50	100.00

[a]Point at which accident rate increases faster than the accumulated percentage of days.

Figure 13. Frictional effects of emulsified petroleum resin.

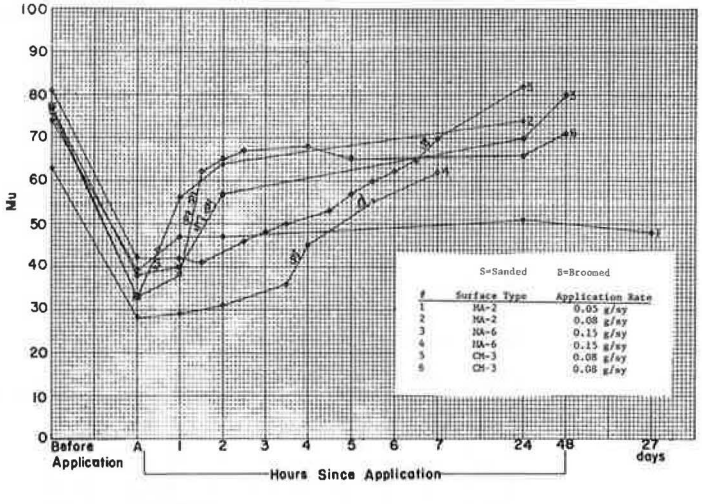

The surface friction was measured prior to the application of the agent. As soon as the agent was placed and demulsified (turned brown), the friction was remeasured and the value recorded (shown as point A). The friction level was measured each hour after the application demulsified. In some cases, the pavement was sanded or broomed; these points are shown on the graph as the letters S and B respectively. A marked increase in the friction can be seen after each of these procedures. From these tests, the following conclusions can be drawn:

1. The application of an asphalt rejuvenating agent (emulsified petroleum resin) causes an initial drop of approximately 53 percent in the Mu-meter reading;
2. The application of sand is beneficial but, when combined with brooming, increases the surface friction significantly and raises it to a satisfactory level;
3. In all of the cases tested, a satisfactory level of friction was achieved when the surface was sanded and broomed;
4. In the cases tested, all of the surfaces that were sanded and broomed regained most of their original friction within 24 hours;
5. The pavement can reach an acceptable level without sanding or brooming, but may take a much longer time and, in some cases, may never recover its original level;
6. When an agent is applied to a pavement, the wet friction is the same as the dry up to a Mu-meter reading of 60 (this phenomenon is unique and has only been observed after such applications); and
7. If a surface originally has a low friction value, an application of an agent may create a hazardous condition that may not be easily corrected.

Present tests indicate that it is possible to safely use an asphalt rejuvenating agent if the pavement is sanded and broomed afterward. If the original pavement friction is low, however, friction tests should be performed before the pavement is opened to traffic, thus ensuring that the pavement has risen to an acceptable friction level.

CONCLUSIONS AND RECOMMENDATIONS

1. The Mu-meter, when modified, is a highly accurate friction-measuring trailer. It has a standard deviation of 1.4 and correlates extremely well to other skid trailers and the stopping distance car. A wet Mu-meter reading of 43 at 40 mph appears to correlate best with wet values of other skid trailers of 35 at 40 mph.
2. At a total cost of $10,600, including tow truck and modifications, the Mu-meter test unit is inexpensive compared to other skid trailers. General savings for this unit could range from $25,000 to $85,000.
3. This unit can test 250 lane-miles of highway per day with a minimum of maintenance. It is sturdy and more maneuverable than most skid trailers.
4. The Mu-meter inventoried 3,439 miles of the Arizona highway system with the following results: Only 2.8 percent of the system had a Mu-meter reading lower than 40, but 29 percent of the wet-weather accidents were in the same range. Only 23 percent of the wet-weather days had greater than 0.11 in. of rain, but 74 percent of the wet-weather accidents occurred on those days. This indicates that it may be necessary to have greater than 0.1 in./day of rain to create a hazardously wet condition under similar conditions.
5. The seasonal variation was studied, but temperature and days since last rain do not satisfactorily explain the phenomenon. The variation seemed consistent for all pavement in a particular area.
6. The effect of different wheelpath frictions was also studied. A difference of 10 wet stopping distance numbers between wheelpaths can cause a braking car to spin out of control even though both wheelpaths have an acceptable level of friction. For this reason, it may be necessary to test both wheelpaths in the future.
7. Initial studies indicate that chip seals, slurry seals, and heater scarifying are acceptable short-term solutions to slick pavements, but an open-graded asphaltic finishing course should be considered as a permanent remedial action.
8. Asphalt rejuvenating agents can be safely applied if the surface is then sanded and broomed and if it initially had an acceptable friction level.

9. Consideration should be given to the development of a complete pavement evaluation system other than the acceptance or rejection based solely on a recorded friction number.

10. Further research should be initiated to investigate various deslicking methods including methods to ensure permanent skid-resistant surfaces on portland cement concrete pavements. The studies should evaluate texturing techniques, addition of skid-resistant aggregate to the finished concrete, and the frictional effects of grooving.

REFERENCES

1. Burns, J. C., and Peters, R. J. Surface Friction Study of Arizona Highways. Materials Division, Arizona Highway Department, Aug. 1972, 75 pp.
2. Gallaway, B. M., and Rose, J. G. Comparison of Highway Pavement Friction Measurements Taken in the Cornering Slip and Skid Modes. Texas Transportation Institute, Texas A&M Univ., Jan. 1971.
3. Kummer, H. W., and Meyer, W. E. Tentative Skid Resistance Requirements for Main Rural Highways. NCHRP Rept. 37, 1967.

TIRE-PAVEMENT FRICTION: A VITAL DESIGN OBJECTIVE

Don L. Ivey and Bob M. Gallaway, Texas Transportation Institute,
Texas A&M University

This paper presents the argument that tire-pavement friction should be considered during the design of a new highway facility. The concept of balanced friction design for safety is presented, and is based on the precept that different maneuvers require different levels of available friction and that different highway geometrics produce the need for different maneuvers. Presented in support of these arguments are the most pertinent results of various research and development studies. The information and examples should be useful not only in designing new highways but also in making decisions concerning the correction of deficiencies in existing highways.

•THE REDUCTION of the losses due to skid-initiated, wet-weather accidents is a goal that has been set by highway officials. Working toward this goal has generated a tremendous amount of research on specific aspects of the problem, but use of this information to evaluate the causative factors has been limited.

The purpose of tire-pavement friction is to allow the driver of the vehicle to perform those maneuvers that he can reasonably expect to accomplish; maneuvers range from the normal driving realm to an emergency avoidance maneuver. When the driver cannot perform an attempted maneuver, whether it be because the tire-pavement interface cannot accept the imposed loads, the capabilities of the vehicle are exceeded, or driver's skills are poor, the result is likely to be an accident. In trying to accommodate all factors that enter into wet-weather accidents, Hankins, Gregory, and Berger (1) prepared a skidding-accident systems model that included 40 separate variables; a simplified representation is shown in Figure 1. Even though complex, this model includes only those most obvious influencing factors, which constitute only a small part of the problem.

Since the 1930s when Moyer (2, 3, 4) conducted a comprehensive study of the requirements of motor vehicles for tire-pavement friction, writers on this subject have been making recommendations for those levels of friction they judged to be appropriate for a range of highway geometrics and conditions. For example, Kummer and Meyer (5) recommended a coefficient of friction of 0.37 for a mean traffic speed of 50 mph and 0.41 for a mean traffic speed of 60 mph. These are not radically different from those made by Moyer in 1932 but were developed from extensive information that was not available to Moyer.

The concept of maintaining certain values of friction over an entire roadway network is an important contribution and undoubtedly has led to much improvement in highway safety. Today, however, we should be prepared to design pavement surfaces to resist the specific horizontal shear loads that are imposed on them, these loads being a function of the maneuvers that can be reasonably expected. This design concept is analogous to designing a beam for the loads that are imposed on it. This same concept, in a generalized way, has been used to derive the levels of friction that were previously mentioned, but it has been done in a research environment and limited to normal maneuvers rather than in the highway design environment where design for friction can interact appropriately with geometric design decisions. The reason for this is partly the seeming complexity of the problem and partly the preoccupation of highway engineers with the vertical wheel loads a pavement must resist under traffic. In many

Publication of this paper sponsored by Committee on Surface Properties-Vehicle Interaction.

early designs pavement friction was something that just happened when a roadway was built. Sometimes it was good, sometimes it was bad, but the concept of actually designing for friction is comparatively new to most highway engineers.

Engineers have accepted the simple concept of a single friction value to satisfy all parts of a highway system and have neglected a more permanent solution to the problem and the potential long-term gains it would bring. Experience and data now available make it possible to design tire-pavement friction to accommodate most maneuvers that drivers will attempt.

BALANCED FRICTION DESIGN FOR SAFETY

The thesis is this: A single skid number is not appropriate for all roads and all positions on any given road. We would not think of designing a building by using the same beam cross section for each span and every load condition. An engineer is taught to design a beam to resist the shear and moment that it must resist, i.e., those internal reactions directly related to the geometry of the beam and the loads that are imposed. Similarly, as shown in Figure 2, a pavement surface should be designed to resist anticipated tractive loads.

This means that available tire-pavement friction must be set at some level above the demand for tire-pavement friction (essentially a function of roadway geometrics), just as yield point is above the working stress, as shown in Figure 3. Figure 4 shows another illustration of the design concept of a balanced friction design for safety. The numbers on the abscissa relate to the numbers on the plan view at the top of the figure. The curves show the demand for friction by a certain percentage of drivers. For example, the 98 percent curve means 98 percent of the drivers do not exceed this friction demand. The supply level is the amount of friction that is available. Any demand above this level could not be accommodated, and skidding would result. The main point is that we should put our costly high-friction surfaces at the locations where demand is greatest.

The equations needed to design pavement friction are presented in several reports (5, 6). The engineering approach to using them is, in most cases, to determine the appropriate input data in terms of speed, stopping distance, cornering radius, and acceleration or deceleration and, thus, to determine the demand for friction. These same equations are suggested for a similar application in the recent report by Weaver, Hankins, and Ivey (7). In that report the available friction is determined empirically and used to determine the safe driving speed, the reverse operation of the friction design process. The equations are presented in detail in the next section of this paper. Empirical determinations of the demand for friction to be available soon from an NCHRP project for certain types of curves and intersections will be a valuable supplement to the information now available for use in the design equations.

The equations presented here are far from perfect, and their application requires something no computer program has succeeded in duplicating—considerable engineering judgment. Aside from the basic design equations and the necessary input data for their use, the other item needed to apply the balanced friction design concept is a consistent way of measuring tire-pavement friction.

A new federally coordinated program for highway safety, initiated by the Federal Highway Administration, seeks to encourage new studies where gaps exist in the present work and undertakes the closure of other gaps by direct administrative contracts. The federally coordinated program for the reduction of wet-weather accidents has undertaken, among other things, the elimination of the large differences among skid number values acquired by different ASTM E 274 skid test units. These differences have been so great that we have been operating during past years under an act not unlike the Mann Act (8): that is, it has been illegal to transport a skid number across state lines for engineering purposes.

To repeal this act, the FHWA is committed to providing a network of inventory skid measurement systems and guide specifications for inventory equipment and field-testing procedures. The National Bureau of Standards will provide the national reference skid measurement system. There will be 3 field test and evaluation centers at Texas A&M

Figure 1. Driver-vehicle-roadway-environment interaction.

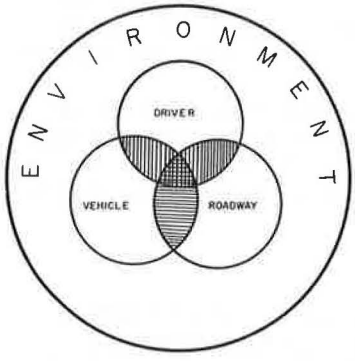

Figure 2. Beam design analogy.

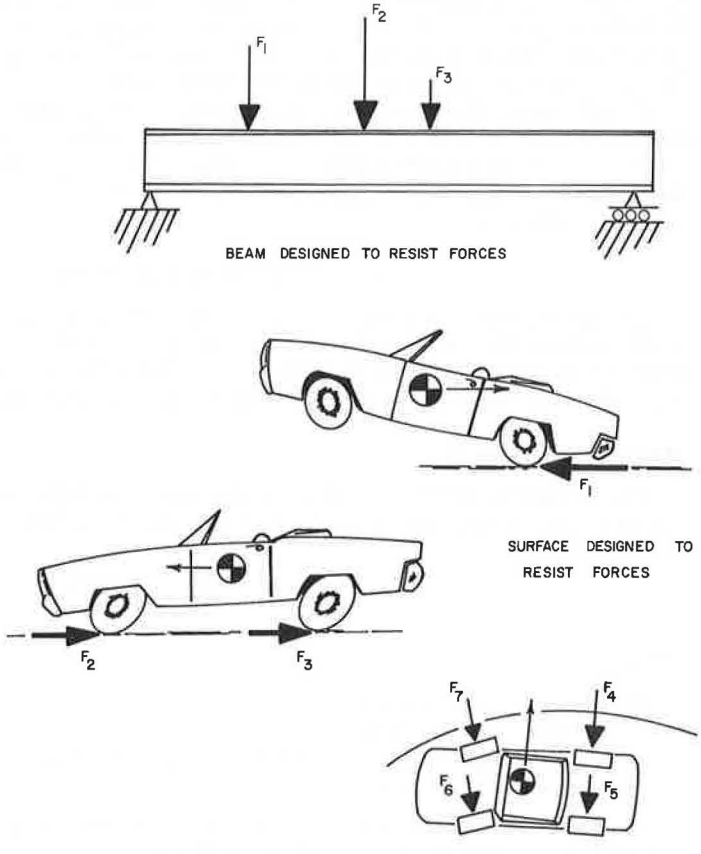

Figure 3. Yield point analogy.

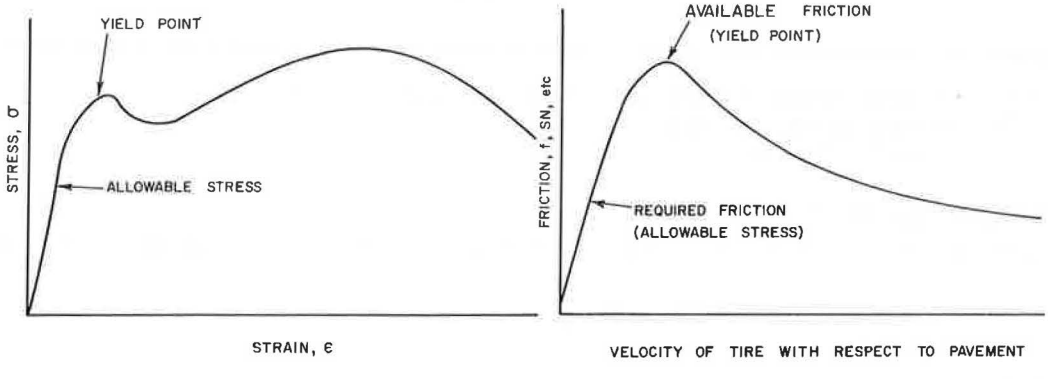

University, at the Ford Proving Grounds (Yucca, Arizona), and at Ohio State University. At each of these centers, there will be an area reference skid measurement system that will be calibrated at the appropriate center and correlated with the center area reference system at designated intervals. When all inventory systems have been related to the NBS in this way, it will then be possible to relate skid number values taken in one state to those observed in any other state.

At this time, there will be a great temptation for governmental agencies to specify certain values of skid numbers on highways. Reasonable decisions must be made concerning the value of tire-pavement friction needed at specific points on highways; or, better still, a balanced friction design policy should be established based on appropriate design equations.

DESIGN EQUATIONS

Design equations are presented as concisely as possible; previously published information is incorporated by the use of appropriate references. Friction numbers are used for continuity with skid numbers. The numbers are the required values of friction multiplied by 100, just as skid numbers are observed values of friction multiplied by 100.

Stopping Maneuvers

The AASHO code (9) provides an acceptable relation between stopping distance and the demand for friction as shown by the following equation:

$$d = \frac{V^2}{30\,f} + 1.47\,Vt$$

where

d = stopping distance, ft;
V = vehicle speed, mph;
f = coefficient of friction between tires and roadway; and
t = perception-reaction time, sec.

Rearranging Eq. 3 and using a 2.5-sec perception-reaction time currently recommended by AASHO (9) relate the demand friction for stopping maneuvers to speed by

$$FN_d = \frac{V^2}{0.3(d - 3.67V)}$$

where

FN_d = demand friction number for stopping within the available distance;
V = vehicle speed, mph; and
d = available distance, ft.

Cornering Maneuvers

The equation used by AASHO in the development of standards for horizontal curves is

$$e + f = \frac{V^2}{15R}$$

where

e = superelevation rate, ft/ft;
f = coefficient of friction;
V = vehicle speed, mph; and
R = curve radius, ft.

This equation was found to give a reasonable estimate of the available friction in a dynamically stable cornering maneuver in a recent study (10) conducted for AASHO.

Rewriting the equation for consistent comparison to values of skid number yields

$$FN_c = \frac{6.67V^2}{R} - 100e$$

where $FN_c = 100(f)$, the demand for lateral friction during cornering.

The friction demand determined from this equation is only appropriate provided the vehicle smoothly traverses the path of the highway curve. Therefore, it should only be used for curves having spiraled transitions or at points significantly removed from abrupt transitions. It there is no transition from tangent to curves with a curvature of 2 deg or greater, the equation developed by Glennon and Weaver (11) should be used:

$$FN_c = \frac{V^2}{0.786R + 40.3} - 100e$$

Combination Maneuvers

Many maneuvers involve some combination of cornering and braking or accelerating. A common way to determine the total friction demand is the vector sum of the demand for the individual changes in speed or direction (5).

If the maneuver is a combination of cornering and braking as might be found in traversing a freeway exit ramp, individual values of FN_c, the friction demand for cornering, and FN_d, the friction demand for decelerating, may be calculated. The total friction demand, FN_t, is found by

$$FN_t = \sqrt{FN_c^2 + FN_d^2}$$

From observations of traffic, Glennon (12) derived the following expression for cornering in the nonconstrained passing maneuver:

$$FN_p = \frac{V^2}{220} + 2$$

This equation was based on a number of other assumptions as described in Weaver's report (13). If the forward acceleration is assumed to vary linearly from 40 to 60 percent, full throttle at 40 and 80 mph respectively, the FN_a needed in accelerating can be found from

$$f(W/2) = \frac{W}{g} a$$

$$FN_a = 2 \frac{a}{g} (100)$$

The appropriate acceleration, a, at 40 percent full throttle was reported by Kummer and Meyer (5) as 6.4 ft/sec^2. The acceleration at 60 percent was 5.0 ft/sec^2. From the vector sum of these 2 effects, the resultant demand for friction was found. The same procedure can be used in any maneuver where estimates of the degree of cornering and braking or accelerating can be supplied.

AVAILABLE FRICTION

Any moving object possesses kinetic energy proportional to the square of its velocity. Dissipation of this energy is required to stop the body. Energy of the wheeled vehicle (neglecting wind resistance and changes in elevation) is dissipated between the tire and

the pavement and in the braking system by the creation of a friction force opposing the direction of motion of the vehicle. After wheel lockup, the total friction force available to oppose the motion of the vehicle must be generated at the tire-pavement interface.

There are many causes of pavement slipperiness. In general it is due to (a) the presence of water or other friction-reducing materials in the tire-pavement contact area and (b) high traffic volumes that, through pavement wear and aggregate polish, drastically reduce the friction of pavement surfaces. Many parameters affect the interactions at the tire-pavement interface. Considered to have major effects are (a) mode of operation, i.e., rolling, slipping, or sliding; (b) pavement-surface characteristics, mainly macroscopic and microscopic roughness and drainage capability, (c) water-film thickness at the interface, (d) tire-tread depth and elastic and damping properties of the tire rubber, and (e) vehicle speed.

Numerous research studies have indicated that almost all pavement surfaces exhibit adequate friction for normal stopping and cornering maneuvers when dry and clean. When wet, however, this is no longer the case. A knowledge of the relative effects of water-film thickness and the water escape mechanism at the tire-pavement interface are therefore of paramount importance.

Relevant Surface Factors

Attempts have been made to characterize properties affecting friction of pavement-surface types by using qualitative terms such as surface macrotexture; aggregate size, shape, microtexture, and mineralogy; and the drainage characteristic of the total surface. Although the relative magnitude of the influence of these characteristics is open to debate, it is generally agreed that they largely determine the ultimate friction properties of surfaces. It is the authors' opinion that the influence of all these characteristics is primarily due to the effect they have on the way water can escape from the tire-pavement interface.

The importance of the type and magnitude of surface texture on the friction properties of pavement surfaces has been studied by several researchers (5, 17, 18, 19, 20). Pavement surface texture refers to the distribution and the geometric configuration of the individual surface aggregates. There is not sufficient agreement among the various researchers to adopt a standard nomenclature for discussing textural parameters. However, general practice today favors the use of the terms macroscopic texture (macrotexture), which refers to the large-scale texture caused by the size and shape of the surface aggregate, and microscopic texture (microtexture), which refers to the fine-scaled roughness contributed by individual small asperities on the individual aggregate particles.

Macrotexture and microtexture respectively provide for gross surface drainage and subsequent puncturing of the water film. Another factor that acts in combination with macrotexture and microtexture is the internal drainage of the pavement surface course itself. Goodwin (19), Hutchinson et al. (20), and Gallaway (21), among others, have postulated that high-void-content surfaces, porous pavements, or vesicular aggregates provide internal escape paths for water under a tire and thus lessen hydrodynamic pressure buildup. This would result in better tire-gripping capability and lessen the need of macrotexture to provide initial, gross drainage. Research directed toward measuring dynamic drainage capabilities of pavement surfaces is in the experimental stage (22).

With respect to the size of the coarse aggregate, the majority opinion seems to be that finer mixes are superior to those that are coarser, at least in bituminous construction (22, 23). However, the advantages of fine mixes are not always apparent, and some investigators have suggested that particle size has actually little or no effect on frictional characteristics (24, 25).

The shape of the aggregate particles is a significant factor in skid-resistance considerations. The individual particles should be angular and sharp in order to give a gritty, sandpaperlike texture (26, 27, 28). Skid-resistance measurements have been found to be about 25 percent higher for bituminous mixes containing angular aggregates than for those containing rounded aggregates (29). The importance of the aggregate shape has also been borne out by laboratory experiments (30, 31, 32).

Wear and polishing under traffic result in skid-resistance variations across the width of the road (32); these may lead to directional control instability during braking regardless of the minimum value of friction. It has been shown analytically (33) that, for a coefficient of friction of 0.40 along one wheelpath and 0.60 along the other, a 3,000-lb vehicle will turn about 17 deg in a locked-wheel stop from 40 mph. This problem is further accentuated on multilane highways where the driving lane is normally more slippery than the passing lane (35, 36).

Because the nature of the wear is directly related to the resistance of the surface aggregate to polishing, wear can actually be desirable on road surfaces. Differential wear, due to variation in hardness of the aggregate constituents or matrix or both (26, 34), greatly contributes to the retention of the rough texture. Particle-by-particle wear, during which aggregate particles are dislodged from the surface before they get excessively polished, continuously rejuvenates the surface (28, 35). In addition, particle-by-particle wear does not just ensure prolonged skid resistance but distributes the energy of stopping to the brakes, tires, and road surface and, therefore, provides instantaneously higher skid resistance.

Test Pavements and Equipment

In a study (37) to test the skid resistance of a number of typical highway surfaces under simulated rainfall, variables included rainfall intensity, pavement macrotexture, tire tread design, tread depth, tire pressure, and vehicle speed. In other tests (38), to evaluate the effectiveness, as measured by skid resistance, of different finishes on a portland cement concrete pavement, variables included rainfall intensity (water depth), tire tread type, tire tread depth, tire pressure, surface finish, and vehicle speed.

A brief description of the experimental and field surfaces is given in Tables 1 and 2 respectively. Major equipment used in the study is shown in Figure 5 and consisted of water tank truck, rainfall simulator, and skid test system.

The framework of the rain simulator is composed of 4-in. wide by 1-in. deep channel iron. A 4-in. diameter pipe serves as the manifold, and 2-in. diameter pipes are used as feeder lines for the shrub-head nozzles. Eight 20-ft long sections of the rain simulator wet an area approximately 210 ft long by 30 ft wide.

A 4,000-gal water truck equipped with a high pressure pump was used to supply water to the system. Desired water depths were measured at various distances along the drainage path. Rainfall intensities were deduced from the amount of water caught in metal cans during a 12-min interval. The number and type of nozzles and header water pressure that were used to produce different rainfall intensities are given in Table 3.

The friction measurements reported were obtained with the Texas Highway Department research skid trailer system, which conforms substantially to ASTM standards (E 274-65T). ASTM standard 14-in. tires (E 249-66) were used and inflated to 24 and 32 psi. The friction force is measured with a strain-gauge instrumented drag link. Figure 5 shows the system under test conditions. Friction measurements were taken at 20, 40, and 60 mph with E-17 tires of 3 tread depths: full tread, half tread, and smooth. Three commercial tires were also tested at 2 pressures and 3 tread depths.

Skid measurements were made by using the trailer's internal watering system; measurements were also made under simulated rain at a minimum of 3 rainfall intensities (6 or more water depths). Reported data represent an average of at least 4 skid test measurements for each variable in the study.

The portland cement concrete field surfaces (Table 2) were tested on a restricted scale because they were formed on a new section of a 4-lane divided highway east of College Station. A summary of the data taken on these surfaces as well as those surfaces previously described in Table 1 is presented and discussed in the following paragraphs.

Test Results

The field sections of PCC were finished by natural bristle brush, plastic bristle broom, metal tines, and a combination burlap drag followed by metal tines. Seven test

Figure 4. Balanced friction design for safety.

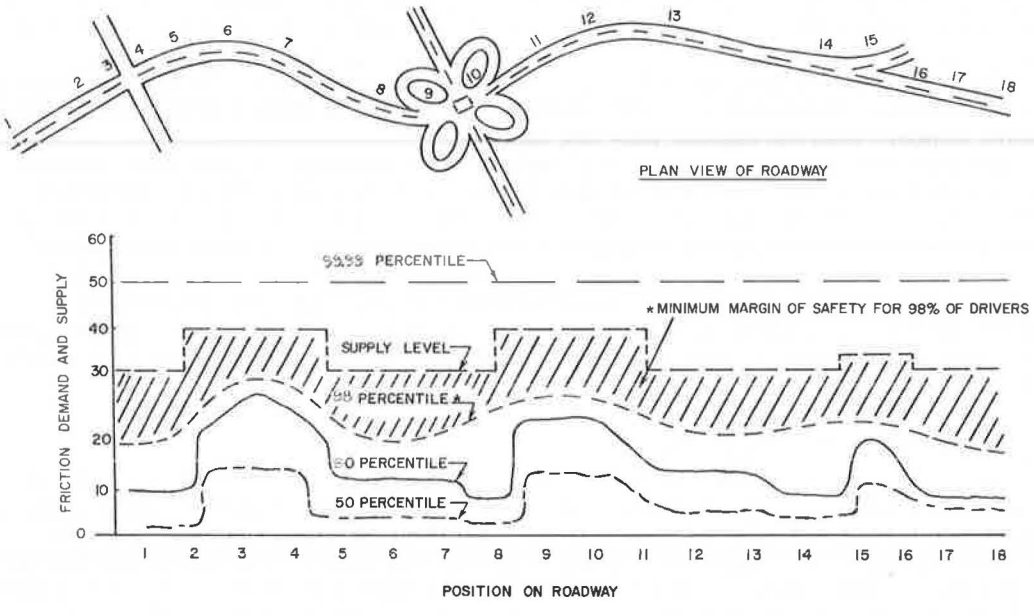

Table 1. Experimental test surfaces.

Test Pad	Surface Type	Aggregate: Weight (percent)	Aggregate: Type	Aggregate: Max Size (in.)	THD Specification	Construction Date	Preparation Prior to Test	Avg Texture Depth[a] (in.)
1	Portland cement concrete (transverse drag)[b]	67	Rounded siliceous gravel	1½	Existing runway surface	1953	Cleaned with water and power broom	0.039
		33	Siliceous gravel					
2	Clay-filled tar emulsion (Jennite), flushed seal	None	None	None	Type E[c]	1968	Scrubbed with water and rubber float	0.005
3	Hot-mix asphalt concrete (terrazzo finish)	35	Coarse crushed limestone	½	Type D	1968	Ground with terrazzo machine and polished with water, fly ash, and rubber float	0.014
		30	Medium crushed limestone					
		25	Fine crushed limestone					
		10	Field sand					
4	Hot-mix asphalt concrete	60	Coarse crushed siliceous gravel	¼	Type F	1968	Polished with water, fly ash, and rubber float	0.029
		20	Fine crushed siliceous gravel					
		20	Field sand					
5	Hot-mix asphalt concrete	30	Coarse rounded siliceous gravel	⅜	Grade C	1968	Polished with water, fly ash, and rubber float	0.024
		25	Fine rounded siliceous gravel					
		35	Crushed limestone fines					
		10	Field sand					
6	Surface treatment (chip seal)	100	Rounded siliceous gravel	½	Grade 4	1970	None	0.119
7	Surface treatment (chip seal)	100	Lightweight aggregate (fired clay)	½	Grade 4	1970	None	0.148
8	Hot-mix asphalt concrete	40	Lightweight aggregate (fired clay)	½		1970	Scrubbed with water and broom and polished with water, fine sand, and rubber float	0.022
		40	Lignite boiler slag aggregate					
		20	Siliceous field sand					

[a]Obtained by impression method.
[b]With respect to direction of vehicular travel.
[c]A 3/16 in. maximum size type E mix composed of slag and limestone screenings used as base for seal.

sections, each 800 ft long, were constructed with initial texture depths, measured by the putty impression method, ranging from 0.039 in. for the burlap drag finish to 0.094 in. for the longitudinal tines finish.

These 7 test sections were constructed in October and November 1971. After construction they were tested for skid resistance by using the Texas Highway Department ASTM trailer at speeds of 20, 40, and 60 mph.

Prior to opening the highway to traffic (June 1972), the rain simulator (Fig. 5) was moved to the project and skid-resistance measurements were taken under simulated rainfall conditions. These data together with data of the skid trailer and the internal watering system were acquired by using the tires previously described.

The skid trailer friction data for the field and experimental test surfaces were analyzed by using a computerized multiple regression program to obtain the best fit of the data. Equations relating the effects of speed, water depth, texture, tire type, tire tread depth, and tire pressure to skid number (SN) were developed, and the equations developed for a selected portion of the research are presented. The data indicate a 10 to 15 percent increase in the SN value for the full-tread ASTM tire over the 3 commercial tires used in the study. This difference, shown in Figure 6, was not shown when a larger sample of commercial tires was under different setting conditions (39).

Figure 7 shows regression lines for a selected commercial tire tested for skid number as a function of speed on experimental test pads with tire pressure, tread depth, and water depth held constant. For comparison purposes, the broken lines show ASTM values of SN as a function of vehicle speed where the various surfaces were wet only by water from an internal watering system of a locked-wheel skid trailer. Although data are given only for pads 2 and 6, they are representative of general findings that show that ASTM skid numbers are significantly higher than locked-wheel friction values determined on naturally wet (rain-slick) surfaces.

Figure 8 shows data developed on the PCC field surfaces given in Table 2. Finish F2 (transverse tines) yields significantly higher SN values than the other finishes used.

A tentative relation defining available friction as a function of the major parameters was developed by Hankins from a portion of the study presented here. This relationship is

$$SN = 0.7483(FM)^{1.03081}\left(\frac{40}{Vel}\right)0.34903$$

when

$$FM = [0.938 + (0.00675 \times Vel - 0.9)(Tread - 2.33)]\,(SN_{40})$$
$$\{29 + [(Vel - 36.4)(75 - 135\,Tread) - 3{,}600]\,(Text)\}(WD)$$

where

Vel = vehicle speed, mph;
SN_{40} = basic friction value, ASTM skid number at 40 mph;
Tread = tire tread depth, value 1 for smooth and value 2 for full-treaded tires;
Text = pavement surface texture, in.; and
WD = water depth on pavement surface, in.

Gallaway (40) had already developed the following equation to determine water depth:

$$WD = \left[3.38 \times 10^{-3}\left(\frac{1}{T}\right)^{-0.11}(L)^{0.43}(I)^{0.59}\left(\frac{1}{S}\right)^{0.42}\right] - T$$

where

WD = water depth above top of texture, in.;
T = average texture depth, in.;
L = drainage path length, ft;
I = rainfall intensity, in./hr; and
S = cross-slope, ft/ft.

Table 2. Portland cement concrete finishes of field surfaces.

Finish			Avg Texture Depth[a] (in.)
Number	Description	Direction	
F6	Burlap drag (control section)	Longitudinal	0.039
F7	Natural fiber brush	Transverse	0.042
F3	Plastic bristle broom	Longitudinal	0.046
F1	Plastic bristle broom	Transverse	0.064
F2	Steel tines	Transverse	0.070
F5	Burlap drag plus steel tines	Longitudinal	0.086
F4	Steel tines	Longitudinal	0.094

[a]Determined by putty impression test.

Table 3. Rain simulation.

Number of Nozzles	Manifold Water Pressure (lb/in.^{2})	Approximate Rainfall (in./hr)
128	30	6
64	30	3
32	20	1½

Figure 5. Equipment used for surface wetting and friction testing.

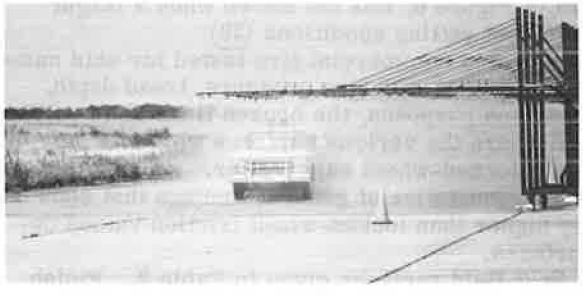

Figure 6. Skid number versus speed on experimental surfaces.

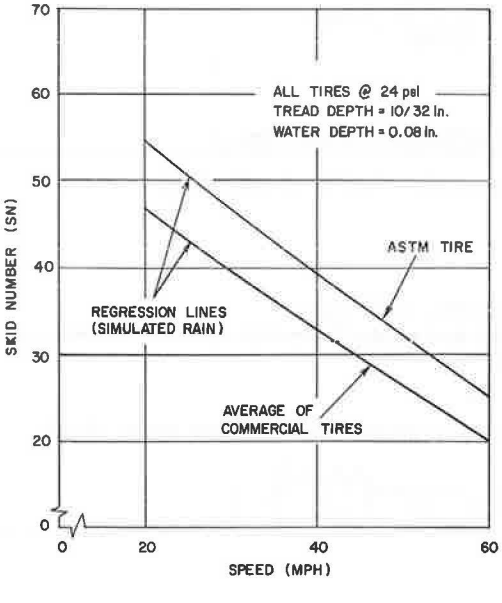

Figure 7. Skid number versus speed for selected tire on experimental surfaces.

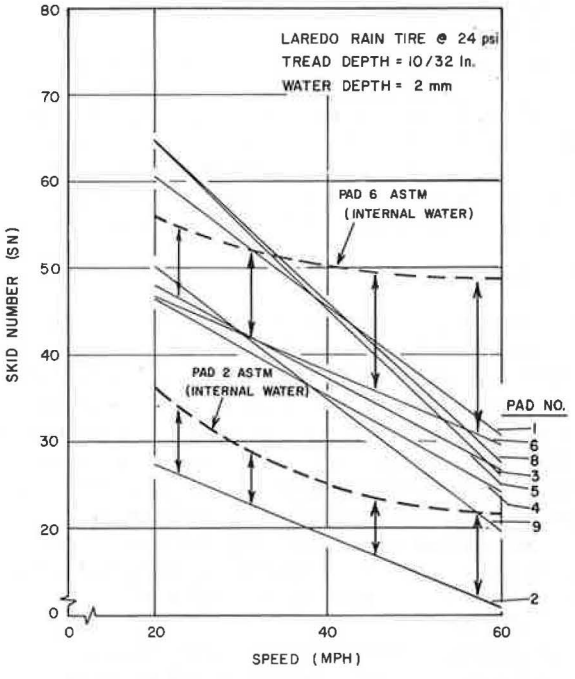

Figure 8. Skid number versus speed on PCC field surfaces.

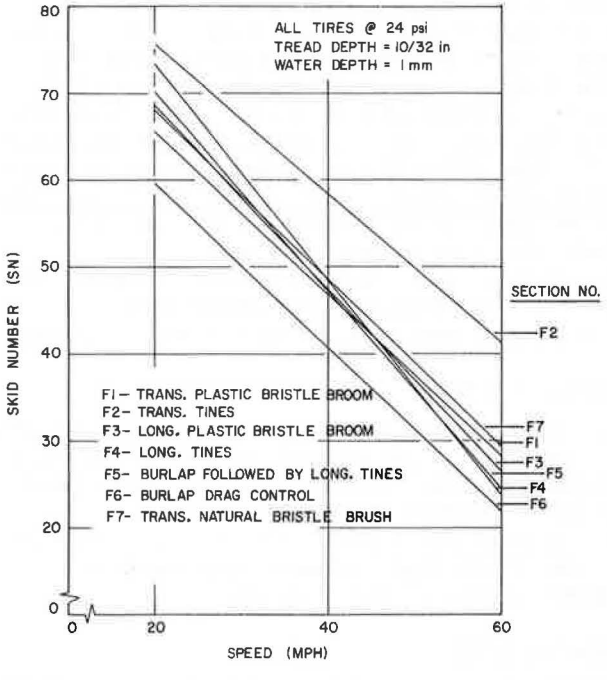

Nomographs for the solution of these equations have been developed by Hankins and are presented in a current report (7). These relations give reasonable approximations for the available friction of a pavement under given rainfall conditions when the value of SN_{40} has been determined in accordance with ASTM E 274-70.

Concerning the way in which the equation fit the data used in its development (data from 5 Texas A&M Research Annex test pads), Hankins (7) states: "The correlation coefficient was 92 with a standard error of estimate of 1.2 skid numbers indicating that the predicted available friction could vary from the measured available friction by ±2.4 skid numbers with a 95 percent confidence level." The authors think that these relations can be productively used to predict available friction from values of SN_{40} until such time that a better relation, based on more comprehensive data, is derived.

SUMMARY

The initiation of design procedures for pavement friction would not invalidate the current AASHO procedures that are addressed most appropriately to common geometric situations. They will allow a more objective evaluation of any given geometric layout in the geometric design stage and allow the prediction of the amount of friction needed. The need for an unusually high friction would probably indicate the need for a geometric layout change, a change obviously more desirable during design than after construction is completed. The AASHO policy has assumed the availability of certain levels of friction, and its assumptions are conservative with respect to the demands of the basic driving maneuvers considered. The major difference in the new approach is that different maneuvers, including those needed in some emergency situations, would also be considered. For these less common maneuvers, we should also consider allowing some margin of safety in terms of available friction.

The implementation of this concept of designing pavement friction will fulfill the highway engineer's obligation to drivers until such time that research and experience indicate that changes and refinements in the basic equations should be made.

The use of these procedures, however, will not result in the elimination of wet-weather accidents, but will result in a significant reduction. The effect of rainfall on visibility (41) is probably one of the most influential factors in the number of wet-weather accidents. Wilson (42) found that, regardless of the speed posted, the average driver will not drive below 38 to 40 mph in a free-flowing traffic condition with visibility limited to 100 to 200 ft and that the distance allowed between vehicles is not decreased at low traffic volumes. It could be concluded that the average driver is in the habit of driving unsafely during low visibility conditions. Moreover, our present social view is that driving is considered to be a right rather than a privilege, and drivers are licensed who are not prepared for normal driving situations, much less emergency conditions. Therefore, drivers will continue to have more accidents in the exceptional environment, i.e., wet weather, than they have under normal conditions.

Although this situation will continue to detract from the effectiveness and safety of highways, it should not deter efforts to design and construct appropriate surfaces to meet the demand, in both normal and emergency conditions, for tire-pavement friction.

ACKNOWLEDGMENT

The information contained in this report is derived primarily from published reports of research studies sponsored by the Texas Highway Department and the Federal Highway Administration. The authors are grateful for the cooperation and encouragement of both the Texas Highway Department and the Federal Highway Administration engineers during the progress of research. In particular we would like to acknowledge the help of K. D. Hankins and J. F. Nixon of the Texas Highway Department and W. J. Lindsey and E. V. Kristaponis of the Federal Highway Administration.

REFERENCES

1. Hankins, K. D., Gregory, R. T., and Berger, W. J. Skidding Accidents System Model. Texas Transportation Institute, Res. Rept. 135-1, March 1971.

2. Moyer, R. A. Skidding Characteristics of Road Surfaces. HRB Proc., Vol. 13, 1933, pp. 123-168.
3. Moyer, R. A. Motor Vehicle Power Requirements on Highway Grades. HRB Proc., Vol. 14, 1934, pp. 147-186.
4. Moyer, R. A. Skidding Characteristics of Automobile Tires on Roadway Surfaces and Their Relation to Highway Safety. Eng. Exp. Station, Univ. of Iowa, Bull. 120, 1934.
5. Kummer, H. W., and Meyer, W. E. Tentative Skid-Resistance Requirements for Main Rural Highways. NCHRP Rept. 37, 1967.
6. Campbell, M. E., and Titus, R. E. Spotting Skid-Prone Sites on West Virginia Highways. Highway Research Record 376, pp. 85-96.
7. Weaver, G. D., Hankins, K. D., and Ivey, D. L. Establishment of Wet Weather Speed Zoning. Texas Transportation Institute, 1973.
8. U.S. Code, 1970, pp. 364-466.
9. A Policy on Geometric Design of Rural Highways. American Association of State Highway Officials, 1965.
10. Ivey, D. L., Ross, H. E., Hayes, G. G., Young, R. D., and Glennon, J. C. Side Friction Factors Used in the Design of Highway Curves. Texas Transportation Institute, June 1971.
11. Glennon, J. C., and Weaver, G. D. The Relationship of Vehicle Path to Highway Curve Design. Texas Transportation Institute, Res. Rept. 134-5, May 1971.
12. Glennon, J. C. A Determination Framework for Wet Weather Speed Limits. Texas Transportation Institute, Res. Rept. 134-8F, Aug. 1971.
13. Weaver, G. D., Hankins, K. D., and Ivey, D. L. Factors Affecting Vehicle Skids: A Basis For Wet Weather Speed Zoning. Texas Transportation Institute, Res. Rept. 135-2, June 1972.
14. Gallaway, B. M. Skid Resistance and Polishing Type Aggregates. Texas Transportation Researcher, Vol. 5, No. 1, Jan. 1969.
15. Schonfeld, R. Skid Numbers From Stereo-Photographs. Ontario Department of Highways, Rept. RR155, Jan. 1970.
16. Sabey, B. E. The Road Surface in Relation to Friction and Wear to Tyres. Road Tar, Vol. 23, No. 1, March 1969.
17. Csathy, T. I., Burnett, W. C., and Armstrong, M. D. State of the Art of Skid Resistance Research. HRB Spec. Rept. 95, 1968.
18. Rose, J. G., Hankins, K. D., and Gallaway, B. M. Macrotexture Measurements and Related Skid Resistance at Speeds From 20 to 60 Miles per Hour. Highway Research Record 341, 1970, pp. 33-45.
19. Goodwin, W. A. Evaluation of Pavement Aggregates for Non-Skid Quantities. Eng. Exp. Station, Univ. of Tennessee, Bull. 24, 1961.
20. Hutchinson, J. W., Kao, T. Y., and Pendley, L. C. Pavement Dynamic Permeability Testing. ASTM, STP 456, 1969.
21. Gallaway, B. M. Skid Resistance Measured on Polishing Type Aggregates. American Society of Safety Engineers Jour., Sept. 1969.
22. Nichols, F. P., Jr. Further Studies on Skid Resistance of Virginia Pavements. Proc., Int. Skid Prevention Conf., Virginia Council of Highway Investigation and Research, Pt. 2, 1959.
23. White, A. M., and Thompson, H. O. Tests for Coefficients of Friction by the Skidding Car Method on Wet and Dry Surfaces. HRB Bull. 186, 1958, pp. 26-34.
24. Mason, D. F. A Preliminary Report on Skid Resistance of Various Asphaltic Highway Surfaces. British Columbia Department of Highways, 1962.
25. Moyer, R. A., and Shupe, J. W. Roughness and Skid Resistance Measurements of Pavements in California. HRB Bull. 37, 1951, pp. 1-34.
26. Moyer, R. A. A Review of the Variables Affecting Pavement Slipperiness. Proc., Int. Skid Prevention Conf., Virginia Council of Highway Investigation and Research, Pt. 2, 1959.
27. Shupe, J. W., and Goetz, W. H. A Laboratory Investigation of Pavement Slipperiness. HRB Bull. 219, 1959.

28. Shupe, J. W., and Loundsbury, R. W. Polishing Characteristics of Mineral Aggregates. Proc., Int. Skid Prevention Conf., Virginia Council of Highway Investigation and Research, Pt. 2, 1959.
29. Sabey, B. E. Pressure Distribution Beneath Spherical and Conical Shapes Pressed Into a Rubber Plane, and Their Bearing on Coefficient of Friction Under Wet Conditions. Proc., Int. Skid Prevention Conf., Virginia Council of Highway Investigation and Research, Pt. 2, 1959.
30. Stephens, J. E., and Goetz, W. H. Effects of Aggregate Factors on Pavement Friction. HRB Bull. 320, 1961.
31. Giles, C. G. Standards of Skidding Resistance: Some European Points of View. Proc., Int. Skid Prevention Conf., Virginia Council of Highway Investigation and Research, Pt. 2, 1959.
32. Zuk, W. The Dynamics of Vehicle Skid Deviation as Caused by Road Conditions. Proc., Int. Skid Prevention Conf., Virginia Council of Highway Investigation and Research, Pt. 1, 1959.
33. Finney, E. A., and Brown, M. G. Relative Skid Resistance of Pavement Surfaces Based on Michigan's Experience. Proc., Int. Skid Prevention Conference, Virginia Council of Highway Investigation and Research, Pt. 2, 1959.
34. Schulze, K. H., and Beckman, L. Friction Properties of Pavements at Different Speeds. ASTM, STP 326, 1962.
35. Kullberg, G. Skiddometer. Swedish State Road Institute, 1959.
36. Mahone, D. C. Variation in Highway Slipperiness Characteristics With Location. ASTM, STP 326, 1962.
37. Gallaway, B. M., Rose, J. G., Hankins, K. D., Scott, W. W., Jr., and Schiller, R. E., Jr. The Influence of Water Depths on Friction Properties of Various Pavement Types. Texas Transportation Institute, Res. Rept. 138-6F, 1973.
38. Ledbetter, W. B., Meyer, A. H., and Davis, J. L. Field Study of Effects of Construction Procedures on Concrete Pavement Surfaces. Texas Transportation Institute, Res. Rept. 141-2, 1973.
39. Neill, A. H., Jr., and Boyd, P. L. Research for the Grading of Wet Tire Traction. ASTM Symposium on Tire Traction, May 1972.
40. Gallaway, B. M. The Effects of Rainfall Intensity, Pavement Cross-Slope, Surface Texture, and Drainage Length on Pavement Water Depths. Texas Transportation Institute, Res. Rept. 138-5, May 1971.
41. Poliakova, G. A. Visibility in Rain. Glanvaia Geofizicheskaia Observatia, No. 100, Leningrad, 1960, pp. 53-57.
42. Wilson, J. E. California's Reduced Visibility Study Helps Cut Down Traffic Accidents When Fog Hits Area. Traffic Engineering, Vol. 35, No. 11, Aug. 1965, p. 12.

WET-WEATHER SPEED ZONING

Graeme D. Weaver, Kenneth D. Hankins, and Don L. Ivey,
Texas Transportation Institute, Texas A&M University

Speed is a significant factor in many wet-weather skidding accidents. Establishing wet-weather speed limits at certain locations, therefore, may be one way to reduce these accidents. This paper assimilates findings from various skid-research efforts to form a basis for equating the available friction at a site (pavement skid resistance) to the expected friction demand for selected maneuvers. Friction normally decreases as speed increases. Because the speeds in question are usually higher than 40 mph, the standard speed at which the skid number is determined, the change in available friction with respect to speed must be considered. Methods to accomplish this are discussed. The paper presents curves to determine, for various pavement frictions, the critical speed for hydroplaning, stopping maneuvers, cornering maneuvers, passing maneuvers, emergency path-correction maneuvers, and combined maneuvers. A design process to establish the wet-weather speed limit is discussed, and examples are presented to illustrate the use of the curves.

•SPEED is a significant factor in many wet-weather accidents. Practically every driver realizes that he must reduce his speed when the roadway is wet if he is to maintain vehicle control. Unfortunately, the degree of speed reduction may not be readily apparent.

Because the potential for skidding is so speed-sensitive, establishing wet-weather speed limits represents one procedure with which to attack the wet-weather skidding problem. Other corrective measures such as geometric improvements and intensive driver education are obviously warranted in many cases. However, these measures represent long-term objectives in the total skid-reduction program, whereas wet-weather speed zoning offers the possibility of relieving the immediate problem in priority locations.

Broadly stated, skidding accidents result from the dynamic interaction of 4 basic elements: vehicle, roadway, driver, and environment. Although simply stated, the problems posed by skidding accidents are complex. Many individual factors affect skid potential; thus, the problem is compounded greatly by the combined factors acting as a total system or sequence of events.

Considerable research has been conducted on isolated factors to determine the influence of each on skid potential. Friction or skid-resistance characteristics of pavements have been investigated both in the field and under controlled conditions. Projects recently completed investigated the relation of highway geometrics to vehicle skidding (1, 2, 3). The hydroplaning phenomenon has received considerable attention by NASA and other agencies, and research is being conducted currently to study its relation to the vehicle skidding problem (4).

The effects of vehicle tire condition, speed, pavement texture, and pavement skid numbers have been studied at accident sites. Extensive tests have been conducted to investigate the combined influence of water depth, tire condition, skid number, pavement texture, and speed (5). Vehicle suspension and steering characteristics are rel-

Publication of this paper sponsored by Committee on Surface Properties-Vehicle Interaction.

atively new research targets. Although the solution to the problem cannot be considered complete, much information exists, and a significant portion of it can be implemented at this time.

As a preliminary step toward reducing the toll of skidding accidents, the Texas legislature placed on the State Highway Commission the authority and responsibility to establish reasonable and safe speed limits when conditions caused by wet or inclement weather require such action. According to the legislation, the establishment of wet-weather speed limits should be based on "an engineering and traffic investigation." A study (6) was recently completed by the Texas Transportation Institute having as its primary objective the assimilation of pertinent findings from various skid-related research efforts to provide an objective basis on which potential wet-weather accident sites can be analyzed and, hence, safe wet-weather speed limits may be determined.

This paper presents the significant findings of that study. A basis is given for equating the available friction at a site (pavement skid resistance) to the expected friction demand for selected traffic maneuvers including hydroplaning, stopping maneuvers, cornering maneuvers, and passing maneuvers. Also discussed is a design process to establish the wet-weather speed limit.

FACTORS AFFECTING VEHICLE SKIDS

Relation of Friction Availability and Demand

The performance of desired maneuvers is dependent on the existence of tire-road surface friction. The friction required (demand) by a vehicle to perform a given maneuver increases with speed. On the other hand, the friction available to the vehicle (skid resistance) at the tire-pavement interface normally decreases with increased speed. The relation between friction demand and friction availability is shown schematically in Figure 1 (7). Loss of control usually occurs when the friction demand exceeds the friction available. The friction at the point where availability and demand are equal is defined in this report as "critical friction." It should be noted that the critical friction for a given maneuver occurs at a critical speed. For speeds less than the critical speed, sufficient friction exists to perform the maneuver. The critical friction concept is used throughout this report as a basis for evaluating the individual factors that influence friction availability and the vehicle maneuvers that affect the friction demand.

Available Friction

A widely accepted measure of pavement friction is the skid number (SN) determined by the locked-wheel skid trailer traveling at 40 mph and using an internal watering system (ASTM E 274-70). In this report, SN (including the effect of speed) is assumed to be equivalent to available friction. Other studies (3, 7, 8) have shown this assumption to be reasonably valid for relatively steady-state cornering and stopping. Although it is well documented that individual tires can develop significantly higher friction forces in a braking or side-slipping condition, these maximum values can rarely be realized simultaneously by all 4 wheels on a vehicle. Consequently, the SN is assumed to provide a reasonable approximation of the average friction available to the vehicle.

Friction measurement by this method, however, is obtained at only one speed, 40 mph. To reiterate, friction decreases with increased speed. Because the speeds in question here are usually higher than 40 mph, the change in available friction with respect to speed must be considered. The available friction, including the effects of speed, may be approximated by 3 methods:

1. By conducting standard skid-trailer measurements at 20, 40, and 60 mph and determining the speed and SN relation graphically;
2. By conducting the 20-, 40-, and 60-mph skid measurement with an external watering system (3); and
3. By conducting standard 40-mph skid measurements and determining the applicable SN at other speeds by using curves similar to those shown in Figure 2.

Using the input factors of pavement surface texture, water depth, vehicle speed, and tire tread depth from Gallaway's studies (5, 12), the Texas Highway Department developed an equation to predict the available friction on wet pavement (6). Also, Gallaway (5) developed an equation to determine water depth on the pavement as a function of texture, drainage length, rainfall intensity, and cross slope. Nomographs have been developed to solve these 2 complex equations for various parameters. So that the determination of available friction can be simplified for operational purposes, representative values have been selected for tire tread depth, pavement texture, water depth, and rainfall intensity. For a texture of 0.050 in. (measured by the putty method), tire tread depth of $^{2}/_{32}$ in., and average 85th percentile rainfall intensity of 0.14 in./hour, the speed-SN relations developed by the Texas Highway Department are shown in Figure 2 (6). Similar curves may be developed from the basic equations for any particular values of the individual factors.

The available friction curves shown in Figure 2 were developed from skid data obtained under an external watering system (rain machine) rather than under the standard ASTM internal watering system. These curves more clearly reflect pavement characteristics under actual wet-weather conditions. The available friction curves are superimposed on the friction demand curves in the remainder of this paper to permit determination of critical speed.

Stopping Maneuvers

The ability to see the roadway ahead is vital to the safe and efficient operation of a vehicle. Although it is desirable to provide ample sight distance for practically unlimited passing opportunity, compromises must be made and the roadway must be designed to less than this optimum. General practice has been (9) that the minimum acceptable design will provide at least sufficient sight distance to allow a driver to safely stop his vehicle before he hits an obstacle in his path.

Rearranging the basic stopping distance equation and substituting a 2.5-sec perception-reaction time gives the following demand friction in stopping a vehicle within the available sight distance (7):

$$FN_s = \frac{V^2}{0.3\,(d - 3.67V)} \qquad (1)$$

where

FN_s = demand friction number for stopping;
d = available sight distance, ft; and
V = vehicle speed, mph.

Figure 3 shows the relation of available friction and friction demand for stopping maneuvers.

Cornering Maneuvers

Findings in a recently completed research study (3) showed that the skid number predicted by an ASTM locked-wheel trailer approximated the average lateral friction available during a cornering maneuver provided that the skid number was considered a function of vehicle speed. Thus, a reliable estimate of critical speed may be obtained from the standard centripetal force equation:

$$e + f = \frac{V^2}{15R} \qquad (2)$$

where

e = superelevation rate, ft/ft;
f = coefficient of friction;
V = vehicle speed, mph; and
R = curve radius, ft.

Figure 1. Relation between friction demand and pavement skid resistance.

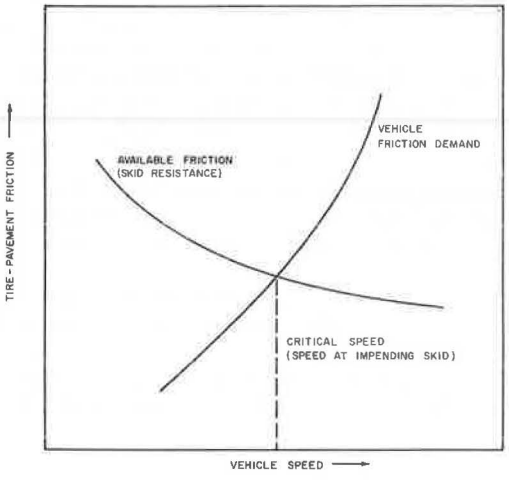

Figure 2. Available friction as predicted by skid number.

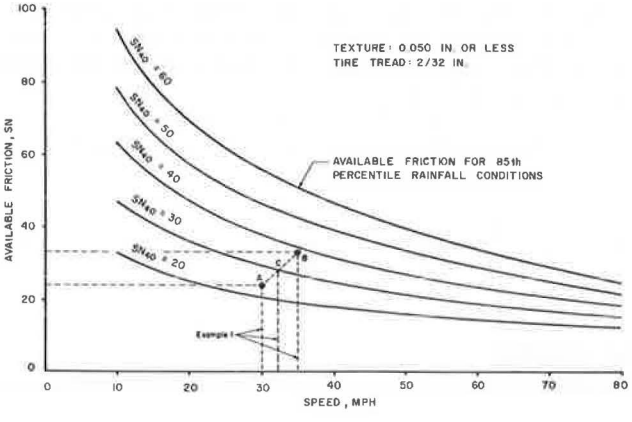

Figure 3. Critical speed for emergency stop imposed by sight distance and available friction.

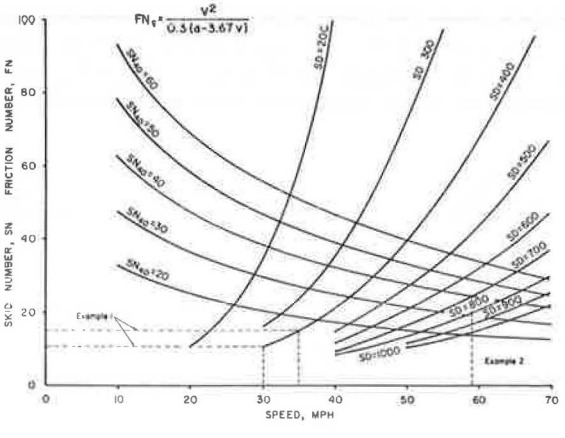

There is the provision that friction, f, be approximated by skid number and considered to be speed dependent. The friction demand for cornering, FN_c, may then be described by

$$\frac{FN_c}{100} + e = \frac{V^2}{15R} \tag{3}$$

Figure 4 shows the lateral friction demand during traversal of nonsuperelevated highway curves for degrees of curvature from 0.5 to 20 deg (1). The variation of SN with speed is superimposed. The critical speed is established by the intersection of the applicable SN curve and the degree of curvature curve.

The curves shown in Figure 4 are developed on a 0-superelevation basis to which appropriate correction factors may be easily applied for a desired superelevation rate. To include the effect of superelevation, the given demand curve, FN_c, is translated vertically by the amount of the superelevation expressed in percent. For example, if a 15-deg curve contained 0.05 positive superelevation, the 15-deg curve would be lowered 5 units of FN as shown by the dashed curve in Figure 4. Similarly, the curve would be translated upward an equal amount if the superelevation were negative.

The critical speeds determined from curves shown in Figure 4 represent allowable speeds provided the vehicle smoothly traverses the path of the highway curve. Therefore, Figure 4 should be used for spiraled transitions or at locations within a curve.

Photographic studies of vehicle maneuvers on highway curves (1) indicated that most vehicle paths, regardless of speed, exceed the degree of highway curve at some point throughout the curve. Results of these studies indicated that the radius of path followed could be expressed by

$$R_v = 0.524R + 268 \tag{4}$$

where

R_v = vehicle path radius, ft; and
R = highway curve radius, ft.

A large percentage of the observed vehicles negotiated the minimum path radius at the ends of the curve near the transition between tangent and curve. Because the friction demand at these locations is more stringent, critical speed should be determined on the basis of this minimum radius. When R_v is substituted in Eq. 3, the friction demand for cornering, FN_c, becomes

$$FN_c = \frac{V^2}{0.786R + 40.3} - 100e \tag{5}$$

Figure 5 shows speed-friction relations for various degrees of curvature (1). It is suggested that these curves be used for determination of critical speeds on curves having abrupt transition regions at either end (nonspiraled curves and at ends of curves).

Passing Maneuvers

The passing maneuver may be one of the most critical nonemergency maneuvers performed on a 2-lane highway. Several characteristics combine during the passing maneuver to influence the demand friction: The maneuver is performed at relatively high speeds; the passing vehicle executes both pullout and return maneuvers against negative superelevation due to normal crown; and the maneuver involves combinations of forward and lateral acceleration.

From studies of actual passing maneuvers on 2-lane highways (10), Glennon (2) determined frictional requirements for the critical portion of the passing maneuver based on maximum lateral friction demand. Assuming an e value of -0.02 to represent the adverse pavement cross slope, Glennon developed the following relation for lateral friction demand during the passing (pullout) maneuver:

$$FN_p = \frac{V^2}{220} + 2 \quad (6)$$

where

FN_p = friction demand number for passing, and
V = vehicle speed, mph.

Based on Kummer and Meyer's (11) relation between forward friction demand and speed for full-throttle acceleration of an American standard automobile, Glennon developed a demand friction-speed relation by using the vector sum of forward and lateral acceleration demand. The demand curve, shown in Figure 6, is based on Glennon's results but does not include his safety margin (2).

Emergency Path-Correction Maneuvers

Drivers are occasionally required to perform corrective maneuvers to avoid leaving the roadway. Although it is not feasible to satisfy the more severe frictional requirements such as might be imposed in attempts to regain control after a violent swerve, the demand friction to correct minor encroachment paths should be considered, particularly on tangent sections.

Glennon (7) calculated frictional requirements for emergency path corrections under several conditions. He concluded that the friction demand was highly sensitive to the encroachment angle and the initial distance from the edge of the roadway. Assuming a -0.02 cross slope, Glennon developed the following friction demand for path correction (Fig. 7):

$$f = \frac{V^2 (1 - \cos \theta)}{15 (W - 1.47V \sin \theta)} + 0.02 \quad (7)$$

where

V = vehicle speed, mph; and
θ = encroachment angle, deg.

Hydroplaning

Numerous factors influence the hydroplaning potential; the more significant are pavement texture, speed, water depth, tire inflation pressure and tread depth, and wheel load. Martinez, Lewis, and Stocker (4) considered these influencing factors on a portland cement concrete and a bituminous pavement.

Although no single critical speed is appropriate for the range of pavement, tire pressure, and tire parameters investigated, it is obvious that partial hydroplaning and thus some loss of vehicle control results at speeds significantly below the speed limit on most major rural highways. No critical speeds lower than 40 mph were found. The approximate median value for all parameters investigated resulted in a 50-mph critical speed, and this speed could be increased by providing a high surface macrotexture. It is suggested that critical wet-weather speed for hydroplaning be determined from curves shown in Figure 8.

Combined Maneuvers

Many common maneuvers include some combination of acceleration, braking, and cornering. The total friction demand may be determined by vector summation of the friction demand for the individual maneuvers. The following example illustrates the manner in which the critical speed may be determined for a combination maneuver. The maneuver involves combined braking and cornering such as might be experienced at an exit ramp to a stop-controlled service road.

Engineering studies revealed the following site characteristics:

1. Available friction, FN, 30;
2. Available stopping sight distance, SD, 400 ft; and

Figure 4. Critical speed for smooth transition on nonsuperelevated horizontal curves.

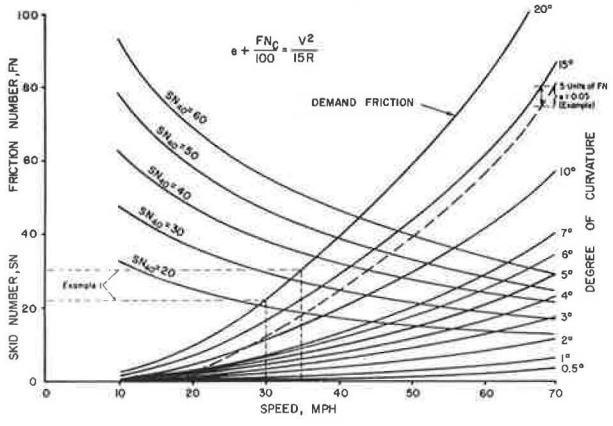

Figure 5. Critical speed for abrupt transition on nonsuperelevated horizontal curves.

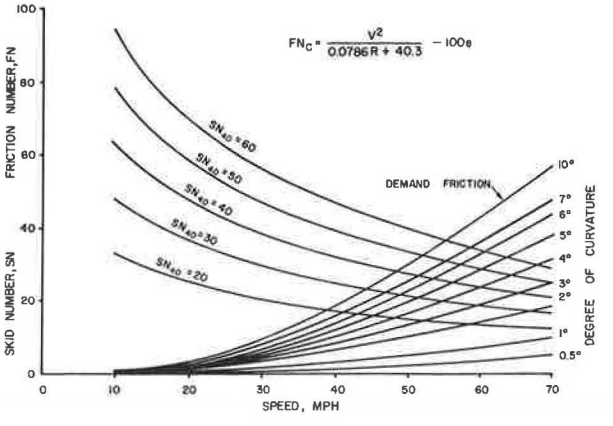

Figure 6. Critical speed for passing maneuvers.

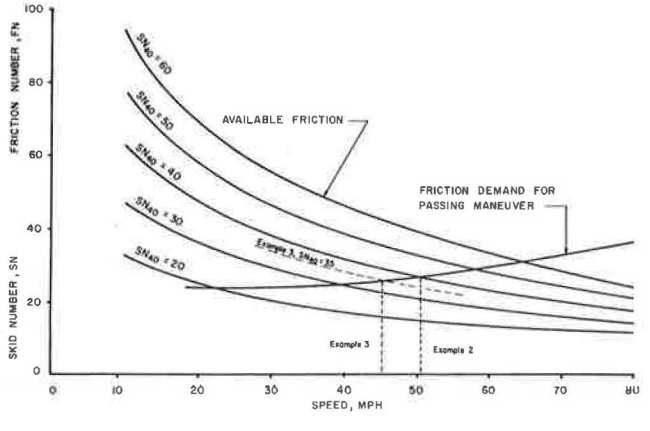

Figure 7. Critical speed for emergency path corrections on 2-lane highway.

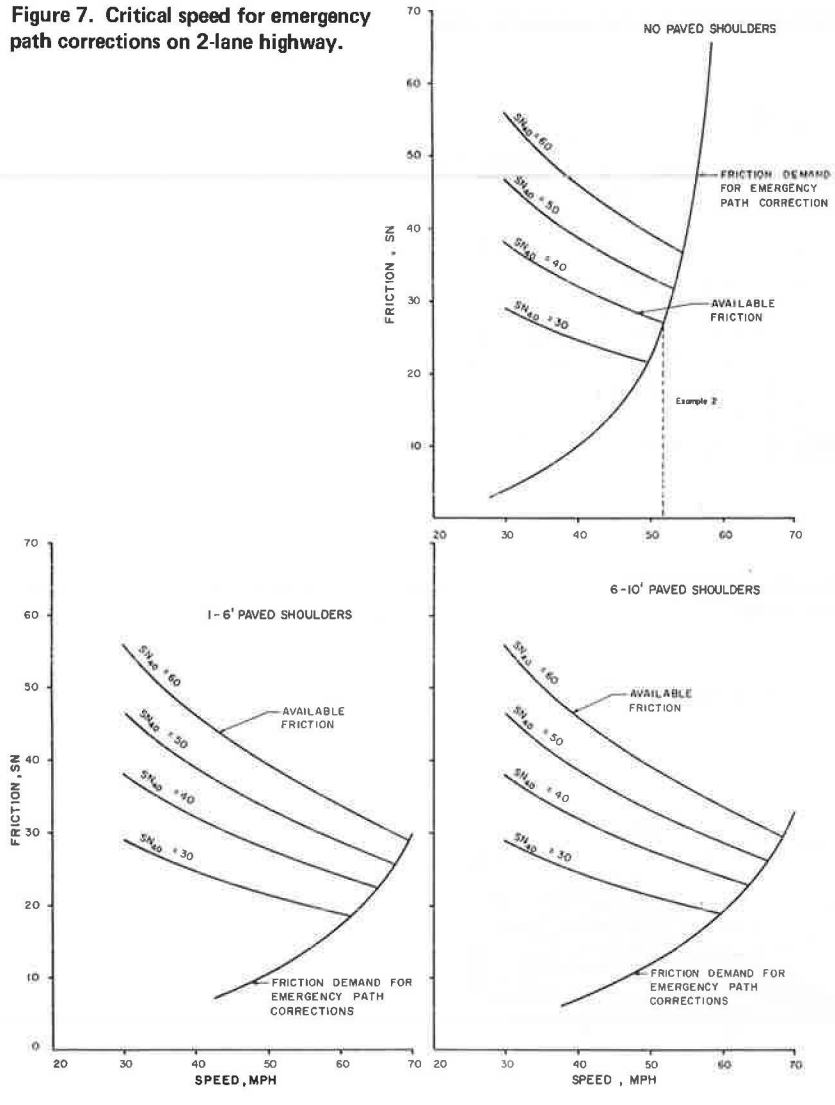

Figure 8. Critical hydroplaning speed imposed by water depth and pavement texture.

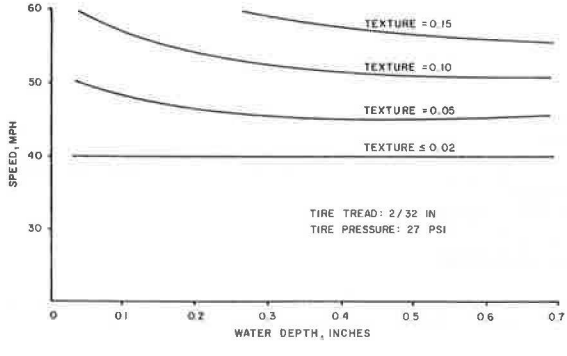

3. Spiral transition curve on ramp to a 20-deg maximum curvature with no superelevation.

The procedure is as follows:

1. Make an initial assumption of critical speed, say V_o = 30 mph.
2. From Figure 4 (or Figure 5 for abrupt transition) and the friction demand curves, determine the friction number demand for cornering, FN_c, by using the assumed speed, V_o. As shown by the dashed line in Figure 4, FN_c = 22.
3. From Figure 3, determine the friction number demand for stopping, FN_s, by using the assumed speed, V_o. As shown by the dashed line in Figure 3, FN_s = 10.
4. Compute the total friction demand number for the combined maneuver, FN_t. The total friction demand is the vector sum of the cornering demand, FN_c, and the stopping demand, FN_2.

$$FN_t = \sqrt{FN_c^2 + FN_s^2}$$

$$= \sqrt{(22)^2 + (10)^2}$$

$$= 24.2$$

5. Because FN_c, FN_s, and, hence, FN_t are dependent on the assumed speed, the resultant interaction point (point having coordinates V_o, FN_t) must be located in Figure 2. If the point lies above the available friction curve applicable to the site (in this case, the SN_{40} = 30 curve) a lower initial speed, V_o, must be assumed, and the above process (steps 1 through 4) repeated. Similarly, if the point lies below the applicable available friction curve, a higher speed, V_o, must be assumed, and the process repeated. The critical speed (the speed at which the point falls on the applicable SN-versus-speed curve) may be closely approximated in 2 or 3 trials.
6. Plotting the interaction point having coordinates V_o = 30 and FN_t = 24.2 on Figure 2 reveals that the point lies slightly below the applicable SN_{40} = 30 curve (point A, Fig. 2). Therefore, a higher speed, V_o = 35 mph was assumed, and the process was repeated. For V_o = 35 mph, FN_c = 30 (Fig. 4), FN_s = 15 (Fig. 3), and FN_t = 33.5. The interaction point (coordinates 35, 33.5) is plotted as point B in Figure 2 and lies slightly above the SN_{40} = 30 curve. A straight line between points A and B indicates a critical speed for the combination maneuver of approximately 32 mph (speed at point C).

WET-WEATHER SPEED ZONING

In many instances, the safe wet-weather speed must be less than the existing 70-mph statewide posted speed where the available friction simply does not provide the capability of performing certain maneuvers at 70 mph. Thus, if speed reduction is the single criterion, the problem is one of establishing, at these points, a reasonable wet-weather speed that is compatible with available friction.

The primary advantage of wet-weather speed zoning at selected sites is that it offers a method to alleviate the most hazardous locations (those that exhibit a history of skid-related accidents) on a priority basis. Although introduction of a statewide wet-weather speed limit would probably represent the most expedient attempt to reduce traffic operating speed during inclement weather, it offers one distinct disadvantage: The speed limit on all highways would be dictated by the safe wet-weather speed on lower quality highways. Thus, under blanket speed control, the speed would be reduced unnecessarily on many highways that provide surfaces and geometrics less susceptible to skidding.

The process outlined in the research (6) report for determination of the safe wet-weather speed limit involves equating the available friction at the selected site to friction demand for traffic operational maneuvers expected at that site. Therefore, certain engineering characteristics of the site must be known from which the available friction may be determined. Similarly, certain traffic operating characteristics must be determined. A critical speed is determined for each expected maneuver. The speed limit will be governed by the expected maneuver producing the lowest critical speed.

Several examples are presented to illustrate the design process for establishing the wet-weather speed limits at sites exhibiting different engineering and expected traffic operating characteristics.

Determining Wet-Weather Speed Limit on Tangent Section

The following site characteristics are assumed:

1. SN_{40} = 40;
2. Sight distance, SD = 700 ft;
3. Highway section is level tangent and has no paved shoulders;
4. Pavement texture = 0.05; and
5. Pavement exhibits good drainage with no evidence of rutting or ponding.

The procedure is as follows:

1. Identify the traffic maneuvers (stopping, passing, and emergency correction) that would be expected at the site. (Because the site is a level tangent section, cornering or combination maneuvers would not be expected. Therefore, critical speeds for these maneuvers would not be applicable at this site. Similarly, because there is no evidence of rutting or ponding and good drainage is provided, critical speed to produce hydroplaning is not applicable at this site.)
2. From Figure 3, the critical speed for a stopping maneuver (SN_{40} = 40, SD = 700 ft) is 59 mph.
3. From Figure 6, the critical speed for a passing maneuver (SN_{40} = 40) is 51 mph.
4. From Figure 7, the critical speed for an emergency path correction (SN_{40} = 40, no paved shoulders) is 52 mph.
5. The lowest critical speed from steps 2, 3, and 4 is 51 mph, governed by friction demand for a passing maneuver.
6. Rounding off to the nearest 5-mph increment, the wet-weather speed limit would be 50 mph.

Determining Wet-Weather Speed Limit on Horizontal Curve

The following site characteristics are assumed:

1. SN_{40} = 35.
2. Horizontal curvature = 3 deg with an abrupt transition from tangent section to the circular curve (that is, no spiral was used at the transition).
3. Superelevation, e = 0.05 percent.
4. Seal course pavement surface is slightly flushed in the wheelpaths. The texture in the wheelpaths is 0.020 and 0.065 other than in the wheelpaths. The flushed wheelpath is considerably wider throughout the curve than on the tangent approach.
5. The pavement grade is 0.4 percent.
6. The pavement surface is slightly rutted in transition area from normal crown to superelevated section. Based on string-line measurements of rut depth, observations of a flat area in the superelevation transition, and the differential texture between the wheelpath and surrounding surface, expected water depth is approximately 0.160 in.
7. Sight distance, SD, is more than 1,000 ft.

The procedure is as follows:

1. Identify the traffic maneuvers (passing and cornering) that would be expected at the site.
2. Because appreciable water depths are expected and rutting is evident, the critical speed for hydroplaning should be determined.
3. Because adequate sight distance is available, stopping maneuvers are not critical.
4. From Figure 5, the critical speed for cornering (SN_{40} = 35, D = 3 deg, e = 0.05) is more than 70 mph.
5. From Figure 10, the critical speed for hydroplaning (texture = 0.02, water depth = 0.160 in.) is 40 mph.
6. From Figure 6, the critical speed for a passing maneuver (SN_{40} = 35) is 45 mph.

7. The lowest critical speed determined in steps 4 through 6 is 40 mph, governed by hydroplaning.
8. The wet-weather speed limit would be 40 mph.

REFERENCES

1. Glennon, J. C., and Weaver, G. D. The Relationship of Vehicle Paths to Highway Curve Design. Texas Transportation Institute, Res. Rept. 134-5, May 1971.
2. Glennon, J. C. Friction Requirements for High-Speed Passing Maneuvers. Texas Transportation Institute, Res. Rept. 134-7, July 1971.
3. Ivey, D. L., Ross, H. E., Hayes, G. G., Young, R. D., and Glennon, J. C. Side Friction Factors Used in the Design of Highway Curves. Texas Transportation Institute, June 1971.
4. Martinez, J. E., Lewis, M. J., and Stocker, A. J. A Study of Variables Associated With Wheel Spin-Down and Hydroplaning. Texas Transportation Institute, Res. Rept. 147-1.
5. Gallaway, B. M. The Effects of Rainfall Intensity, Pavement Cross-Slope, Surface Texture, and Drainage Length on Pavement Water Depths. Texas Transportation Institute, Res. Rept. 138-5, May 1971.
6. Weaver, G. D., Hankins, K. D., and Ivey, D. L. Factors Affecting Vehicle Skids: A Basis for Wet Weather Speed Zoning. Texas Transportation Institute, Res. Rept. 135-2, June 1972.
7. Glennon, J. C. A Determination Framework for Wet Weather Speed Limits. Texas Transportation Institute, Res. Rept. 134-8F, Aug. 1971.
8. Glennon, J. C. Evaluation of Stopping Sight Distance Design Criteria. Texas Transportation Institute, Res. Rept. 134-3, Aug. 1969.
9. A Policy on Geometric Design of Rural Highways. American Association of State Highway Officials, 1965.
10. Weaver, G. D., and Glennon, J. C. Passing Performance Measurements Related to Sight Distance Design. Texas Transportation Institute, Res. Rept. 134-6, June 1971.
11. Kummer, H. W., and Meyer, W. E. Tentative Skid-Resistance Requirements for Main Rural Highways. NCHRP Rept. 37, 1967.
12. Gallaway, B. M., Rose, J. G., Hankins, K. D., Scott, W. W., Jr., and Schiller, R. E., Jr. The Influence of Water Depths on Friction Properties of Various Pavement Types. Texas Transportation Institute, Res. Rept. 138-6F, 1973.

SKID RESISTANCE TESTING FROM A STATISTICAL VIEWPOINT

T. D. Gillespie, W. E. Meyer, and R. R. Hegmon,
Pennsylvania Transportation and Traffic Safety Center,
Pennsylvania State University

Standards of minimum skid resistance for highway pavements must be compatible with the limitations of locked-wheel skid testers and skid resistance characteristics of the highways. Variance of skid testing data arises from the testers, test tires, and pavements. The magnitude of each source is illustrated, and some of the causes are explained. The influence of the variance is examined with respect to the confidence of skid test data in repeat and survey modes; the point is made that a large number of tests should be conducted whenever possible. It is concluded that the reduction of variance due to the tester and the test tire, though desirable, will not eliminate the need for statistical methods in skid test data analysis. The way in which minimum skid resistance standards should be defined is discussed as is a proposed method by which statistical uncertainty can be reflected in the interpretation of results from survey testing.

•A UNIFORM method for measuring pavement skid resistance has long been needed. The locked-wheel pavement skid tester has become accepted in the United States as the best current means of skid resistance measurement. The Federal Highway Administration is expected to soon adopt a set of minimum skid resistance requirements applicable to all highways that fall within the purview of the National Highway Safety Program Standards. Individual states will be required to conduct surveys to achieve these standards. As this time approaches, there is need to consider in detail how the standards must be defined to be compatible with the performance limitations of the tester and with the skid resistance characteristics of the highways.

MEASUREMENT STANDARD OF SKID TESTERS

The locked-wheel skid tester is a measuring device that is not entirely precise and accurate. That is illustrated by the use of a micrometer to measure a particular dimension of a machine part. If a large number of measurements are made, they will not all be identical, but will be distributed (usually normally distributed) about some mean that can be calculated from the individual measurements. If, with an infinite number of tests, the mean of the measurements is equal to the "true" dimension as determined from a reference standard, the micrometer is accurate. Whether accurate or not, the spread of the measurements is indicative of its precision. An NCHRP project (1) and the FHWA Area Reference Center Program formally address themselves to the problem of skid tester accuracy. Though accuracy and precision are interrelated, the following discussion will be primarily addressed to the problem of precision.

The precision of a skid tester relates to its ability to reproduce data in a number of repeat tests. Repeat tests here refer to any number of tests on the same pavement and under the same conditions during one continuous effort, aside from day-to-day tester variability, variability of test tires, and other such factors that may also be considered

Publication of this paper sponsored by Committee on Surface Properties-Vehicle Interaction.

in the category of accuracy problems. In repeat tests, the data exhibit either systematic or random variations; the latter are usually distributed normally about a mean. The standard deviation or variance (which is the square of the standard deviation) is used as a measure of the precision; for a normal distribution, 68 percent of the data points fall within ±1 standard deviation of the mean, and 95 percent of the data points fall within ±2 standard deviations.

Because of variability it is only possible to determine the true mean obtained by the tester or the true skid resistance as measured by that tester by taking an infinite number of tests. (The true means obtained by different testers will also differ because of systematic errors that affect their accuracy.) Fortunately probability theory provides an alternate approach, which is more practical and economically acceptable than conducting an infinite number of tests. Using statistical methods, one can draw inferences about the tester's true mean from only a limited number of skid tests.

Any finite number of random tests has a mean value that is probabilistically related to the mean of an infinite number of tests; the closeness and certainty of the relation are determined by the variance of the data and the number of tests. That is, the less variance in the data and the larger the number of tests are, the closer the sample mean is expected to be to the true mean.

One way to express this relation is shown in Figure 1 (2). For a given number of tests, Figure 1 shows the confidence interval of the data mean when the standard deviation of the tester has been estimated. The standard deviation of the tester is obtained from a reasonably large number of similar tests while the measured parameter (i.e., pavement skid resistance) remains constant. The confidence coefficient (0.90) and probability (0.90) used in constructing these curves were selected because they yield practical sample sizes and reasonable ranges that subjectively agree with typical tester behavior. The choice of higher or lower values has a marked effect on the location of the curves and the implied relation, suggesting the need for further research in this area.

Nevertheless, if this graph is accepted for purposes of illustration, a simplified though approximate interpretation is that, for a given set of test data, one may be 90 percent confident that the true mean of the tester is within the indicated interval of the data sample mean.

Thus, it is demonstrated that the locked-wheel tester can provide only an estimate of skid resistance. This statement applies to any measuring device; however, it carries particular significance with respect to the practical employment of locked-wheel skid testers.

Table 1 gives data taken by 6 testers in 10 repeat tests at the same location on a pavement during a skid-tester calibration and correlation study (3). At other speeds (30 and 60 mph) the standard deviations for the individual testers changed significantly, although the data spread over all testers remained at about the same magnitude. The standard deviation of each tester was estimated by the standard deviation given in Table 1 on the basis of 10 tests. Figure 1 shows that the best tester is 90 percent confident of obtaining a mean skid number within 0.6 SN of its true mean; the poorest tester is only within 2.4 SN.

The data given in Table 1 were assembled from the tests of 6 typical testers operated under closely controlled conditions. The average standard deviation for all 6 testers is approximately 2 SN and may be considered to be representative of typical testers in use today. Applying this standard deviation to Figure 1, one can see that at the stipulated confidence level a typical tester can only be expected to measure a mean skid number within 2.5 SN of its true value for 5 tests and within 1.5 SN for 10 tests. On a percentage basis, these figures translate into roughly 6 percent and 4 percent for 5 and 10 tests respectively on pavements such as those on which Table 1 data are based. Practically, these values may be taken as an indication of the accuracy of a tester in determining the skid resistance of a particular pavement location relative to the number of tests that are made.

According to the data shown in Figure 1, the best skid resistance data are obtained when a large number of tests are made with a tester having a low standard deviation. The key question then becomes, What are the sources of data variance, and how can they be controlled?

The answer is that variance of skid test data has many sources that can be grouped into 3 major sources: pavement, test tire, and tester. Within each of these, the variance includes influences from sources such as the operators, test procedures, and data evaluation methods. Figure 2 shows data from several series of tests that illustrate the magnitude of the variance from each of the 3 major sources. On a specific pavement site 50 tests were run with an ASTM E 249 test tire and a commerical steel-belted radial tire. The reduction in standard deviation between the first 2 series of tests was attributed to the greater uniformity of the steel-belted test tire. Tests with the ASTM tire on a textured steel plate yielded a reduction in standard deviation, suggesting a reduction in pavement variability. In this case, the downward drift of the data with successive tests was accommodated by using a sloping "best fit" control line because the metallic surface was visibly burnishing. Finally, the steel-belted tire was tested on the textured steel surface and yielded an even smaller standard deviation. Regarding this last test condition, it may be concluded that both the ASTM test tire and the pavement (even in repeat tests at the same location) each roughly double the spread of the test results.

The tests described illustrate the nature of data variance and the typical magnitudes of the influence from pavement, test tire, and tester. To expect all users to run such extensive tests with locked-wheel skid testers is both impractical and unnecessary. Because all survey work must be done with the ASTM test tire, the standard deviation of interest is that of the tester and the tire combined.

To obtain an estimate of the standard deviation for a tester with test tire would require at least 50 tests to be conducted on the most uniform available pavement sites. The pavements should have adequate side slope to prevent water accumulation; however, complete drying of the site between tests is impractical because the time for tests would become excessive. The testing rate should not exceed 1 test per minute. If a data drift is observed that can logically be attributed to changes in test conditions (and can be substantiated by control tests), a best fit straight line may be applied to the data as was done in the cited example (Fig. 2).

The tests should be conducted over a variety of surfaces and speeds representative of those found in routine testing. If the standard deviations obtained are clearly and repeatably functions of speed or friction level, they may be applied accordingly.

The standard deviation thus obtained is still only an estimate and applies to the combination of tester and tire. The actual deviations should be kept to a minimum by maintaining test tires in good condition and discarding those that have been dry skidded or have become visually nonuniform. Similarly, operators have an influence on the data, especially through the procedures used. Every effort should be made to maintain consistency of performance through accurate speed holding, controlling lateral placement of the tester, and consistently evaluating skid records. Good tester design and high quality equipment are essential in keeping variability to a minimum. Consistent water system performance and low drift in the gain and zero of the instrumentation are important in this respect.

PAVEMENT FRICTION VARIANCE

The discussion thus far has dealt with skid-tester variability and its influence on the confidence interval of the skid resistance determined by sampling at just one pavement site. However, the friction of a pavement varies laterally, longitudinally, and temporally. The last factor affects the ultimate level of significance in a skid resistance survey, but for now the interest may be confined to the first 2 factors.

Figure 3 shows typical skid number profiles across 2 typical pavements. The profiles were obtained by averaging the skid numbers from 10 longitudinal pavement sites when the lateral position was closely maintained with a tracking device. Though not shown by the average, typical variations as large as 20 percent were observed at individual longitudinal locations when the tester moved into or out of the wheel track. For this reason, close control of lateral position in skid resistance testing is important. A skilled and experienced driver can keep variations due to this source to a minimum but cannot eliminate them because, as shown by the graph, a 10-in. deviation

Figure 1. Statistical relation of number of skid tests and confidence interval associated with data mean.

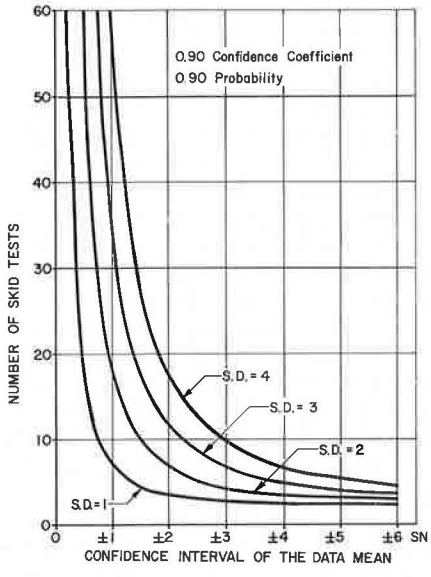

Figure 2. Repeatability tests with 2 tires and 2 surfaces.

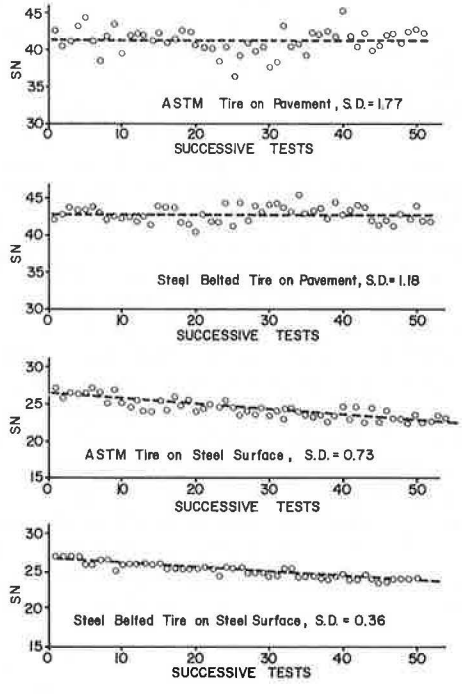

Table 1. Repeat data for 6 testers at test speed of 40 mph.

	Tester					
Test	1	2	3	4	5	6
1	48.2	55.7	47.9	46.5	46.0	40.0
2	48.2	48.7	44.8	42.0	46.0	40.0
3	49.3	49.7	45.8	43.5	52.0	39.0
4	47.1	51.7	49.9	42.0	46.0	40.5
5	49.3	48.7	49.4	46.5	42.0	39.5
6	52.4	51.7	44.3	44.5	49.0	41.0
7	48.2	48.7	47.4	42.0	44.0	41.0
8	50.2	49.7	46.3	48.5	46.0	41.5
9	49.1	49.7	44.3	50.0	48.0	40.5
10	—	50.7	44.8	—	46.0	39.0
Mean	49.11	50.50	46.49	45.05	46.50	40.20
Standard deviation	1.525	2.149	2.074	2.99	2.718	0.856

from the intended path can produce a 2 to 3 percent variation. Because of the problem of wheel track detection and tester control, lateral placement errors are an ever-present cause of variance in survey testing data.

Figure 4 shows the skid number profile measured longitudinally along 3 miles of a 2-lane highway that has few access points. The tests were run so as to eventually obtain 20 evenly spaced data points per mile. The pavement was homogeneous in age, design, and construction method. The data suggest that the pavement is frictionally homogeneous because no noticeable trend appears even though the data vary over a 30 percent range. On the other hand, the homogeneity would not have been apparent had only 5 or 10 consecutive tests been made, for example, between test numbers 25 and 35.

The element of risk or chance in skid testing can be illustrated by closer examination of the data shown in Figure 4. Table 2 gives the means, standard deviations, and confidence intervals for the case in which either 3, 5, 15, or 64 tests are conducted over the test distance. For the cases with 3, 5, and 15 tests, the data points are selected at uniform intervals from the sequence of 64 points to simulate the way data might be acquired in routine testing. Neither the means nor the standard deviations show a clear trend but are statistically a result of pure chance. The fact that the standard deviation for the case of 15 data points is less than that for 64 is a result of chance and demonstrates the risk involved in estimating the standard deviation from a limited amount of data. When, however, the statistical significance of the data is considered and the confidence interval is determined (by using Fig. 1), the importance of a large number of tests becomes obvious.

The data given in Table 2 were obtained with a locked-wheel tester using an ASTM test tire so that the calculated standard deviations include the composite of tester-tire and pavement variability. Assuming the variances do not interact, the standard deviations combine according to the relation

$$s_c^2 = s_T^2 + s_p^2$$

where

s_c = composite standard deviation,
s_T = tester-tire standard deviation, and
s_p = pavement standard deviation.

Using 2.0 SN as a conservative estimate of the tester-tire standard deviation, the pavement standard deviation can be computed and is given in the last column in Table 2. From the set of 64 tests for which the statistical confidence is highest, the pavement contribution to the test data variance is greater than that of the tester-tire combination. Thus, even when testers and test tires have been improved to the point where they become insignificant as sources of variance, the statistical problem in skid resistance surveying will remain because of the nonhomogeneous nature of the pavements.

From the standpoint of homogeneity, the pavement used as an example is typical and far better than many encountered in skid resistance surveys. Yet, to obtain an estimate of pavement skid resistance that has a precision of 3 or 4 percent (in this case less than a 2 SN confidence interval) requires far more than 5 tests specified as minimum in ASTM Method E 274-70. On the other hand, there is a practical limit to the number of tests that can be accomplished with a single tester in routine use. Figure 5 shows the mean skid number, standard deviation, and confidence interval versus the number of tests for tests conducted according to the ASTM Method E 274-70 and at the rate of 4 tests/min. The mean skid number, standard deviation, and confidence interval values are cumulative from the first to the n th test so that the values at the n th test are the result that would have been obtained if testing had been discontinued at that point.

The 4-tests/min rate is high enough that tire heating occurred and caused a downward trend in the skid resistance data. A similar effect might just have well been observed on a pavement that is nonhomogeneous. The trend shows up as a downward drift in the mean skid number and an eventual upward drift in the standard deviation. The confidence interval itself starts high and settles down, in this case a little faster than

expected because of a chance low point in the standard deviation. In theory, the confidence interval will continue to decrease with increasing number of tests such that the data mean is expected to approach the true mean of the tester. In this case, as in others that will occur in practice, systematic changes in test conditions take place in the course of the testing and, thus, prevent the confidence interval from approaching zero. A total of 10 or 20 tests appears to represent the point of diminishing returns. A data drift as shown in Figure 5 might also arise from pavement nonhomogeneity, and the more complicated problem of defining homogeneous test sections would be raised.

CONCLUSIONS

From the discussion of the application of statistical methods to the problem of variability in skid testing and some typical examples of actual tests, certain conclusions can be drawn about the limitations of using the locked-wheel method for skid resistance measurement.

1. The skid tester-test tire variance is of the same order or somewhat smaller than the variance of typical pavements.
2. Even if skid tester and test tire variances could be eliminated, the necessity of statistical analysis of skid test data remains because of the variance in pavements themselves.
3. The optimum number of tests is a compromise between precision and practicality. The point of diminishing returns appears to be about 10 to 20 tests per test section.
4. The practical limit of precision in skid testing appears to be typically 3 to 4 percent and to depend primarily on pavement homogeneity and obtaining a statistically significant number of tests.
5. Precision skid resistance data in short pavement sections or at discrete locations cannot be obtained without multiple passes through the test section to achieve statistical validity of the data.

SETTING MINIMUM SKID RESISTANCE STANDARDS

In the establishment of minimum skid resistance standards, 2 factors must be recognized: Skid resistance cannot be determined to an arbitrarily high degree of precision, and the definition of requirements in terms that necessitate discrimination of skid resistance at discrete pavement locations will greatly increase the effort involved in testing.

In the final analysis the standards must recognize traffic demands created by factors such as grades, curves, speed limits, and intersections and must likewise allow for skid resistance determination wherever possible by averaging from a large number of tests.

The suggested method is to define skid resistance standards by categories based on the design standards of each test section as measured by the criteria for design of curves, grades, shoulders, speed, and other factors that affect traffic friction requirements. The acceptability of a given highway would then be determined by comparison of the mean skid resistance, reduced by a weighted portion of the associated confidence interval, and the minimum requirement.

Methods that require discrete minimum friction levels in individual curves or other traffic situations have been postulated. To include the degree of refinement that recognizes singular locations of low skid resistance level or high traffic demand will require adoption of repeat testing methods and will increase the effort required in survey testing by an order of magnitude.

APPLICATION TO SKID RESISTANCE SURVEYS

Extensive effort is required to ensure high statistical confidence in all skid resistance surveys. A logical alternative is to conduct 2 surveys: a general survey to identify highway sections suspected of failing to meet minimum requirements and a precision survey of the suspected sections to obtain the precision data necessary for final

Figure 3. Average lateral profiles for 2 highways.

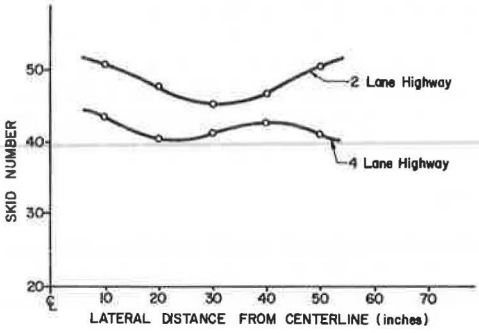

Figure 4. Longitudinal skid number profile on 2-lane highway.

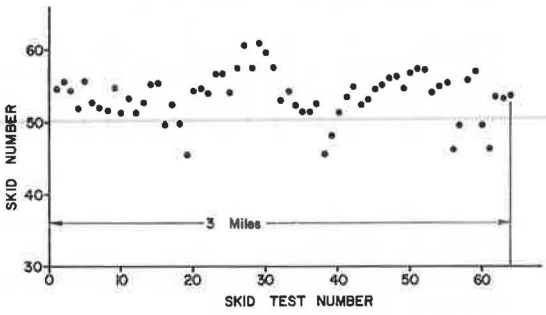

Table 2. Statistical characteristics of data of different sizes.

	Skid Number			
Number of Tests	Mean	Standard Deviation	Confidence Interval	Pavement Standard Deviation
3	53.0	6.00	>±6	5.65
5	52.7	4.50	±6	4.03
15	54.5	2.77	±1.6	1.91
64	53.9	3.39	±0.8	2.74

Figure 5. Data drift obtained at 4 tests/min.

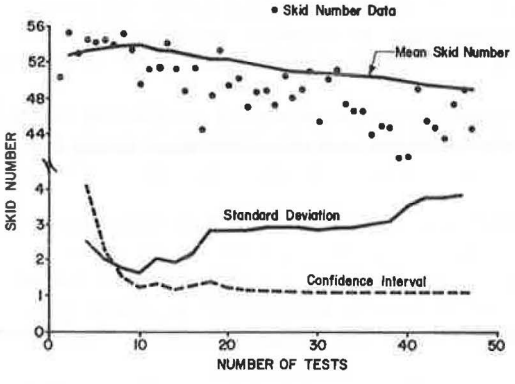

Figure 6. Comparison of skid resistance data with minimum standards.

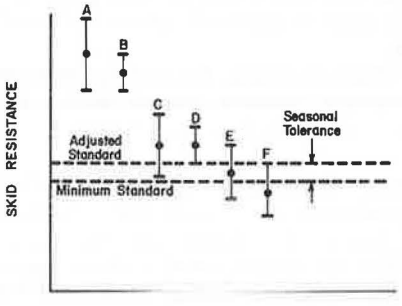

judgment on compliance with requirements and to determine the maintenance action required.

Judgment of individual pavement sections might be done in both types of surveys in the fashion shown in Figure 6. Rather than consider only the skid number means one should, it is suggested, consider the mean minus one-half the confidence interval. The skid resistances of surfaces A and B are clearly above the minimum requirement and may be judged adequate even though they differ in mean and confidence interval. Even when the confidence interval is large because of a low number of data points, such as on surface A, further testing is not required. Surfaces E and F have means that are respectively above and below the minimum requirement. Surface F is clearly substandard, and surface E should likewise be considered substandard because the confidence interval indicates that portions of it are substandard. If the confidence interval in this latter case is large because of a low number of test data, a precision survey is called for. The larger number of data points may possibly reduce the confidence interval enough so that the mean minus one-half the interval will no longer fall below the minimum standard.

Surfaces C and D are more difficult to judge because of the closeness of their skid number means to the minimum requirement, and the judgment must take into account other phenomena in skid resistance testing. For instance, temperature and seasonal effects are known to influence skid resistance, and the effects are variable throughout the country. If it is postulated that surface must be adequate at all times, a seasonal tolerance based on empirical knowledge of such effects in the local geographic area can be added to the minimum and used to adjust the requirement. As illustrated, this would make surfaces E and F clearly substandard.

In the general survey, the suggested criterion for identifying suspected substandard surfaces is whether the skid number mean less one-half its confidence interval falls below the adjusted requirement. For such surfaces, precision surveys should then be conducted during that portion of the test season when the minimum skid resistance prevails.

A frequent second objective in skid resistance surveys is predicting when highways will reach substandard skid resistance levels, and statistical methods can also be used for that. The use of data means with confidence intervals can be implemented in existing procedures, thereby placing the predictions on a more rational basis because the data variances can be transformed into variance on the predictions as well.

In this paper no attempt has been made to set statistical criteria for methods in the use of locked-wheel skid testers or for decisions on pavement skid resistance adequacy. The criteria used in the discussions illustrated how and why pavement skid resistance is a statistical quantity. The valid use of skid resistance data requires statistical methods, and it is hoped that its importance and some potential methods may be recognized.

ACKNOWLEDGMENTS

The data used for illustration in this paper were obtained in connection with the conduct of the NCHRP Project 1-12(2).

REFERENCES

1. Meyer, W. E., Hegmon, R. R., and Gillespie, T. D. Locked-Wheel Pavement Skid Tester Correlation and Calibration Techniques. Pennsylvania Transportation and Traffic Safety Center, Pennsylvania State Univ., May 1973, 360 pp.
2. Guenther, W. C. Concepts of Statistical Inference. McGraw-Hill, 1965, App. D-11.
3. Neill, A. H., Jr., and Boyd, P. L. Calibration Study Should Eliminate Variations in Skid-Testing Trailers. Highway Research News, No. 45, Autumn 1971, pp. 31-36.

PAVEMENT ROUGHNESS: MEASUREMENT AND EVALUATION

Rolands L. Rizenbergs, James L. Burchett, and Larry E. Davis,
Bureau of Highways, Kentucky Department of Transportation

Vertical accelerations of a passenger traveling in an automobile on a section of road at 51.5 mph (23.0 m/s) are automatically summed. A roughness index is obtained by dividing this sum by the time elapsed during the test. Continuity in measurements since 1957 has been preserved through correlations among successive vehicles involved and reference pavements. In general, bituminous construction has smoother riding surfaces than concrete construction. The smoothness of concrete pavements, however, has improved on those projects where slip-form paving was used. Interstate highway and parkway construction continues to yield smoother pavements than other major construction. The rate of increase in roughness was found to be different for each pavement type and varied according to the original or as-constructed roughness of the pavement, structural number, and type of highway facility involved.

•IN EARLY road-roughness testing in Kentucky, local irregularities in pavement profiles were detected by a roller type of straightedge. Although this method continues to be used to control construction tolerances, it was recognized in the early 1950s that a rapid method of recording profile characteristics more closely associated with riding quality was needed. Attention was then directed toward the response of a vehicle traveling on a highway at a normal speed. Various parameters associated with vehicles in motion were investigated; this led to the adoption of a triaxial arrangement of accelerometers mounted on the chest of a test passenger. Multichannel recording equipment was installed in an automobile to record passenger accelerations (1). A number of analytical approaches were tried (2). Finally, it was decided to sum the area under the vertical acceleration trace only and to express this measurement in terms of a roughness index (3, 4). The manual method of analysis was both tedious and time-consuming. Subsequently, instrumentation was added to automatically sum the vertical accelerations. This automatic system enabled an extensive survey program. Several variables affecting the results were investigated, and test procedures were developed to minimize their influences (5). Subsequent investigations have been concerned with the frequency content of vertical accelerations and the contribution of various frequencies to the roughness index. Test sedans were periodically replaced. Each change required a correlation between the old and the replacement vehicle.

Roughness measurements were obtained on more than 50 representative bituminous and concrete paving projects completed before 1957. Those projects have been retested periodically. Major bituminous and concrete paving projects completed since 1957 have also been added to the testing program and periodically retested. Projects largely involved Interstate highways and parkways (expressways). By 1970, 234 projects were being monitored for roughness.

Measurements were used to evaluate quality of workmanship and construction, to quantify rates of deterioration, and to identify contributing causes. Roughness indexes were related to service age, cumulative traffic, and equivalent axle loads (EAL).

Publication of this paper sponsored by Committee on Surface Properties-Vehicle Interaction.

AUTOMOBILE METHOD OF RIDE-QUALITY TESTING

Instrumentation

The automatic roughness-measuring system (ARMS) is shown in Figure 1. The accelerometer is powered and balanced by circuits in the control console. The output signal is amplified and rectified by a selenium bridge and integrated by a solion cell. The integrator output is read on a dc digital voltmeter, which is also used for monitoring the ARMS in performing component adjustments and for calibrations. A recorder provides a chart for visual field or laboratory inspection. Figure 2 shows the instrumentation installed in the automobile and the test passenger with the accelerometer on his chest.

Procedures

Pressure in the tires was adjusted to 24 lb/in.^{2} (1.7 kg/cm^2) when cold and did not exceed 28 lb/in.^{2} (2.0 kg/cm^2) during a test; the gas tank was at least half full. The instrumentation power was turned on at least 10 minutes prior to testing to allow for adequate warm-up. Temperature in the vehicle was maintained at about 75 F (24 C). The accelerometer was balanced and calibrated; integrator output was nulled, and a full-scale calibration was performed.

The test passenger, of medium build and frame and weighing 150 to 170 lb (68 to 77 kg), was seated erectly, but relaxed, in the right front seat of the test vehicle with his arms resting in his lap. The accelerometer, mounted on an aluminum platform, was suspended from a cloth strap looping over his shoulders and behind his neck and resting against his chest. A mirror mounted on the right sunvisor permitted the test passenger to view a bubble level on the mounting platform to maintain the proper positioning of the accelerometer.

Sufficient starting distance preceded the test section to permit the vehicle to attain the test speed, normally 51.5 mph (23.0 m/s). At the end of each test excursion, the integrator output and elapsed time were recorded, and, by substitution into the appropriate equation (6), a roughness index (RI) was calculated. If a retest yielded an RI differing by more than ±4 percent, the pavement was retested. The closest values were averaged. Roughness measurements were not conducted under rainy or wet conditions or at temperatures below 45 F (7 C).

Vehicle Replacements

During the past 13 years, 3 full-sized Ford sedans have been employed in roughness testing: a 1957 Ford from January 1957 to May 1963, a 1962 Ford Galaxie from May 1963 to July 1968, and a 1968 Ford Galaxie from July 1968 to the present. Odometers in the first 2 vehicles at the time of retirement from roughness testing indicated approximately 90,000 miles (145,000 km).

Each vehicle replacement required a correlation of roughness measurements obtained with the old and replacement vehicles. Test sections of both flexible and rigid pavements were selected to represent pavements with excellent to poor ride qualities. The correlation in 1963 was primarily conducted on 2-lane roadways that exemplified the prevailing routes of travel. By 1968, emphasis in roughness testing was shifted to Interstate highways and parkways, and correlation between vehicles, therefore, was conducted on those projects. Consequently, the range in pavement roughness was greatly reduced, and pavements having very high RI values were no longer available.

Results of vehicle correlations in 1968 are shown in Figure 3. Separate linear regression equations were warranted for each pavement type. Because of the high vehicle correlations, periodic replacement of the test automobile has not perceptibly affected continuity in roughness measurements. Equations used in calculating the roughness index incorporated, among other considerations, differences in ride quality of the automobiles. Thus, all measurements are relative to the original test vehicle.

Figure 1. Automatic roughness-measuring system.

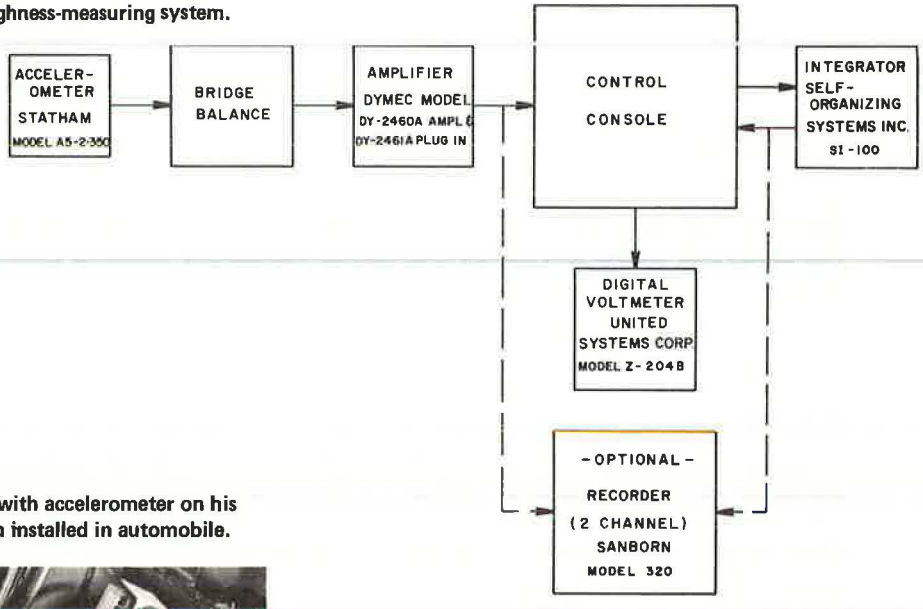

Figure 2. Test passenger with accelerometer on his chest and instrumentation installed in automobile.

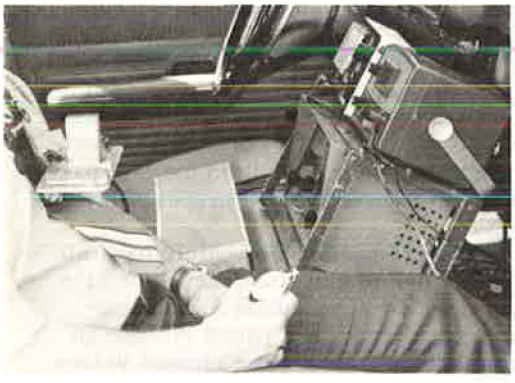

Figure 3. 1968 vehicle correlation.

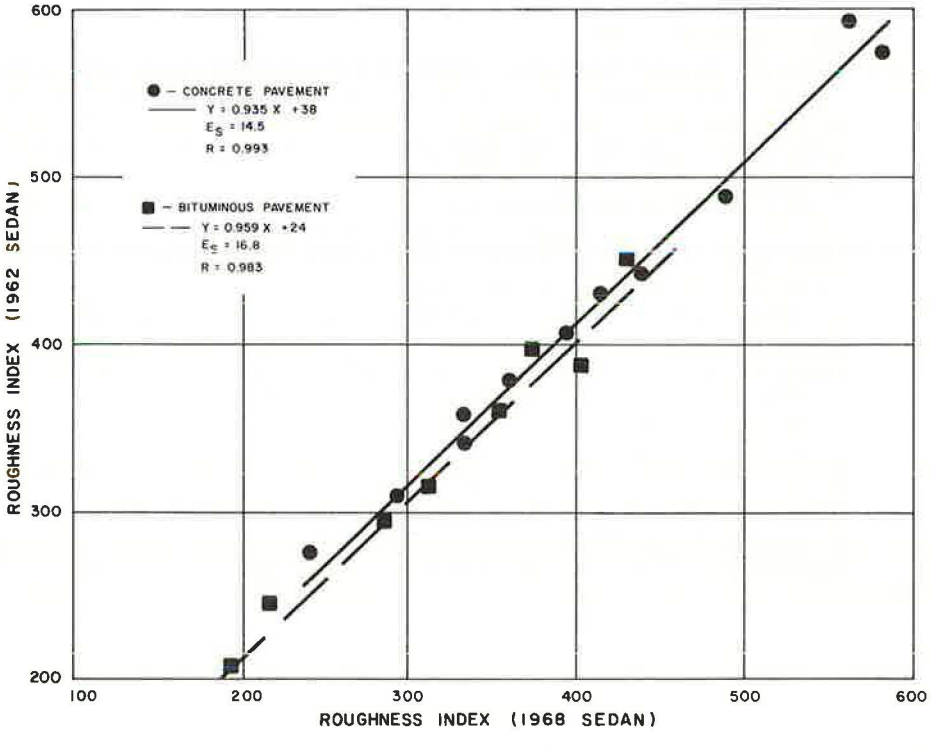

Tire Replacement

Tires on the test vehicles were replaced with identical kind. The new tires were preconditioned on the test automobile, or another sedan, for at least 500 miles (800 km) prior to their use in roughness testing. The front end of the automobile was then inspected and aligned, and the tires were balanced. Tires were not permitted to wear below $^1/_8$ in. (3.2 mm) tread depth and were replaced when flat spots, out-of-roundness, or any other defects were detected. Performance of replacement tires was checked on reference surfaces.

Reference Surfaces

The dynamic response of the test vehicle was continuously monitored to achieve reliable roughness measurements. Deterioration of the suspension system or tires affects test results and may introduce serious errors. Two low-traffic roadway sections, one bituminous and one concrete, were selected as reference surfaces and periodically tested.

The addition or removal of weights from the vehicle was found to be the most expeditious procedure by which to alter test results. In the event the RI on the reference surfaces was judged to be too high, addition of weights improved the ride quality and thereby reduced the RI. Before such remedies were applied, however, a careful investigation was initiated to pinpoint the source of the problem. Some fault was usually found with one or several tires due to improper front-end alignment or wheel balance, and the defective tires were replaced or the wheels were rebalanced and the front end aligned. Close attention was always given to regular maintenance of the vehicle.

Measurements on the 2 reference surfaces were at times supplemented with measurements on other pavements for which previous data were available before final judgment was made as to vehicle condition. At times, roughness data were simply corrected on the basis of previous measurements obtained on the reference pavements when their retesting yielded values outside acceptable limits. These procedures were generally satisfactory in providing reasonable means to ensure short-term and, to a lesser extent, long-term reproducibility of roughness measurements.

Most pavements become rougher with age. Available evidence suggested that the reference pavements have become rougher, but not nearly so much as most other projects under surveillance. Data revealed a slight trend toward increased RI during a 3-year period. Whether this increase can be attributed solely to changes in the pavement profile or to the deterioration in ride quality of the vehicle cannot be conclusively stated. Discrepancies created by using data from the reference surfaces as outlined created errors in roughness measurements and, thus, underrated the roughness of pavements with the passing of time. The end result, of course, is that recently constructed pavements may indicate a somewhat smoother ride quality than their surface profiles may warrant, and retesting of projects constructed several years ago may show less deterioration than had actually occurred.

Frequency Composition of Measured Accelerations

Accelerations sensed with the accelerometer reflect the composite characteristics of the pavement profile, vehicle, and passenger. The pavement profile, therefore, cannot be specifically described unless the frequency response of the entire system between the sensor and the pavement is known. We were somewhat compelled to inspect the measured accelerations in terms of discrete frequency ranges and to note their contribution to the roughness index.

A bituminous surface and a concrete surface having nearly the same roughness indexes were selected for this analysis. The pavements could be described as representative of those pavement types in terms of their wavelength characteristics. A filtering device was incorporated into the ARMS instrumentation to allow recording of filtered output. Pavement sections were tested repeatedly with the filter acting as a low-pass filter. Several frequency ranges were used.

A roughness index was also obtained for each frequency range. Results of the low-

pass filter measurements are shown in Figure 4 in terms of cumulative percentage of the total roughness index. Several observations are noteworthy. First, profile characteristics of the 2 pavements were quite different, even though their roughness indexes were the same. Profile amplitudes associated with shorter wavelengths were somewhat larger on concrete pavements than on bituminous pavements. Second, accelerations associated with 20- to 100-ft (6- to 31-m) waves contributed a major portion of the roughness index. Third, acceleration frequencies of 1 Hz or less contributed significantly to the RI even though their amplitudes were quite low. The explanation for what appears to be a contradiction lies with the method by which the RI was obtained. The method entailed summing of acceleration signals, or areas under the acceleration trace, which were random in nature. The higher frequency signals were superimposed on the lower frequencies and thereby added to or subtracted from the amplitude of the lower frequency signals. The net effect was a disproportionately lower contribution from the higher frequency accelerations.

Test Speed

It was recognized that the ride quality of vehicles changes with speed; therefore, a standard speed was necessary if pavements were to be compared and rated. A speed of 51.5 mph (23.0 m/s) was chosen because it approximated the average running speed on rural roads at that time. Statewide road improvement programs and construction of the Interstate and parkway systems have significantly raised running speeds, which now approach 70 mph (31 m/s) on expressways.

Sections on Interstate highways were selected for testing at 51.5 mph (23.0 m/s) and 70 mph (31 m/s). Data and results of linear regression analysis are shown in Figure 5. The following observations are made.

1. Profile characteristics of the 2 pavement types were sufficiently dissimilar to warrant separate regression equations.
2. Roughness indexes at 70 mph (31 m/s) were significantly higher than at the normal test speed. On bituminous pavements, the RI was 44 percent to 49 percent higher. On concrete pavements, the RI was 23 to 28 percent higher.
3. Differences between RI for the 2 speeds were somewhat affected by the roughness level of the road. On rougher pavements, the percentage differences between RI for the 2 speeds were the greatest.
4. Pavement profile characteristics for the same type of pavements were rather similar as reflected by the statistical parameters for the regression lines.

Figure 5 shows the influence of speed on roughness measurements and permits extrapolation of roughness indexes to higher test speeds. The measurements were made with the 1962 vehicle and not with the current test automobile, and, as pointed out earlier, each automobile responds somewhat differently to roadway excitations.

EVALUATION OF PAVEMENT ROUGHNESS

There are 2 sources of roughness: that which is built or constructed into the pavement and that which develops after construction through use or abuse. It is recognized that a pavement may change with age even if it were not used at all; embankments settle, and the pavement heaves. Heavy loads, and especially overloading, cause damage and may induce roughness. Roughness has been one of the major factors considered in resurfacing programs, and a history of the development of roughness is a significant descriptor of the service life of a pavement. Initial roughness thus alludes to the construction process and to quality of workmanship; changes in roughness with age and traffic are meaningful from the standpoint of structural design of pavements.

To this end, testing for roughness has been continued since 1957; some historical records include one or more resurfacings. All Interstate and parkway projects and many major construction projects have been tested for initial or as-constructed roughness. Insofar as possible, outer lanes on 4-lane roads have been tested annually; inside lanes of several selected projects have also been tested.

Figure 4. Roughness index with increasing acceleration frequencies obtained with low-pass filter.

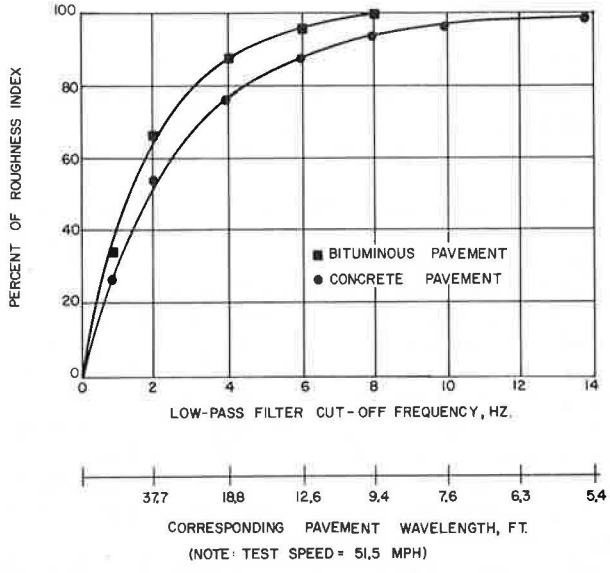

Figure 5. Roughness indexes at test speeds of 51.5 and 70 mph on bituminous and concrete pavements.

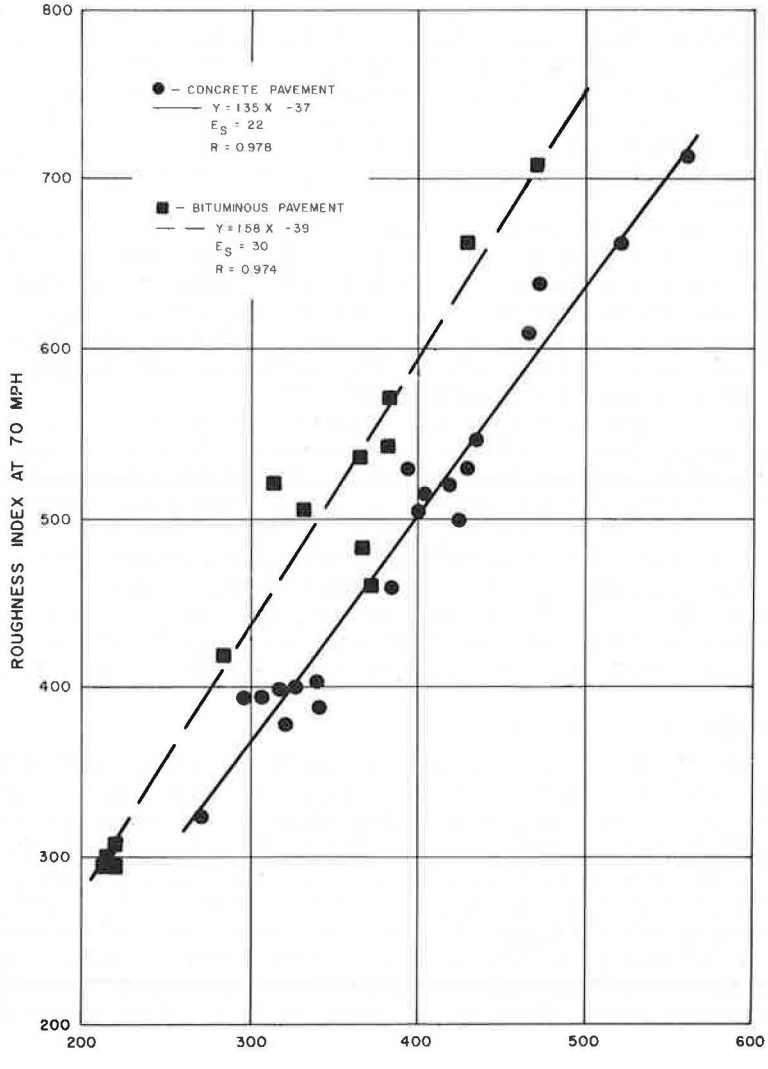

Constructed Roughness

Since 1959, Interstate, parkway, and other major roads tested totaled approximately 4,000 lane-miles (6,400 lane-km) and involved 177 projects, of which 71 were bituminous. The remaining 106 projects were concrete and included 14 projects constructed by slip-forming.

Distribution of initial roughness values is shown in Figure 6. Word ratings were first introduced in 1962 (4) and have remained unaltered, although they were established from a limited data set. By 1970, 55 percent of the concrete pavements and 71 percent of the bituminous pavements were rated excellent or good.

At the time of construction, roughness generally showed small variation throughout the length of a particular lane or among lanes. There were some notable exceptions. The greatest differences between any 2 lanes in Interstate and parkway construction were 41 and 36 percent for bituminous and concrete pavements respectively. Within each paving project, concrete pavements showed the smallest differences between the smoothest and the roughest lanes—an average of 13 percent. On bituminous pavements, the differences averaged 17 percent. On the whole, the smallest differences in roughness, of course, were found between adjoining lanes—3 percent in bituminous construction and 1 percent in concrete construction.

Comparisons of roughness indexes for Interstate, parkway, and other pavements for each construction year are given in Table 1. Parkways were somewhat smoother than Interstate highways, and other major construction projects were usually rougher than either. These comparisons are valid only for the same test speed (51.5 mph, 23.0 m/s). When additional consideration was given to driving speeds, such as 70 mph (31 m/s) on Interstate highways and parkways and 60 mph (27 m/s) on other highways, the ride quality was significantly reduced. Whereas direct comparisons were made at the standard testing speed, tests made at permissive running speeds showed clearly that control of pavement profile quality is not improved in commensurate proportion to design speed.

According to the roughness index, bituminous construction yielded smoother riding surfaces than concrete construction. As discussed earlier, caution should be exercised in directly comparing pavements having different surface characteristics. Concrete pavements typically exhibit a greater proportion of shorter wavelength irregularities that do not contribute significantly to the roughness index obtained with the Kentucky method of roughness testing, but they may be annoying to the driver and, therefore, influence ride-quality judgments.

The smoothness of concrete pavements was improved on those projects where slip-form paving (7) was used, with the exception of the first 2 projects completed in 1967. One project constructed in 1968 with continuous reinforcement and slip-form paving exhibited particularly excellent ride quality. Bituminous pavements constructed in the past several years, however, have not materially improved when contrasted with paving in the earlier years of Interstate and parkway construction. Voluntary adoption of electronic screed controls on pavers probably accounts for earlier quality improvements. Figure 7 shows the average roughness indexes of projects for each construction year on 4-lane Interstate highways and parkways. The median roughness for all projects was 270 for bituminous pavements and 325 for concrete pavements.

Bituminous Resurfacing

In 1957, more than 50 bituminous pavements were tested for roughness in connection with a pavement design study (8). These pavements represented a high type of construction and were located throughout Kentucky. Monitoring for roughness has continued although most of the pavements have been resurfaced. Bituminous overlays significantly reduced roughness; the average reduction in roughness index was 36 percent. Bituminous overlays on several concrete pavements exhibited similar improvements—an average of 39 percent. The greater reduction in roughness seemed to be realized on the rougher pavements as indicated by data given in Table 2. Cited improvements, however, are not precise because measurements were not made just prior to or shortly after resurfacing. Either the terminal roughness of the pavement was not obtained in

Figure 6. Initial roughness values for newly constructed bituminous and concrete pavements.

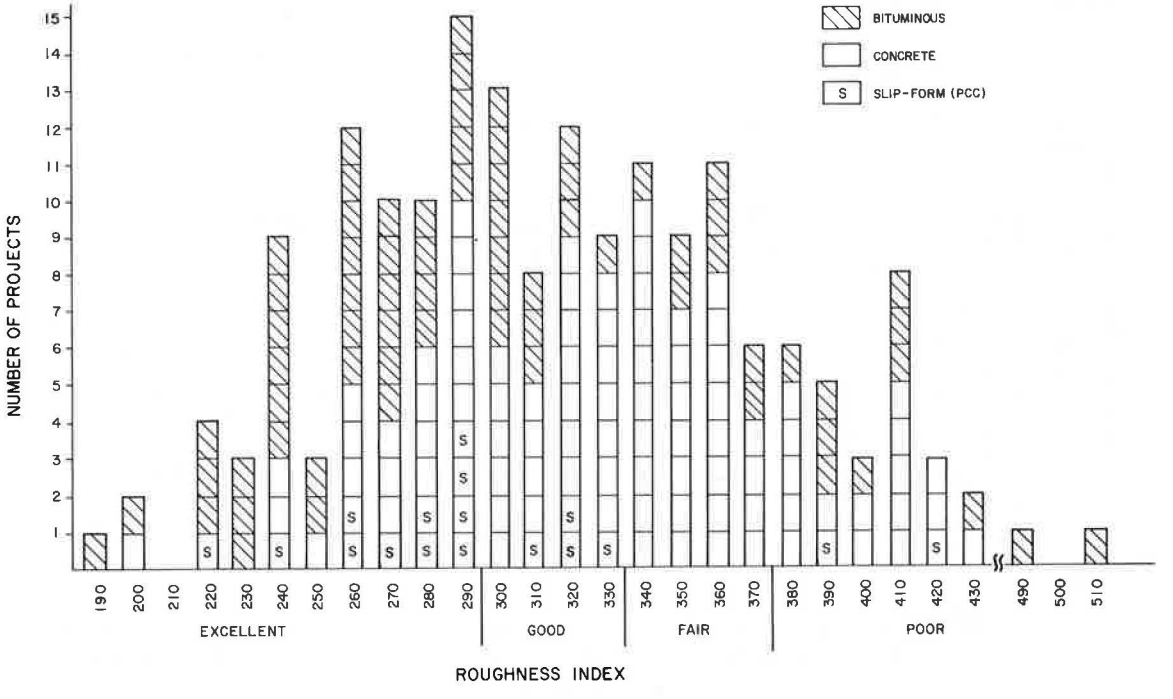

Table 1. Constructed roughness of pavements.

Pavement	Construction Year	Interstate		Parkway		Combined	Others	
		Number of Projects	Avg RI	Number of Projects	Avg RI	Avg RI	Number of Projects	Avg RI
Concrete (conventional)	Before 1962	10	331			331	4	382
	1962	8	332	9	332	332	2	325
	1963	7	329	12	302	312	3	350
	1964	3	337			337	1	300
	1965	3	317	4	325	322	1	420
	1966	4	340			340	1	410
	1967	6	368			368		
	1968	3	343	3	290	317		
	1969	3	297	2	360	322		
	Avg		334		317	328		363
Concrete (slip-form)	1967	2	405			405		
	1968	5	276	3	273	275		
	1969	4	285			285		
	1970			3	305	305		
	Avg		303		289	298		
Bituminous	Before 1962	2	295			295	8	362
	1962	2	330			330	6	368
	1963	2	355	13	277	287	3	303
	1964	3	270			270	2	290
	1965	2	260	3	233	244	3	267
	1966						5	320
	1967	2	280			280		
	1968	2	265	7	269	268		
	1969	4	262			262	2	325
	Avg		286		269	275		332

Figure 7. Average roughness index for each construction year on bituminous and concrete pavements of 4-lane Interstate and parkway highways.

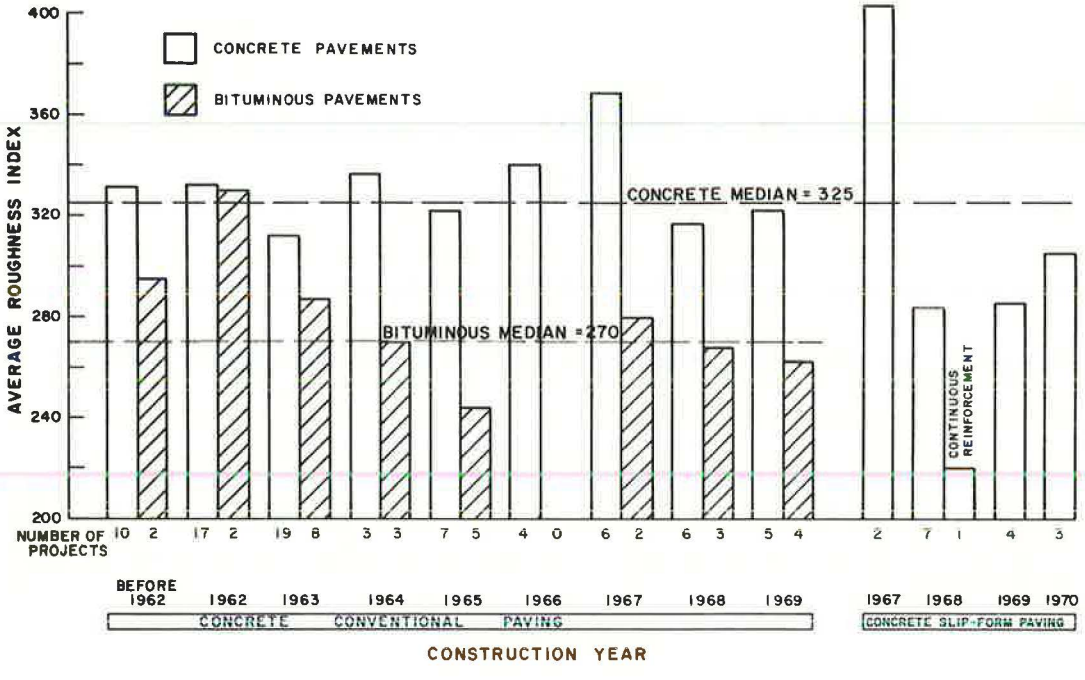

Table 2. Roughness of resurfaced flexible pavements.

Item	Before Resurfacing			After Resurfacing		
	Number of Projects	Avg Years in Service	Avg RI	Avg RI	Avg RI Improvement (percent)	Avg Annual RI Change Since Resurfacing (percent)
RI Range						
900	2	Unknown	942	538	43	0.9
800-900	4	9	819	456	44	2.3
700-800	9	11	744	489	34	1.8
600-700	8	12	658	425	35	3.2
500-600	6	11	566	392	31	3.7
Year Resurfaced						
1958	2	8	898	562	37	1.7
1959	3	9	745	485	34	2.4
1961	4	8	752	389	48	2.4
1962	5	11	718	500	30	0.6
1963	3	12	750	448	40	3.4
1964	3	12	585	437	25	6.3
1965	1	6	635	370	42	1.6
1966	6	13	662	442	33	3.1
1967	1	17	710	390	45	
1968	1	9	565	355	37	6.3
Avg		10.8	707	450	36	2.7

the year of resurfacing or the pavement was tested a year after resurfacing. Several pavements were excluded from consideration because the measurements were delayed by more than a year.

Criteria governing selection of the projects for resurfacing were not documented. Roughness data do suggest that strong consideration was given to pavement serviceability; and, of course, serviceability is foremost related to roughness. Figure 8 shows that the rougher pavements were generally chosen for resurfacing, and, in spite of ongoing deterioration of pavements with age, the remaining surfaces exhibited at least the same roughness as they did in the preceding years. The net result of resurfacing efforts on the subject pavements was a substantial improvement in ride quality by 1970. Although these pavements were not statistically chosen, they may be considered representative of the older, higher type of construction on U.S. and state routes. Therefore, a reasonably legitimate claim may be made that ride quality on most 2-lane highways in Kentucky has materially improved since 1957.

Roughness Inventory

The latest available test results for various highways are given in Table 3. Interstate highways and parkways had lower roughness indexes than other roads; however, ride quality of high-speed facilities diminished significantly when tested at the speed limit. In other words, a person traveling 70 mph (31 m/s) on an Interstate highway may experience more discomfort than he would traveling 50 mph (22 m/s) on a 50-mph (22-m/s) road.

Bituminous overlays on older surfaces have eliminated many of the very rough pavements in Kentucky. Only a few road sections in the current inventory had RI's higher than 600; in 1960 almost half of the projects monitored were rougher.

Service Roughness

After being tested for as-constructed roughness, each project was periodically retested to monitor changes in roughness during the life of the pavement. On Interstate, parkway, and other multilane roads, the outside lanes were usually tested. A cursory inspection of data indicated that increases in roughness were associated with time-dependent variables or influences. This increase was quantified and the contributing influences were identified by relating roughness to service period, cumulative traffic, and equivalent axle load. Cumulative traffic for a given lane was determined from lane distribution factors, average daily traffic, and the number of days the pavement was in service. EAL was calculated according to the modified AASHO procedures and traffic parameters developed by Deacon and Deen (9).

Roughness data for every Interstate highway and parkway project were plotted versus time in service, cumulative traffic, and EAL. Curves were manually fitted for all projects for which 4 or more roughness measurements were available. No attempt was made to delete any data, even though some roughness measurements were obviously in error when contrasted with measurements in preceding or subsequent years or both. A straight line was found to best describe the relations although there were notable exceptions. Computerized, linear regression analysis provided equations of best fit straight lines. Graphs of 6 bituminous pavements are shown in Figure 9 for illustration. Similar procedures and analyses were employed for bituminous concrete, bituminous overlays on bituminous base, and concrete pavements involving other high type of construction projects on U.S. and state highways. However, roughness data were related only to months in service and cumulative traffic.

The rate of increase in roughness, expressed here as the slope of regression lines, was different for each pavement type, as shown in Figures 10 through 16, and varied according to the original or as-constructed roughness of the pavement. Concrete pavements on Interstate highways and parkways deteriorated at a considerably lower rate than the bituminous pavements on the same type of facility. On bituminous pavements, the smoother constructed surfaces deteriorated more rapidly, with the exception of the 4-lane parkways. On the other hand, concrete pavements on U.S. and Interstate highways deteriorated more rapidly on projects where the constructed roughness was the highest. Here again, parkways exhibited opposite trends.

Figure 8. Average roughness index of bituminous pavements monitored since 1957.

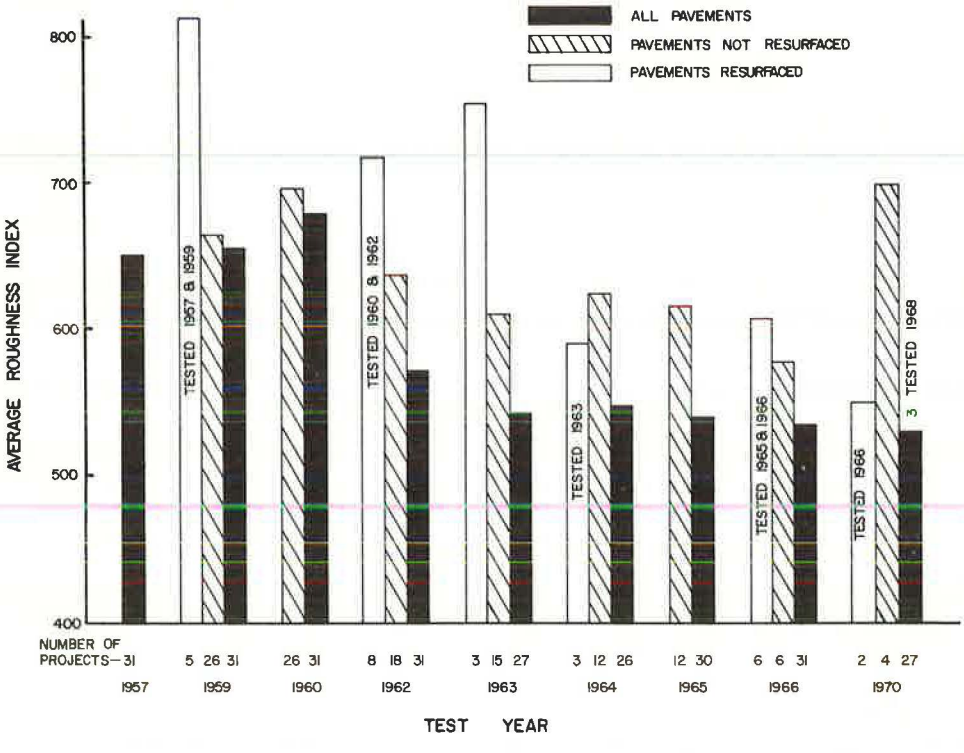

Table 3. Roughness of various highways.

Pavement	Highway	Number of Projects	Roughness Index		Equivalent, Median RI[a]	
			Median	Avg	60 mph	70 mph
Bituminous	Interstate	19	350	345		515
	Parkway	23	325	358		475
	U.S. and state	80	465	444	540	
Concrete	Interstate	58	350	354		435
	Parkway	36	345	357		430
	U.S. and state	18	440	457	495	

[a]Extrapolated from data shown in Figure 4.

Figure 9. Relation of roughness index and pavement age, cumulative traffic, and EAL for 6 bituminous Interstate projects.

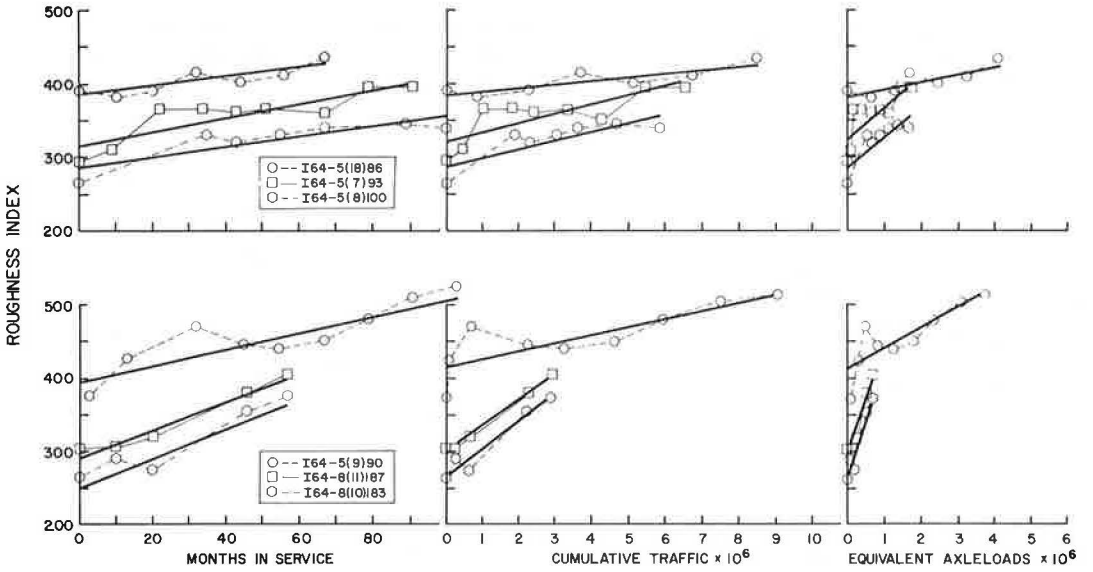

Figure 10. Combined regression equations relating roughness to age of bituminous pavements on Interstate highways.

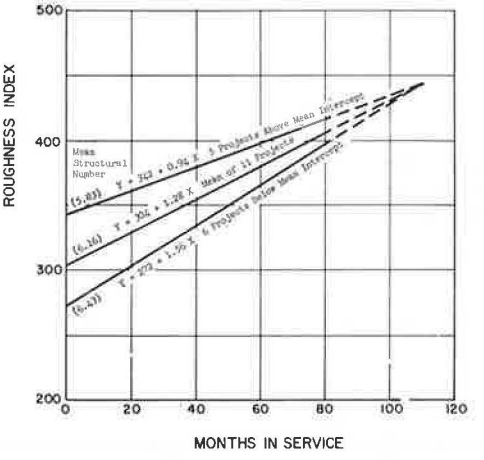

Figure 11. Combined regression equations relating roughness to age of bituminous pavements on 4-lane parkways.

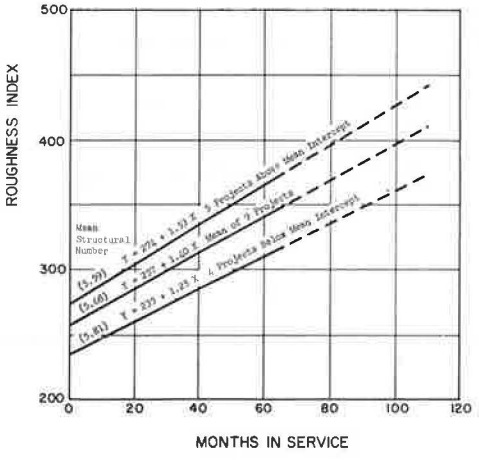

Figure 12. Combined regression equations relating roughness to age of concrete pavements on Interstate highways.

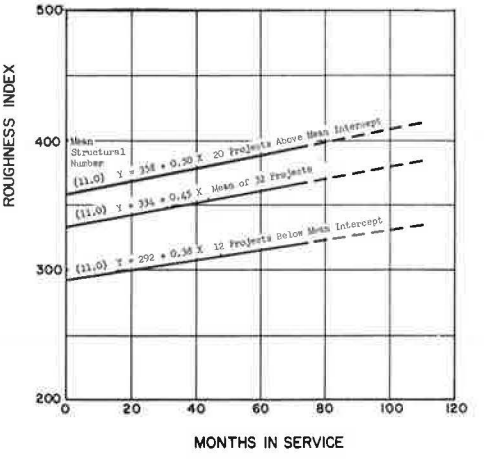

Figure 13. Combined regression equations relating roughness to age of concrete pavements on parkways.

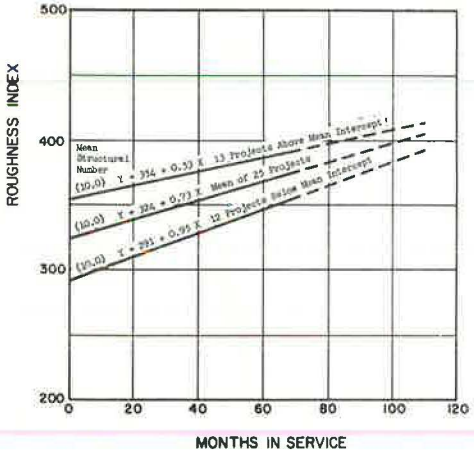

Figure 14. Combined regression equations relating roughness to age of concrete pavements on U.S. highways.

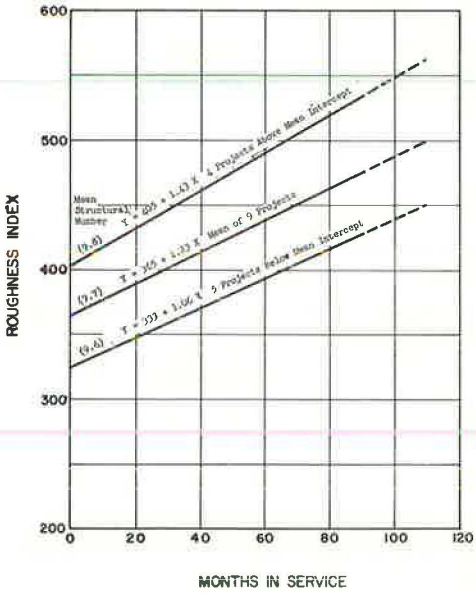

Figure 15. Combined regression equations relating roughness to age of bituminous pavements on U.S. and state highways.

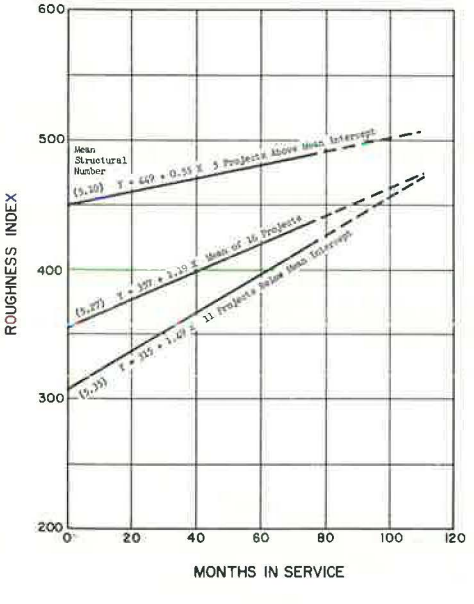

Figure 16. Combined regression equations relating roughness to age of bituminous resurfacing on U.S. and state highways.

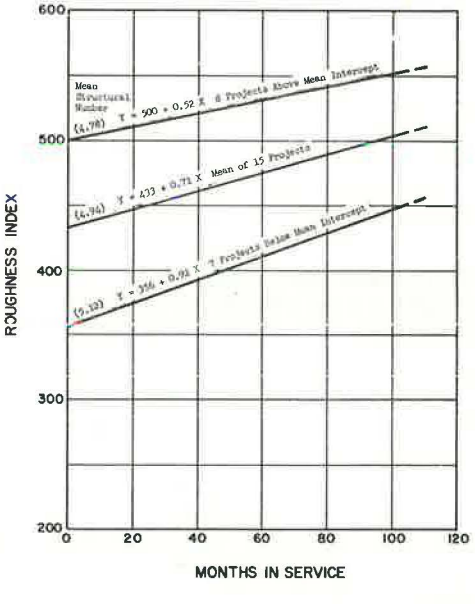

Structural numbers (SN) for bituminous pavements were calculated and ranged between 2.9 and 7.0. No conclusive evidence was found to suggest that the SN had a significant bearing on the rate of increase in roughness. An interesting trend, however, was noted between the magnitude of the as-constructed RI and SN when several bituminous projects for a given highway facility were combined. In every case, the smoother constructed pavements were associated with a higher structural number. Concrete pavements were designed with a fixed SN of 11 for Interstate highways. On U.S. highways, the SN was either 9 or 10. A definite trend of increasing roughness was noted as the structural number decreased.

Correlations between RI and service period, cumulative traffic, and EAL yielded equally valid statistical results (6). The contribution of traffic and loading to roughness, therefore, could not be isolated from service period. Each of the parameters was time dependent and correlated well with one another. Further consideration must be given to other unaccounted influences, such as rate of differential settlement and rutting, and the interrelations among parameters considered.

In general, pavements involving high type of construction do not exhibit rapid changes in roughness. For example, several bituminous pavements on I-64 and I-75 required resurfacing because of severe cracking in the surface course and significant depth of rutting in the wheelpaths. Yet, the RI of those projects had increased by only 50 to 145 above the as-constructed roughness. The level of service provided by these highways in regard to roughness, therefore, was foremost related to the as-constructed roughness of the pavements.

The pavement serviceability performance concept originated in conjunction with the AASHO Road Test. Determination of present serviceability index (PSI), a scalar expression of pavement condition, has continued on a limited basis for Interstate projects. The PSI can be obtained either directly from the roughness index by using appropriate regression equations or from roughness measurement and a survey of the pavement by quantifying the extent of major cracking, patching, and rutting depth. The choice as to which yields the proper expression of pavement serviceability has been of some concern. The PSI determined from RI alone was consistently higher. If the PSI is to be used as an expression of pavement condition, the better choice would be to use the equations that incorporate cracking, patching, and rutting. Although it can be argued that serviceability is important from the standpoint of the road user, insidious fatigue of the structure is not necessarily manifested in roughness or serviceability at the half-life stage. Fatigue is revealed only by breakup of the pavement. Therefore, if fatigue were the only factor affecting roughness, trend lines [for 18-kip (8,200-kg) axles] for all pavements considered would be horizontal; that is to say, none would show an increase in roughness. Therefore, any increasing roughness surely becomes attributable to other causes. The question then arises as to whether the available regression equations properly characterize high type of construction. A Purdue University study (10) considered test sections on primary and secondary roads, none of which was comparable to Interstate highways. Surely the pavement rater would apply somewhat different standards for those highways and would, therefore, rate them accordingly.

SUMMARY AND CONCLUSIONS

Accelerometer measurements of a passenger's torso, using the automatic roughness-measuring system, has been an invaluable tool in evaluating roughness of road surfaces in terms that are closely associated (here by inference only) with riding comfort. The test can be conducted at a speed that is compatible with the normal flow of traffic and, thereby, can be carried out with maximum safety to testing personnel. Test results are available immediately and are closely repeatable. Reasonably good long-term reproducibility of test results has been achieved through strict adherence to carefully developed procedures and practices. Replacement of test vehicles has not seriously detracted from continued data collection. The automobile as a testing device does present inherent deficiencies and limitations; and the measurements, in the form of either roughness index or an acceleration recording, do not fully characterize the pavement.

In general, bituminous construction has yielded smoother riding surfaces than con-

crete construction. No major improvements in workmanship were noted on bituminous pavements in Kentucky since 1962. The roughness of concrete pavements, however, was improved on those projects where slip-form paving was used. A pavement constructed in 1968 with continuous reinforcement and slip-form paving exhibited especially excellent ride quality and may be indicative of results from similar construction in the future. Interstate highway and parkway construction continues to yield smoother pavements than other major construction. These comparisons, of course, are valid only for the same speed of travel, for the tests were conducted at 51.5 mph (23 m/s). However, roughness was found to be related to vehicle speed; and when consideration was given to actual travel speed, such as 70 mph (31 m/s) on Interstate highways and parkways and 50 mph (22 m/s) on other highways, the ride quality became significantly degraded on the higher speed facilities and greatly offset cited improvements. Assessments and requirements for pavement roughness, therefore, must be coupled with due consideration to the anticipated speed of travel for each highway facility.

Bituminous overlaying of the older surfaces has eliminated most of the very rough pavements. As a result of these resurfacing efforts, a reasonably valid claim may be made that the ride quality on most primary, 2-lane highways has materially improved since 1957 in spite of the ongoing deterioration of pavements with age, increased traffic, and vehicle loads.

The rate of deterioration in roughness was found to be different for each pavement type and varied according to the original or as-constructed roughness of the pavement, structural number, and type of highway facility involved. Concrete pavements on Interstate highways and parkways deteriorated at a considerably lower rate than bituminous pavements on the same facilities. An interesting trend was found between as-constructed roughness, structural number, and rate of pavement deterioration. On Interstate highways, the smoother constructed surfaces of bituminous pavements deteriorated more rapidly, while the rougher surfaces of concrete pavements deteriorated more rapidly. Completely opposite trends, however, were realized on parkways. For a given highway facility involving bituminous construction, the lower original roughness indexes were associated with those projects where the structural numbers were higher. A definite trend to increased roughness was noted for concrete pavements as the structural number decreased.

The correlations between roughness index and service period, cumulative traffic, and EAL were valid. The contribution of traffic or loading to roughness, therefore, could not be isolated from service period. Each of the parameters was time dependent and correlated well. Further consideration must be given to other unaccounted influences, such as rate of differential settlement and rutting, and the interrelations among parameters considered. Refined measurement of pavement roughness and improved information on volume, distribution, and composition of traffic may be needed to clearly identify those elements that cause pavements to become rougher.

Pavements involving high type of construction generally do not exhibit rapid changes in roughness. The level of service provided by these highways in regard to roughness, therefore, is foremost related to the as-constructed roughness of the pavement. Clearly then, every effort should be pursued to construct the smoothest possible surfaces. Other considerations such as structural adequacy of the total pavement system, structural integrity of the surface course, and slipperiness will primarily dictate the need for resurfacing.

ACKNOWLEDGMENTS

The work reported in this paper was done by the Kentucky Department of Transportation in cooperation with the Federal Highway Administration. The contents of this paper reflect the views of the authors and not necessarily the official views or policies of the agencies involved.

REFERENCES

1. Gregg, L. E., and Foy, W. S. Triaxial Acceleration Analysis Applied to the Evaluation of Pavement Riding Qualities. HRB Proc., Vol. 34, 1955, pp. 210-223.

2. Foy, W. S. Analysis of Pavement Ride Quality. Kentucky Department of Highways, Nov. 1956.
3. Rizenbergs, R. L. Analysis of Pavement Roughness. Kentucky Department of Highways, March 1961.
4. Rizenbergs, R. L., and Havens, J. H. Pavement Roughness Studies. Kentucky Department of Highways, April 1962.
5. Rizenbergs, R. L. Accelerometer Method of Riding Quality Testing. Kentucky Department of Highways, Feb. 1965.
6. Rizenbergs, R. L., Burchett, J. L., and Davis, L. E. Pavement Roughness: Measurement and Evaluation. Kentucky Department of Highways, Dec. 1971.
7. Magan, K. P. Slip-Form Paving. Kentucky Department of Highways, Feb. 1970.
8. Drake, W. B., and Havens, J. H. Kentucky Flexible Pavement Design Studies. Eng. Exp. Station, Univ. of Kentucky, Bull. 52, June 1959.
9. Deacon, J. A., and Deen, R. C. Equivalent Axle Loads for Pavement Design. Highway Research Record 291, 1969, pp. 133-143.
10. Yoder, E. J., and Milhous, R. T. Comparison of Different Methods of Measuring Pavement Condition. NCHRP Rept. 7, 1964.

EFFECT OF ROAD ROUGHNESS ON VEHICLE STEERING

B. E. Quinn, Purdue University; and
S. E. Hildebrand, International Harvester Company

The roughness of a pavement influences the steering behavior of a vehicle by producing variations in the normal forces between the tires and the pavement that in turn affect the lateral forces needed to control the vehicle. A simple mathematical model of a passenger car is used to compute the position of the car relative to a set of axes fixed in the pavement as the vehicle executes different maneuvers. Pavement roughness is introduced indirectly by using, as inputs to the model, the actual normal tire forces that were measured experimentally on a smooth and a rough pavement. For vehicle paths having large radii of curvature and for low vehicle velocities, the lateral forces required to control the vehicle are relatively small. Under these conditions pavement roughness is relatively unimportant. For vehicle paths having small radii of curvature and for high vehicle velocities, the required lateral forces can be quite high. Developing these forces may not be possible if the pavement is too rough, and this can cause loss of control of the vehicle. Such a condition may exist on a rough road when an overtaking vehicle changes lanes at a high velocity to pass a slower vehicle and then is suddenly forced to return to the original driving lane because of oncoming traffic. Safe vehicle handling can thus be adversely influenced by pavement roughness.

•MANY FACTORS influence the steering behavior of a vehicle. In designing the vehicle the manufacturer makes decisions relative to the length of the wheelbase, the steering linkage geometry, and other properties that influence the handling characteristics of the car. In addition, the tire manufacturer imparts certain properties to the tire that will greatly affect the steering characteristics. One such property, the cornering stiffness of the tire, is of considerable importance in the study of vehicle steering characteristics. Moreover, the driver can also influence the behavior of the vehicle by deciding how the vehicle is to be loaded. Different steering characteristics will be produced if a large proportion of the vehicle weight is on the rear tires than if the same proportion of weight is on the front tires. The characteristics of the pavement on which the vehicle is operated will also influence the handling of the vehicle. If the pavement is very slippery, it may be quite difficult to control the vehicle.

The property of the pavement of primary concern in this paper is that of the pavement roughness, which imparts a vertical motion to the vehicle tires and is independent of the slipperiness of the pavement. The task of providing a vehicle with safe handling characteristics is thus the responsibility of many groups. This paper is primarily concerned with pavement roughness as a factor influencing safe vehicle handling characteristics.

LATERAL TIRE FORCES

Lateral tire forces are needed to control the motion of a vehicle. These are the forces that act on the tread of the tire parallel to the surface of the road and at right angles to the wheel plane. Figure 1 shows a top view of a wheel moving in the direction

Publication of this paper sponsored by Committee on Surface Properties-Vehicle Interaction.

shown by the arrow. It should be noted that the direction of motion is not parallel to the wheel plane but is rather at the angle α, which is indicated as the slip angle.

As a consequence of this motion, a lateral force is developed on the tire. This is a horizontal force exerted by the road on the tire perpendicular to the plane of the wheel for the motion as indicated. The magnitude of this force depends on the slip angle α and the normal force. In general this is a nonlinear relation.

Figure 1 does not show the normal tire force. This force would be acting on the bottom of the tire and is perpendicular to the plane of the paper.

The relation among the normal force, the lateral tire force, and the slip angle for a typical tire is shown in Figure 2 in which the lateral force is plotted as a function of normal force for various slip angles. Information of this type is obtained experimentally and is usually shown in the form of carpet plots (1) rather than as in Figure 2.

In obtaining the information shown in Figure 2, a flat surface representative of a pavement is used. A reasonable coefficient of friction exists between the tire and the flat surface. The effect of a slippery pavement would be to greatly reduce the lateral forces that can be developed for a given normal force and a given slip angle. In this paper it is assumed that slipperiness is not a factor in the behavior of the vehicle.

Of particular interest is the nonlinear relation shown in Figure 2. For a normal force of 1,000 lb and a slip angle of 6 deg, the corresponding lateral force is 760 lb. If the normal force is reduced by 300 lb, the lateral force is reduced by 160 lb. If, however, the normal force is increased by 300 lb, the lateral force is only increased by 140 lb.

This observation is of utmost importance because it means that, if the normal force fluctuates, the resulting average value of the lateral force for an average value of 1,000 lb will not be 760 lb but less.

Figure 2 shows the mechanism whereby pavement roughness influences the ability to control a vehicle. Pavement roughness causes variations in the normal tire force. On a relatively smooth pavement these variations are very small, but on a rough pavement these variations can be quite large. The net result as far as the lateral force is concerned is that there is a reduction in the average value of the lateral force available to control the vehicle. For those situations in which large lateral forces are necessary, this loss of force may mean loss of control of the vehicle.

The mechanism shown in Figure 2 is important for 2 reasons: It provides an explanation for the loss of lateral force when there is a variation in the normal tire force, and it provides a basis for defining the following 3 terms in a theoretical context.

1. Rough road is a road that causes a variation in the normal tire forces (and consequently a variation in the lateral forces).
2. Road having no roughness is a road that does not cause any variation in the normal tire forces (the normal tire forces are always equal to the static wheel loads) but that has a coefficient of friction such that the lateral forces shown in Figure 2 can be developed.
3. Slippery road is a road having a low coefficient of friction such that the lateral forces shown in Figure 2 cannot be developed.

From a practical viewpoint a road having no roughness does not exist, but this concept is useful in theoretical studies.

PREDICTING VEHICLE BEHAVIOR

The problem of predicting vehicle-handling characteristics has been of great concern to the automotive industry. Not only normal steering characteristics but also problems dealing with instability have been studied. Milliken (2), Bundorf (3), and many others have done research in this area. Various mathematical techniques have been developed, and mathematical vehicle models of varying degrees of complexity have been employed.

In this investigation a very simple model of the vehicle, known as the bicycle model (4), was employed. In this model, shown in Figure 3, the 2 front wheels of an automobile have been replaced by a single wheel and the 2 rear wheels have also been replaced

Figure 1. Tire slip angle.

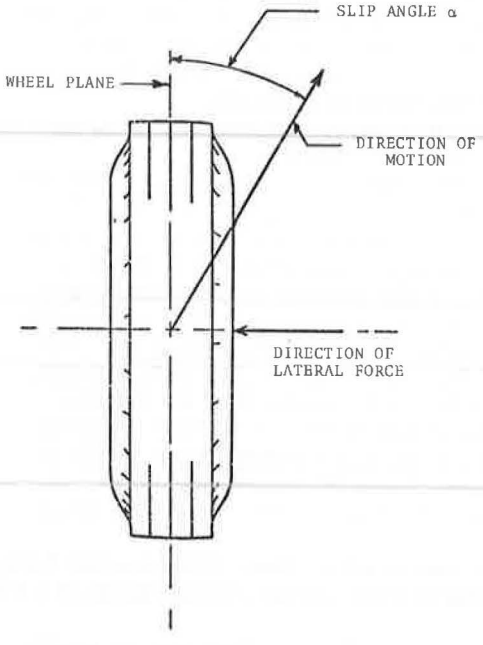

Figure 2. Tire force characteristics.

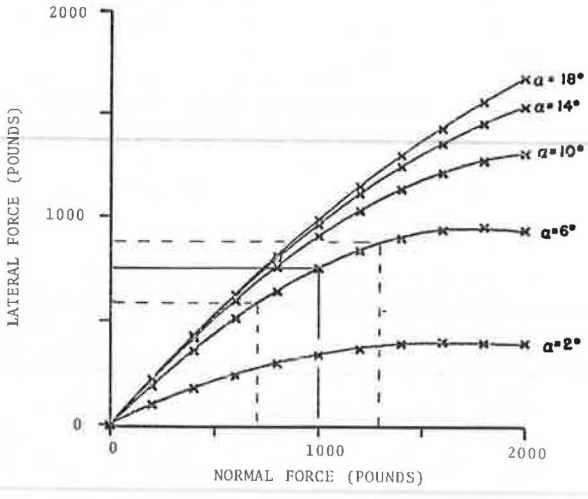

Figure 3. Bicycle model of automobile.

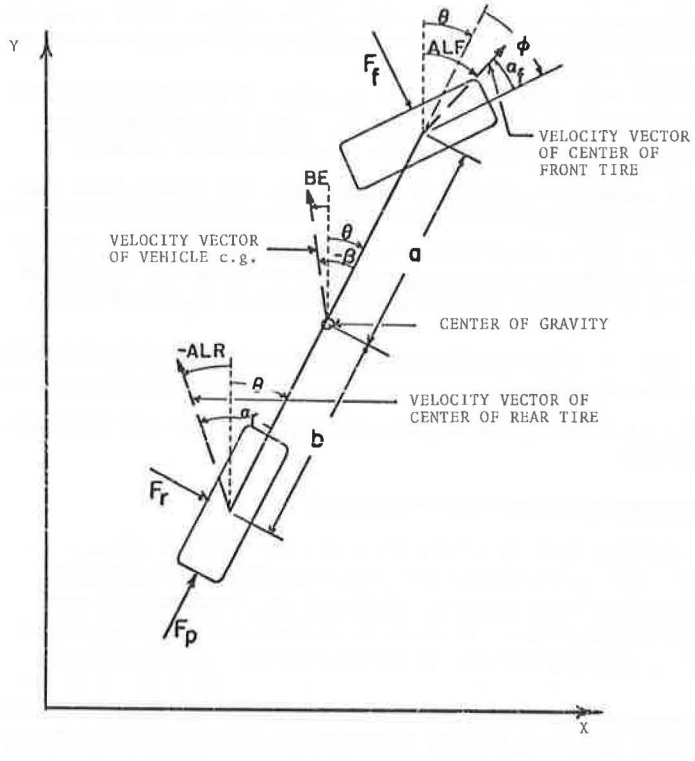

by a single wheel. The single front tire is therefore assumed to have the property of the 2 front tires on the actual vehicle, and the single rear tire is assumed to have the properties of the 2 rear tires.

In this model the wheelbase is the same as in the actual vehicle. The same weight is used, and the fore and aft location of the center of gravity is the same as in the prototype vehicle. In addition, the mass moment of inertia about a vertical axis through the center of gravity and perpendicular to the plane of the paper (Fig. 3) is assumed to be the same as that of the actual vehicle.

The use of this model immediately imposes limitations on the quantities that can be considered. Using this simple model makes it impossible to include the effect of pitching of the vehicle or to consider any of the riding qualities.

Moreover, no rolling of the actual automobile can be considered, and thus the transfer of load from the inner to the outer wheels cannot be introduced in a model of this simplicity. In brief, the effects of the suspension system of the vehicle cannot be taken into account with this model as it is normally employed.

This model does permit a consideration of yaw (rotation about an axis perpendicular to the paper as shown in Figure 3). In addition it is possible to consider the x and y locations of the center of gravity of the model relative to a set of X and Y axes that are always fixed in the pavement. It is possible to compute the coordinates of the path of the center of gravity of the vehicle and to compute the angular position of the vehicle relative to the axes. In brief, the motion of the vehicle as seen from above can be approximated by using this technique.

The derivation of the equations necessary for making these calculations is given in the Appendix.

The question may be asked as to how the effect of pavement roughness can be introduced when such a simple model is employed, particularly since it is impossible to introduce a road profile into the calculations because neither the springs nor the shock absorbers of the suspension system are included.

In this investigation the effect of road roughness was introduced in the following manner. The dynamic tire forces (normal forces) were measured experimentally by using an actual passenger vehicle operated over both a rough and a smooth road at various speeds. These normal tire forces were obtained as time-varying quantities.

The equations given in the Appendix were solved numerically by using time as the independent variable. The time was increased by small increments, and at each interval of time it was necessary to obtain values for the lateral forces at the front and back wheels. Because the normal tire forces were available as functions of time, it was possible to obtain values for these forces from the available records. Having these normal forces and knowing the slip angles, it was then possible to compute the corresponding lateral forces from the tire characteristics shown in Figure 2. The x and y coordinates of the center of gravity and the corresponding angular position θ of the vehicle were then computed. In all cases the vehicle speed was maintained at a constant value during the maneuver.

The smooth road used in this investigation had a BPR roughometer rating of 62 in./mile, and the rough road had a BPR roughometer rating of 122 in./mile.

EFFECTS OF PAVEMENT ROUGHNESS

To summarize the effects of pavement roughness on the steering properties of a vehicle is difficult. This is because the resulting motion of a vehicle can be quite complex, and no simple criteria are available for discussing whether the vehicle has satisfactorily executed a particular maneuver. Because of this difficulty, results are depicted in different ways in an attempt to describe the effect of pavement roughness on the vehicle-handling characteristics.

Step-Steer Input

One way of evaluating vehicle steering behavior is to subject the vehicle to identical steering conditions for pavements having different amounts of roughness. Accordingly, the steer angle of the vehicle (see Appendix) was suddenly increased at $x = 0$, $y = 0$, and

Figure 6. Effect of roughness on vehicle path at 30 mph.

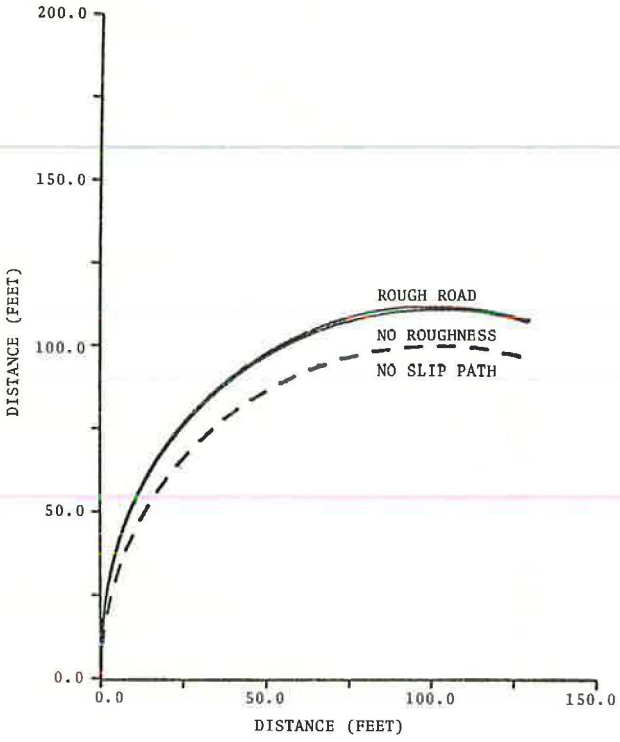

Figure 7. Effect of roughness on vehicle path at 50 mph.

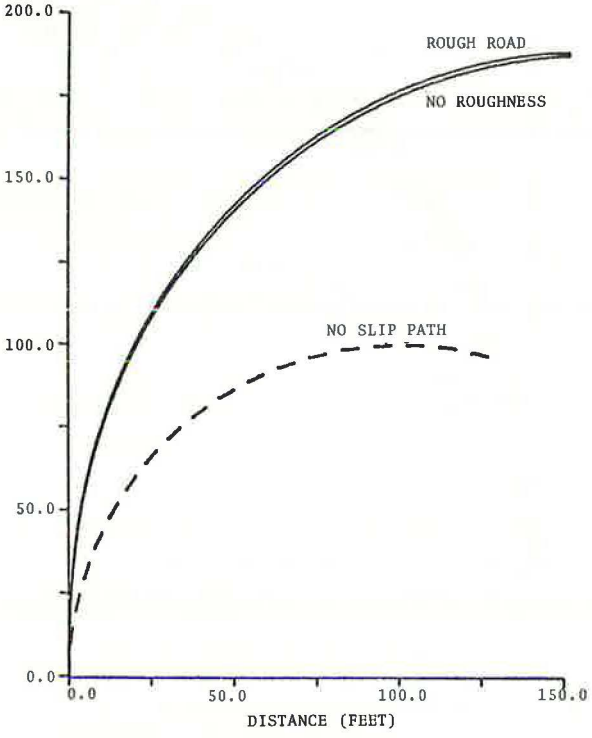

Lane-Change Maneuver

In the previous figures, a constant steer angle was used to control the vehicle. At this point a different approach is taken. In the work that follows, the path that the vehicle is to travel is specified, and the steer angles necessary to accomplish this maneuver are computed together with the associated sideslip angles. This is a more complex condition and requires a modification of the techniques used for solving the equations given in the Appendix. These details will be omitted, however, in the interest of brevity.

If a path is selected for a vehicle to follow, there will be a theoretical relation between the steer angle and the position of the vehicle on the path. If the vehicle moves at very low velocities and the steer angle is varied in the theoretical fashion, the center of gravity of the vehicle will follow the desired path. As the speed of the vehicle is increased, it is necessary to change the steer angle at different points along the path in order to develop the necessary lateral forces to keep the vehicle moving in the desired path. Under certain circumstances, it is possible that no value of the steer angle will produce lateral forces sufficient to control the vehicle in the desired manner. When this point is reached, it is assumed in this investigation that control of the vehicle has been lost, and the calculations are not continued beyond this point.

The sideslip angle is another criterion for evaluating the behavior of a vehicle during a maneuver. As shown in Figure 3, this is the angle between the centerline of the vehicle and the velocity of the center of gravity. When this angle is equal to 0 deg, the vehicle is pointed in the direction that the center of gravity is moving; when this angle is equal to 90 deg, the vehicle is sliding sideways. Figure 5 shows a situation in which the sideslip angle becomes excessive.

For the maneuvers shown in Figures 8 and 9, the sideslip angles are compared with those that would exist if these maneuvers were executed at very low velocities.

Consider the lane-change maneuver shown in Figure 8. This occurs when a vehicle overtakes a slower moving vehicle and swings out in the adjacent lane to pass. The following equation was used to describe the desired path:

$$y = A \tan^{-1} (x/B)$$

where

x = x coordinate of path, ft; and
y = y coordinate of path, ft.

The constants A and B can be varied to change the severity of the maneuver. For this analysis, A was set equal to 4 ft and B was set equal to 30 ft.

The broken-line curves shown in Figure 9 indicate the values for the steer angle and the sideslip angle that are required for the vehicle to follow the path shown in Figure 8 at a very low velocity and with no variation in the normal tire forces (no pavement roughness).

When this maneuver is executed at 30 mph on the smooth pavement section, the required steer angles and sideslip angles are virtually identical to those obtained for a very low velocity and no pavement roughness.

When the rough pavement section is considered, the associated steer angles and sideslip angles are indicated by the solid lines shown in Figure 9. At 30 mph on the rough pavement, there is virtually no difficulty encountered in executing the passing maneuver. The same can be said, of course, for the smooth pavement.

Ninety-Degree Turn

Another common maneuver required in highway driving is that of going around a turn of changing radius. The desired path is shown in Figure 10 and is described by the following equation:

$$y = k/x$$

Figure 11. Ninety-degree turn on smooth road at 30 mph.

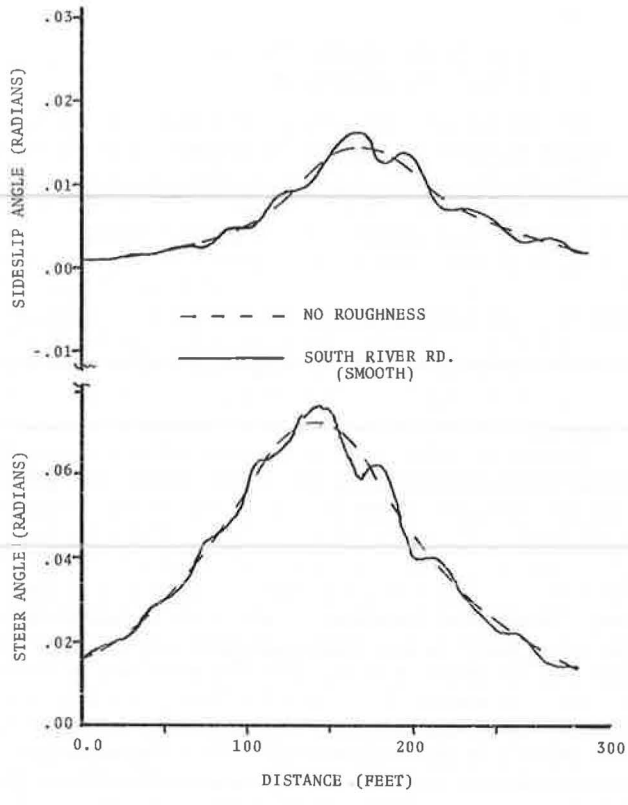

Figure 12. Ninety-degree turn on rough road at 30 mph.

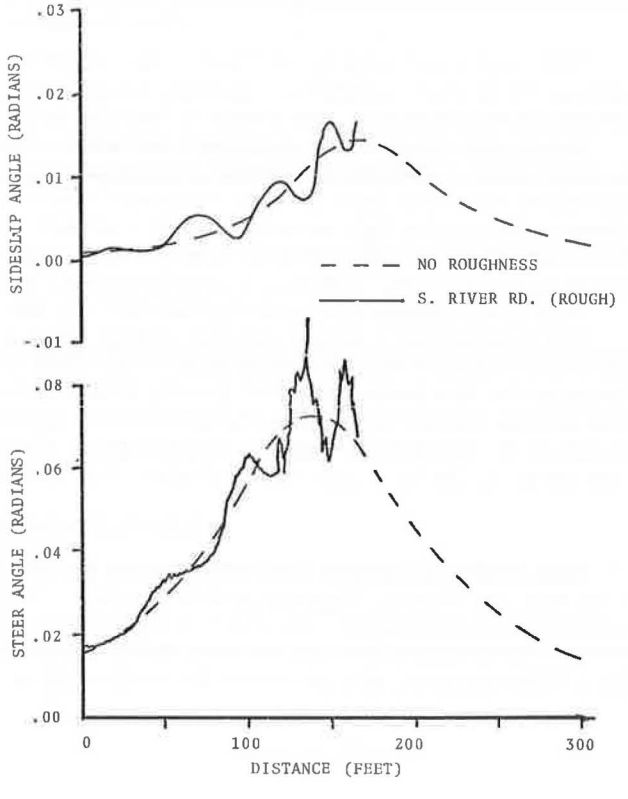

REFERENCES

1. Nordeen, D. L., and Cortese, A. D. Force and Moment Characteristics of Rolling Tires. SAE, Paper 713A, 1963.
2. Milliken, W. F., Jr., Whitcomb, S. W., Segel, L., et al. Research in Automobile Stability and Control. Institution of Mechanical Engineers, London, 1956.
3. Bundorf, R. T. The Influence of Vehicle Design Parameters on Characteristic Speed and Understeer. SAE, Paper 670078, 1967.
4. Bundorf, R. T. A Primer on Vehicle Directional Control. General Motors Technical Center, Warren, Mich., Publ. A-2730, 1968.
5. James, M. L., Smith, G. M., and Wolford, J. C. Analog and Digital Computer Methods in Engineering Analysis. International Textbook Co., 1964, p. 344.
6. Quinn, B. E., and Hildebrand, S. E. The Effect of Pavement Roughness on Safe Vehicle Handling Characteristics. Purdue Univ., Lafayette, Ind., 1972.
7. Quinn, B. E., and Sattaripour, A. Measurement and Prediction of the Dynamic Tire Forces of a Passenger Vehicle on a Highway. Purdue Univ., Lafayette, Ind., 1972.

APPENDIX

DERIVATION OF MATHEMATICAL MODEL OF VEHICLE FOR STEP-STEER INPUT

Figure 3 shows the bicycle model of an automobile and the forces acting upon it in the x-y plane. The position of the vehicle is described by the x and y coordinates of the center of gravity, and the orientation of the vehicle is described by the absolute angular rotation θ. The variables shown in Figure 3 are defined as follows:

a = distance from vehicle center of gravity to front tire;
b = distance from vehicle center of gravity to rear tire;
F_f = front tire lateral force;
F_r = rear tire lateral force;
F_p = rear tire propulsion force;
x = abscissa of vehicle center of gravity;
y = ordinate of vehicle center of gravity;
θ = angle between +y axis and vehicle centerline measured clockwise;
ϕ = steer angle measured clockwise from vehicle centerline to centerline of front tire;
ALF = angle measured clockwise between +y axis and velocity vector of front tire;
ALR = angle measured clockwise between +y axis and velocity vector of rear tire;
α_f = front tire slip angle;
α_r = rear tire slip angle;
BE = angle measured clockwise between +y axis and velocity vector of vehicle center of gravity; and
β = vehicle sideslip angle.

Because the position of the center of gravity of the vehicle is determined by the coordinates x and y and the angular orientation of the vehicle is determined by the angle θ, then

$\dot{x}$ = velocity of vehicle center of gravity in +x direction,
$\dot{y}$ = velocity of vehicle center of gravity in +y direction, and
$\dot{\theta}$ = angular velocity of vehicle.

Let

$\dot{x}_f$ = velocity of front tire in +x direction, and
$\dot{y}_f$ = velocity of front tire in +y direction.

From examination of Figure 3,

$$\dot{x}_f = \dot{x} + a\,\dot{\theta}\cos(\theta)$$
$$\dot{y}_f = \dot{y} - a\,\dot{\theta}\sin(\theta)$$

Also,

$$ALF = \tan^{-1}(\dot{x}_f/\dot{y}_f) \tag{1}$$

Therefore,

$$ALF = \tan^{-1}\left[\frac{\dot{x} + a\,\dot{\theta}\cos(\theta)}{\dot{y} - a\,\dot{\theta}\sin(\theta)}\right] \tag{2}$$

Similarly,

$$ALR = \tan^{-1}\left[\frac{\dot{x} - b\,\dot{\theta}\cos(\theta)}{\dot{y} + b\,\dot{\theta}\sin(\theta)}\right] \tag{3}$$

Also,

$$BE = \tan^{-1}(\dot{x}/\dot{y}) \tag{4}$$

The sum of the forces acting on the vehicle in the +x direction equals the product of the mass of the vehicle and the component of acceleration of the vehicle center of gravity in the +x direction.

$$\Sigma F_x = M\,\ddot{x} \tag{5}$$

or

$$F_f\cos(\theta + \phi) + F_r\cos(\theta) + F_p\sin(\theta) = M\,\ddot{x} \tag{6}$$

The sum of the forces acting on the vehicle in the +y direction equals the product of the mass of the vehicle and the component of acceleration of the vehicle center of gravity in the +y direction.

$$\Sigma F_y = M\,\ddot{y} \tag{7}$$

or

$$-F_f\sin(\theta + \phi) - F_r\sin(\theta) + F_p\cos(\theta) = M\,\ddot{y} \tag{8}$$

The sum of the moments acting on the vehicle about the center of gravity equals the product of the moment of inertia of the vehicle and its angular acceleration.

$$\Sigma M_{c.g} = I\,\ddot{\theta} \tag{9}$$

or

$$a\,F_f\cos(\phi) - b\,F_r = I\,\ddot{\theta} \tag{10}$$

In order for the vehicle to move at constant speed, the acceleration of the center of gravity of the vehicle in the direction of the velocity vector of the center of gravity must equal 0. For this to be true, the sum of the forces acting on the vehicle in this direction must equal 0.

$$F_p\cos(\beta) - F_r\sin(-\beta) - F_f\sin(\phi - \beta) = 0 \tag{11}$$

$$F_p = \frac{F_r \sin(-\beta) + F_f \sin(\phi - \beta)}{\cos(\beta)} \tag{12}$$

The lateral tire forces F_f and F_r are determined from α_f, α_r, and the normal tire forces by using the tire characteristics as shown in Figure 2. Because each tire used in this model replaced 2 tires on an actual vehicle, it is necessary to double the lateral tire force obtained from the tire characteristic curves.

The tire slip angles α_f and α_r can be determined as follows (Fig. 3):

$$\alpha_f = \theta + \phi - \text{ALF} \tag{13}$$

$$\alpha_r = \theta - \text{ALR} \tag{14}$$

Because of the nonlinearities involved in these equations, a numerical technique was used to obtain a solution.

Various numerical methods for solving equations of this type are available (5), and further details of solution are omitted in this paper.

EFFECT OF ROAD ROUGHNESS ON VEHICLE BRAKING

J. C. Wambold, A. D. Brickman, and W. H. Park, Pennsylvania State University; and J. Ingram, Rex Chainbelt, Inc.

The loss of tire braking friction due to road roughness was simulated and measured experimentally in a test machine designed to produce simultaneous wheel slip and vertical vibration of the contact surface. Equivalent roughness amplitudes as great as 0.7 in. and roughness frequencies (velocity/wavelength) as high as 14 Hz were covered. Wheel slip was varied by discrete amounts to include the values normally associated with maximum friction. The dynamic friction force found in each test run was time-averaged and expressed as a percentage of the highest observed average to minimize the effects of temperature, surface conditions, and other secondary considerations. Results show simulated roughness amplitude and frequency to have a strong influence on the average force available for braking: Friction losses were 30 percent at 0.04 in. and 14 Hz, and 90 percent at 0.71 in. and 6 Hz. Wheel slip and the dead-weight load on the tires were found to have a less dramatic effect over the range tested. The most important conclusion reached is that friction predictions without road profile consideration can result in gross errors and may be one of the causes of lack of correlation of friction data.

•WITH THE exception of the body aerodynamic resistance, all other forces necessary for accelerating, braking, and steering a moving automobile depend on tire friction. Friction force is relatively large on a smooth, dry, plane pavement, but may be reduced on an uneven and undulating pavement. On a washboard road containing numerous holes and ruts that cause wheels to bounce and chatter, the accompanying loss of traction can be readily observed as the vehicle's brakes are applied without producing any noticeable deceleration.

Recent papers on tire friction indicate that most investigations focus on the microsurface structure of the pavement, that is, its texture and the polishing of the texture asperities. No work has been found that deals with effects of road roughness on tire friction, where road roughness refers to roughness amplitudes on the order of 1 in. and larger (what one feels as "roughness" when riding in a car).

This paper is concerned with the effects of bulk road roughness on the frictional forces developed by a tire operating in a slipping mode. A stationary test apparatus was employed to produce controlled sliding of a rotating tire against a vertically oscillating metal plate, simulating a tire operating under brake slip on a rough road. Tests were run over a range of 5 roughness amplitudes (0.041 to 0.707 in.) and a range of 10 roughness frequencies (0 to 14 Hz). Three measured sliding speeds—0.18, 0.30, and 0.46 mph—were tested that result in actual sliding speeds near and above the critical sliding speed of 0.1 mph at which the adhesion peak occurs.

The frictional force produced by the tire slipping against the plate was measured by a quartz load cell. The proportional output voltage was then averaged with an analog circuit and read from a digital voltmeter. The average normal force between tire and plate was measured by a strain gauge load cell. For a given roughness amplitude and normal preload, the average normal force was found to be essentially constant over the range of tested frequencies.

Publication of this paper sponsored by Committee on Surface Properties-Vehicle Interaction.

The smallest amplitude of 0.041 in. produced a traction loss of about 30 percent at 14 Hz, and the largest tested amplitude of 0.707 in. produced traction losses greater than 80 percent at about 6 Hz, the exact values depending on the normal preload and sliding speed.

For larger amplitudes, the average deformation slip increased as the amplitude increased. This means that the average actual sliding speed decreased to a much lower value than the critical speed with the result that the frictional force decreased to a much lower value. On the other hand, the effects of increasing frequency at even relatively small amplitudes reduced the frictional force over the entire range of sliding speeds, the critical speed included.

To explain these conclusions, we briefly review the details of rubber friction.

RUBBER FRICTION

Rubber friction is a complicated viscoelastic process in which the friction force depends not only on the surface but also on load, temperature, and velocity (1). The total friction force developed by a tire slipping on a road surface is generally considered to be the result of 4 contributing factors: adhesion, hysteresis, tearing, and wear. The last 2 make very minor contributions compared to the first 2 and may, therefore, be neglected in most cases (2).

The 2 primary friction mechanisms, adhesion and hysteresis, appear to be different manifestations of the same basic energy dissipation process. The adhesion mechanism may be summarized as the component due to the shearing of molecular junctions at the tire-pavement interface. The hysteresis component is due to the "plowing" of the asperities of the rigid pavement surface through the soft rubber. On dry surfaces under normal conditions the adhesion mechanism is dominant, and hysteresis plays only a minor role. [A more detailed explanation of the friction mechanisms is given by Kummer and Meyer (3).]

For any given tire-pavement combination, there exists a particular sliding speed that produces the maximum possible traction force (Fig. 1). This sliding speed is called the critical sliding speed and has been experimentally determined to be on the order of 0.1 mph (3). Its exact value is influenced by rubber composition, surface parameters, and temperature.

The adhesion component, under normal conditions, provides the contol needed for braking, accelerating, and cornering because it increases rapidly to a high value in a sliding speed range (up to 0.1 mph) without producing noticeable vehicle drift speeds (3). Although the tire has to slip to develop this adhesion force, the slip speed necessary to produce a large friction force is small enough that there is no noticeable loss of control.

SLIDING SPEED

Of most importance is the actual sliding speed—the component of the tread speed tangential to the surface. However, because the tread elements in the contact area are distorted and undergo deformation slip (3), the actual sliding speed in the contact area is very difficult to measure; thus, "measured" sliding speed is commonly used. The measured sliding speed of the tire would be equal to the actual sliding speed if the tread elements in the rubber-pavement contact area were undistorted. In this paper "slip speed" refers to measured slip speed unless otherwise noted.

TEST APPARATUS

A detailed discussion of the test machine and its specifications and components is given by Leary (4). This paper describes only the machine's operational features.

The test machine is an uncomplicated, stationary piece of equipment capable of achieving the same relative velocity between the wheel and a simulated road surface that a given vehicle velocity and measured percentage of slip produce in the real case. This is accomplished by loading a rotating tire down against a vertically oscillating metal plate. (Figure 2 shows a schematic diagram of the test machine's important moving parts.) The rotation of the tire results in a relative sliding speed between the

tread elements and the surface, while the vertical displacement of the plate simulates road roughness.

The tire is connected to a rotating axle that is restrained from any type of translational movement. Thus, effects on the tire load from the spring, shock absorber, and body mass are eliminated. All deflection produced by the vertical displacement of the table (metal plate) occurs in the tire. The amplitude of displacement of the table can be varied in 36 steps from 0 to 1 in. by changing an eccentric. The speed of the tire surface (the measured sliding speed) can be varied from 0 to 0.46 mph by adjusting the rpm of the dc motor that drives the wheel. Table oscillation frequency can be varied from 0 to 30 Hz. The tire is loaded against the table by an air cylinder to normal loads of 600 lb.

The instrumentation system employed monitors both the vertical normal force and the horizontal friction force. A strain gauge network in combination with an amplifier supplies an output voltage proportional to the normal load between the tire and the table. A quartz load cell in combination with a charge amplifier produces a voltage proportional to the horizontal friction force developed by the tire sliding against the table surface. Figure 3 shows the tire, table, load cell, and one of the strain-gauge-instrumented table support struts.

Because the 2 output voltages corresponding to the horizontal and normal forces in their unaltered forms vary periodically with time (Fig. 4), a small analog computer was used to time-average the 2 signals. The average values of normal and horizontal voltages obtained are then used as the inputs to a digital computer program that converts the voltages to pounds and calculates or plots the friction coefficients and percentage loss of friction.

The goal of this study was to investigate effects of road roughness on tire friction only; changes in frictional performance due to temperature and humidity were eliminated by normalizing all coefficients of friction in each group. All tests were made with a layer of water on the plate to reduce the temperature rise due to frictional heating and to reduce tire wear. In tests run earlier with both tire and plate dry, severe heating was noted and a sheet of rubber remained on the plate after the tire was raised. The water-film effects on traction are not at all like those on a real highway. In the real case, the slipping tire rotating at near vehicle speed is continuously moving forward on the film. On the machine, the tire slowly rotates while remaining in the same horizontal position and, as a result, experiences none of the "wedge" effects that tend to cause a real tire to hydroplane.

RESULTS

For a nominal load of 200 lb, the 2 smaller amplitudes of 0.041 and 0.084 in. produce a gradually decreasing friction force with increasing frequency. At 11 Hz the friction force levels off at 60 to 70 percent of its maximum value (a 30 to 40 percent loss). However, over the entire frequency range the highest friction force is produced by the lowest sliding speed. Figure 5 shows these trends for an amplitude of 0.084 in. Increasing the amplitude to 0.173 in. decreases the frictional force about 50 percent at 11 Hz (Fig. 6). In addition, a "crossover" occurs at about 4 Hz. At frequencies lower than 4 Hz, the highest friction force is produced by the lowest sliding speed, the same as with 2 smaller amplitudes; but, at frequencies above 4 Hz, the highest friction force is produced by the highest sliding speed.

At an amplitude of 0.342 in., the friction loss increases to about 80 percent at 9 Hz. The crossover now occurs at a much lower frequency, somewhere below the first test frequency of 2.2 Hz. At 0.707 in., the friction loss is about 90 percent at a frequency of 4 Hz, and the crossover again occurs somewhere below the first test frequency. At this large amplitude, the tread surface was observed to be leaving the table surface during the period that the table is moving through the lower portion of its travel.

For the 400-lb nominal load, the 2 smaller amplitudes exhibit friction losses of about 20 to 30 percent at the upper end of the test frequency range (around 11 Hz). As before with the 200-lb load, for the smaller amplitudes the highest friction force is produced at the lowest sliding speed at all tested frequencies. Increasing the amplitude to 0.173 in. increases the loss to about 30 to 50 percent depending on the sliding speed.

Figure 1. Speed dependence of adhesion coefficient on log of actual sliding speed.

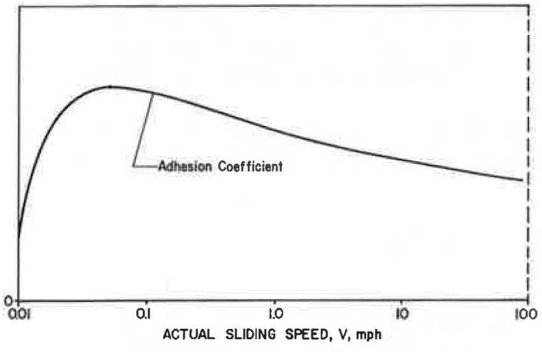

Figure 2. Schematic representation of tire friction test apparatus.

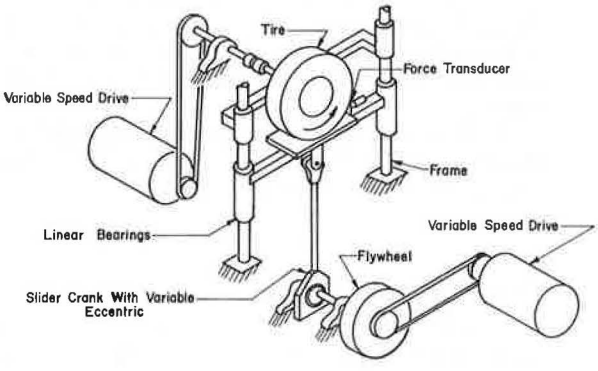

Figure 3. Tire, table, load cell, and strain gauge.

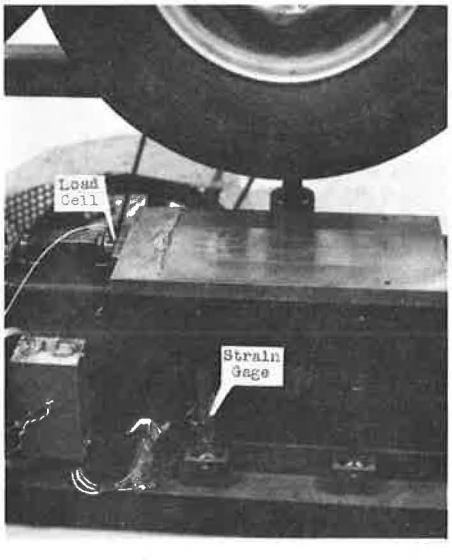

Figure 4. Unaltered normal and horizontal output voltages for measured sliding speed of 0.18 mph.

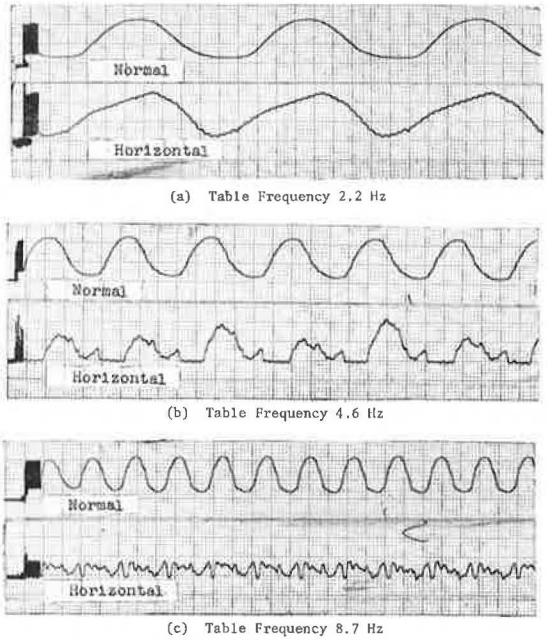

(a) Table Frequency 2.2 Hz

(b) Table Frequency 4.6 Hz

(c) Table Frequency 8.7 Hz

However, unlike the 0.173-in. amplitude at the lighter 300-lb load, no crossover is observed. At an amplitude of 0.342 in. the friction loss increases to about 65 percent at 10 Hz, and a crossover is now observed somewhere below the first test frequency. At the largest amplitude of 0.707 in. the loss is about 90 percent at a frequency above 8 Hz, and a crossover occurs at some very low frequency. As before, with the large amplitudes the tread surface separates from the table surface during part of the table's cycle.

A summary of these curves for the 400-lb nominal load is shown in Figure 7. The figure shows 5 curves, one for each amplitude tested, and each one is an average of the curves for the 3 sliding speeds.

INTERPRETATION OF TEST RESULTS

Mechanism of Friction

For this experimental case of a tire sliding at low speeds on a smooth, wet, flat plate, the dominant friction mechanism is adhesion; there is almost no hysteresis. Thus, a plot of the friction force as a function of the actual sliding speed is similar to that shown in Figure 8, which is valid for a constant sliding speed on a smooth surface.

Because the amount of deformation slip is unknown, the locations on the plot of the 3 actual sliding speeds that correspond to the measured sliding speeds of 0.18, 0.30, and 0.46 mph cannot be precisely determined. However, the 3 points must fall somewhere to the right of the adhesion peak because the lowest measured sliding speed is observed to produce the highest friction force and would appear in the approximate positions shown by points a, b, and c for the case of 0 frequency, 0 roughness.

Influence of Amplitude of Roughness on Friction Loss

For the case where a tire is operated on a rough surface, the amount of tread windup is constantly changing because the friction force is constantly changing. In the tests, as the table moves up against the tire, the tread elements wind up; then as the table moves away from the tire, the friction decreases and the tread elements easily snap forward. Thus, as the table oscillates at larger displacements, the net deformation slip remains about the same because the tread elements have the time required to wind up and then to unwind with less actual slip because contact is reduced as the table moves away.

In the tests, the rotating speed is held constant so that, as the displacement is increased, the actual sliding speed decreases. Thus, the points a, b, and c shift along the curve to the left and eventually reach positions such as shown by a′, b′, and c′. With the points shifted to the left of the adhesion peak, the higher measured sliding speeds now produce higher friction coefficient and there is an overall decrease of the friction coefficient for all 3 points.

Influence of Frequency of Roughness on Friction Loss

At the smaller roughness amplitudes, a loss of friction is still observed even though no crossover occurs to indicate that the actual sliding speed has shifted to the left of the adhesion peak. Thus, the primary mechanism that causes the friction loss cannot be attributed to the increase in deformation slip as in the case with the large roughness amplitudes described above. Instead of simply shifting on the curve on the coefficient plot as before, the operating points a, b, and c must somehow shift to a different curve that is valid for a tire sliding on a rough surface instead of a flat surface (the points a″, b″, and c″ located on a tentative "frequency roughness" curve). Because the adhesion force is dependent on the number and strength of interface junctions formed, the roughness frequency must reduce one or both of these factors to cause a loss of friction.

CONCLUSIONS AND RECOMMENDATIONS

The influence of frequency and amplitude on friction as separate effects was discussed. For the tests performed in this work, both effects occur simultaneously. Be-

Figure 5. Average maximum friction versus table frequency at amplitude of 0.084 in. and nominal load of 200 lb (curves normalized by dividing all coefficients by 0.59).

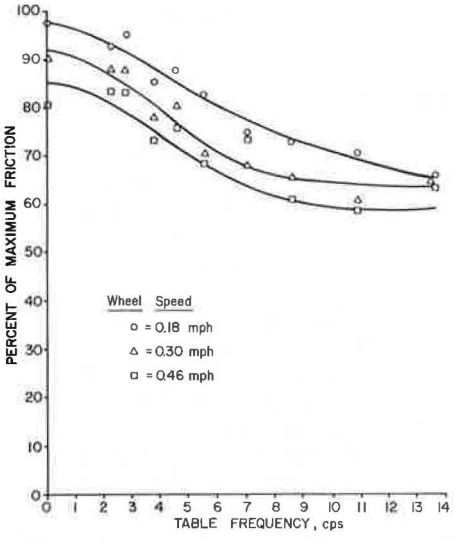

Figure 6. Average maximum friction versus table frequency at amplitude of 0.173 in. and nominal load of 200 lb (curves normalized by dividing all coefficients by 0.46).

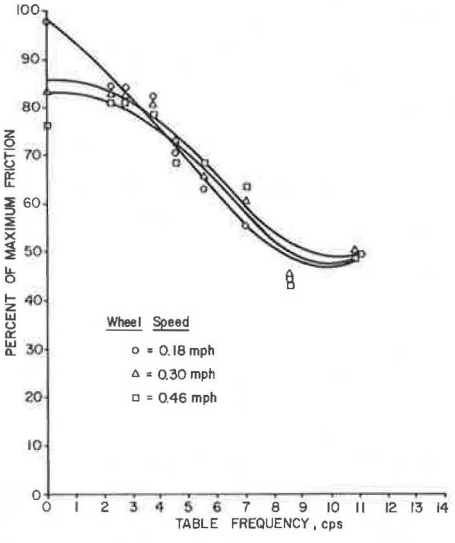

Figure 7. Average loss of friction versus table frequency at nominal load of 400 lb.

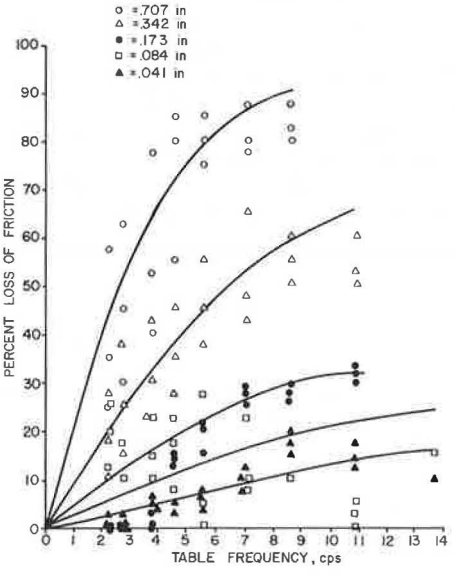

Figure 8. Influence of amplitude and frequency of roughness on friction loss.

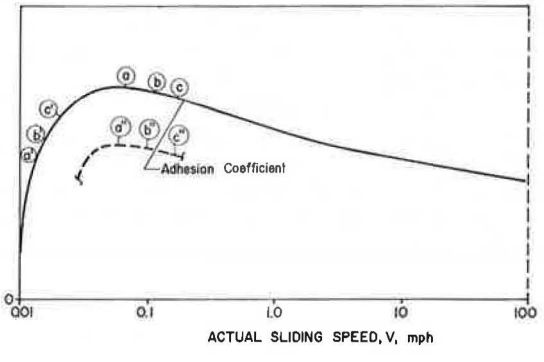

cause each effect always occurs with, and influences, the other, no clear-cut observations can be safely made until one dwells on the combined effects.

The tests demonstrated that increasing roughness amplitudes (from 0.041 to 0.707 in.) and increasing roughness frequencies (from 0 to 14 Hz) result in a decrease in the average coefficient of friction for measured sliding speeds in the range from 0.18 to 0.46 mph. At small amplitudes producing barely observable gross movements of the tire tread, increasing the roughness frequency to 14 Hz causes a friction loss of approximately 30 percent. At a low roughness frequency of around 3 Hz, increasing the roughness amplitude to 0.707 in. can cause a friction loss of 60 to 80 percent, depending on the amplitude.

This loss of friction is due to 2 factors: a reduction of the actual sliding speed caused by the increased deformation slip, and an overall lowering of the coefficient of friction. The reduction of actual sliding speed and the resultant leftward shift on the adhesion coefficient curve due to deformation slip are caused most predominately by large amplitudes of roughness, and the lowering of the coefficient is caused mainly by frequency.

The test machine in its present form restrains the rotating wheel's axle from any vertical motion. Thus, the dynamic effects of the suspension and body are eliminated, and only the dynamic performance of the tire is tested. This departure from an actual car, though it makes an extension of the test observations to an actual driving situation difficult, is done for good reason. Testing performed in this manner can isolate the effects of the tire from the effects of the suspension and the effects of the body mass. If a quarter-car simulation had been done from the start, the separate effects on frictional performance due to the tire, suspension, and body mass could not have been separated. Also, for future study the test machine was so designed as to allow a more complete simulation of a quarter-car by adding a spring, shock absorber, and body mass.

Occasional occurrences of slip-stick and chatter have been noted. The fact that the friction force drops when the tire goes into a condition of chattering may warrant further investigation. For a particular test run where the slip-stick has been briefly explored, it is found that slip-stick is less likely to recur in the next run if there is a sufficient time interval between successive runs. This fact that the chatter can sometimes be avoided if the tire is given time to "rest" suggests the possibility that it may be undergoing some kind of recovery from a strain it undergoes during slip-stick.

Finally, it must be noted that these results clearly show that the traction available is highly dependent on the speed with which one traverses a rough road. Thus, if friction measurements are to be applied at speeds other than the test speed, road profile data must also be utilized. Therefore, friction predictions without profile consideration can result in gross errors and may be one of the causes of lack of correlation of friction data.

REFERENCES

1. Kummer, H. W. Rubber and Tire Friction. Pennsylvania State Univ., PhD dissertation, 1965.
2. Meyer, W. E., and Schrock, M. C. Tire Friction: A State-of-the-Art Review. Automotive Safety Research Program, Pennsylvania State Univ., Rept. S34, 1969.
3. Kummer, H. W., and Meyer, W. E. Skid or Slip Resistance? Jour. of Materials, Vol. 1, 1966, pp. 667-688.
4. Leary, C. P. The Design of an Apparatus to Correlate Road Roughness and Tire Friction. Pennsylvania State Univ., Master's thesis, 1971.

ANALYTICAL PROBLEMS ENCOUNTERED IN THE CORRELATION OF SUBJECTIVE RESPONSE AND PAVEMENT POWER SPECTRAL DENSITY FUNCTIONS

L. F. Holbrook and J. R. Darlington, Michigan Department of Transportation

It is argued and demonstrated that, when human subjective response to road roughness is functionally related through multiple regression to power spectral density frequencies of the road profile, highly unreliable estimates of frequency coefficients result. Hence, one will be misled in assuming that such roads are especially detrimental to ride. The problem, generally designated "multicollinearity," is caused by extremely high intercorrelation of many of these frequencies. This follows from the mathematical treatment required in power spectral density analysis as well as from the inherent nature of road profiles. Nor is the situation any better if frequency selection procedures such as stepwise multiple regression are used in an attempt to capture only the most important frequencies. The presence of high multicollinearity between frequencies makes trivial the statistical selection and rejection criteria and thereby allows sampling error to essentially determine which frequencies are selected. A proposed solution to this problem is taken from the econometrics literature and applied to a small sample of subjective ride data for illustrative purposes only. The conventional full multiple regression estimates of frequency coefficients give totally unreasonable results, and the proposed solution gives results consistent with known automobile pass-band characteristics.

•THE GENERAL MOTORS rapid-travel profilometer is currently the only distortion-free system for profile measurement (1, 2). This does not imply that all wavelengths can be measured, and in practice the device is accurate only for wavelengths extending from 3 in. to approximately 200 ft. This implies that profiles are measured with respect to a linear reference that is no longer than 200 ft. Moreover, the position of this reference is arbitrary and slowly varying as the profile is traversed. This produces the seeming paradox of repeat runs on the same profile appearing different when plotted. Again however, this is merely a consequence of measuring the profile with respect to a linear but slowly varying, arbitrarily positioned reference.

Normally, this situation causes no problems in frequency domain analysis of a single wheelpath profile because, as stated above, the profile is entirely accurate within a given band. A problem does arise, however, in measuring the difference in elevation between inner and outer wheelpaths. This signal, known as the roll component, may have a strong bearing on ride quality as determined by subjective response of passengers in the vehicle. Moreover, the problem is not solved by profilometers with dual wheelpath measuring systems. The separate wheelpath measuring elements are completely independent and produce profiles measured with respect to arbitrary and independent references. In this respect, the dual wheelpath systems provide no improvement over measurement of each wheelpath separately with single wheelpath units. Unfortunately, a process called tipping, which inserts the arbitrary reference of one

Publication of this paper sponsored by Committee on Surface Properties-Vehicle Interaction.

profile into another, thereby permitting crude comparisons, cannot be used because the error introduced is generally similar to most roll components.

In view of the possible importance of roll components in ride quality, it is natural to seek some method of utilizing the separate wheelpath profiles. Although the roll component signal cannot be obtained directly, each wheelpath profile yields a power spectral density (PSD) function that is not affected by the reference differences. It is then possible to combine power between inner and outer wheelpaths at each frequency to provide a power function relating the 2 signals. Three obvious combinations of power at each frequency are (a) the average power between lanes $(I_i + O_i)$, where I_i equals power in the inner lane at frequency I_i and O_i equals power in the outer lane; (b) the absolute difference in power between lanes $|I_i - O_i|$; and (c) the product of $(I_i + O_i) \times |I_i - O_i|$.

Interpretation of function a is straightforward, but functions b and c deserve some comment. If power in each wheelpath is similar, the difference will be small and in theory will not indicate the presence or absence of roll component. It is safe to assume, however, that a small roll component is present because transverse finishing produces parallel roughness components spanning the entire lane. It is also probable that large differences in power between paths imply a high roll component. If this proves to be the case, function b may correlate with subjective response. Function c, which is average power multiplied by difference in power, expresses the interaction between average and roll power. This may prove to be a sensitive measure because rough pavements, particularly flexible, have a high roll component.

THE PROBLEM

As measurement of road profiles with rapid travel profilometry techniques becomes more popular, it is natural to expect that profile PSD will be used to predict human subjective response to road roughness (3). If problems in the measurement of subjective response (SR) can be overcome (4, 5), further problems will arise if conventional multiple regression techniques are used to estimate the β parameters in the linear formulation

$$SR = \gamma + \beta_1 X_1 + \beta_2 X_2 + \ldots + \beta_N X_N \quad (1)$$

where X_i is some form of intensity (usually log variance) of the respective profile frequencies f_i. When the number of frequencies (the N regressors) in Eq. 1 is large, say, 3 or more, a high degree of intercorrelation among them will usually be present. One reason for this is the mathematical smoothing induced by the PSD analysis. To understand why this must be so, we will examine briefly the PSD analysis used in the present study. For this analysis, 4 statistical decisions are important:

1. The analog profile signal from inner and outer wheelpaths is filtered to eliminate all wavelengths outside the band of 2 to 50 ft;
2. The filtered signals are sampled every 6 in. providing 4 points per cycle of the highest frequency present;
3. Twenty-five ordinates are computed providing 13 "independent" estimates of the power spectrum (estimates are spaced 0 to 0.02 cycle/ft apart, and the resolution bandwidth is 0.04 cycle/ft; and
4. A Hanning spectral window is used to smooth the final estimates.

These considerations imply a theoretical correlation among PSD estimates for broadband white noise (6). Adjacent ordinates are correlated about 0.6 if the true spectrum is flat. In addition, 2 other conditions may increase the correlation among ordinates by unpredictable amounts.

1. If a signal from a nonflat power spectrum has a great deal of power in a narrow frequency band and very little in an adjacent band, estimates of power in the weak band will be too high. This occurs because a finite data sample implies a data window that transforms through analysis into a spectral window with nonvertical skirts and side lobes. This simply means that the PSD resolution filter attenuates but does not completely eliminate power in adjacent frequencies. Thus, the resolution filter may not attenuate

power at an adjacent frequency enough to keep it well below power at the frequency being examined. This problem is significant only when the true spectrum has a very steep roll-off of perhaps 40 dB per decade or a narrow band of power perhaps 40 dB above adjacent bands.

2. Consider the case in which the PSD for a number of roads have the same general shape but simply move up or down as a unit depending on general roughness. In this case power in a given band rises or falls along with power from an adjacent band. This would generate the correlation between an ordinate and its neighbors. That the PSD often have similar shapes but different general power levels can be seen from the examination of a number of power spectra. Indeed, neighboring frequencies may be so highly correlated that no useful information is supplied by one that is not supplied by its close neighbors.

High independent variable intercorrelation is frequently encountered in multiple regressions with large numbers of regressors and has been termed "multicollinearity" (7, 8, 9). Multicollinearity in the limit where 2 or more regressors are perfectly correlated aborts the multiple regression estimation of β because the X^TX matrix has 2 or more identical columns and cannot be inverted as required by the multiple regression procedure. Short of this, high multicollinearity induced by either high correlation between 2 variables or moderately high correlation among all variables causes the β estimates to be extremely unreliable. If β is used as a measure of the relative importance of profile frequencies, high multicollinearity will almost certainly lead to erroneous inferences. A second sample will give radically different β weights and consequently inconsistent designation of those frequencies that most seriously affect riding quality.

It might be thought that some of the variable selection procedures such as stepwise multiple regression might solve the problem (10). Unfortunately, this is not the case—these procedures are seriously influenced by multicollinearity (11). What will generally happen with the forward selection procedures is that the variables that first enter the equation do so on the basis of relatively high correlations with the dependent variable. However, PSD frequencies considered as regressors are very highly intercorrelated, and those chosen initially by the selection procedure would be only insignificantly more correlated with SR than neighboring frequencies. However, these latter frequencies will never be selected by the procedure because, by virtue of high intercorrelation with the initial set, their unique relation with SR will not be large enough to permit their inclusion in the regression equation. In other words, when high multicollinearity is present and forward variable selection procedures are used, variables selected early in the procedure drastically militate against the inclusion of potentially important remaining variables. But the initial set chosen by the procedure, being only marginally more correlated with SR than other variables, suggests that it would not be selected initially in subsequent samples. Therefore, if we want to identify important PSD frequencies, we can expect procedures such as stepwise regression to pick a different set every time we process new data.

Similar comments apply to the variable rejection part of stepwise multiple regression: Variables included later may through intercorrelation "rob" earlier variables of their contribution and thereby cause them to be rejected at a later state. Finally, even if a few important frequencies are repeatedly selected by these procedures, their coefficients will vary considerably from sample to sample. This can be seen in the formula for the variance of the $\hat{\beta}_2$ coefficient for the case of only 3 regressors in Eq. 1:

$$\mathrm{Var}(\hat{\beta}_2) = \frac{\sigma^2}{(1 - r_{23}^2) \sum_{i=1}^{K} (X_i - \overline{X})^2} \qquad (2)$$

As the correlation between X_2 and X_3 (r_{23}) increases, Var ($\hat{\beta}_2$) also increases until in the limit, when $r_{23} = \pm 1.0$, Var ($\hat{\beta}_2$) $= \infty$.

ANALYSIS PROCEDURE

To simplify the illustration of problems encountered with road frequency multicollinearity, we will use only 1 of the first of the 3 power combinations discussed and define a roughness measure S_i as $(O_i + I_i)$, where I_i = logarithm of squared amplitude for the i th frequency band of the inside wheel track, and O_i = logarithm of squared amplitude for the i th frequency band of the outside wheel track. S can be thought of as a measure of "average" intensity for the respective frequencies. If S is standardized to s, we will be able to compare the multiple regression coefficients, $\hat{\beta}_i$, directly. If, under ordinary multiple regression specifications, we were to regress subjective response SR on s for each frequency band, we would have

$$\hat{SR} = \hat{\gamma} + \hat{\beta}_0 s_0 + \hat{B}_1 s_1 + \ldots + \hat{\beta}_N s_N \tag{3}$$

which requires the estimation of N + 2 parameters. Suppose now that we require $\hat{\beta}$ to conform to some reasonable function, remembering that it would be unlikely that β would jump around as capriciously as the ordinary multiple regression estimates do (12, 13). Not knowing a priori the form of this function, we should initially use only very general functions such as polynomials. Suppose we specify a k th degree polynomial together with the condition that $\beta_0 = 0$, i.e., that the weight corresponding to the frequency f_0 is 0 (Fig. 1). The equation functionally relating β_i to i will be

$$\beta_i = \alpha_1 i + \alpha_2 i^2 + \ldots + \alpha_K i^K \tag{4}$$

Substituting Eq. 4 into Eq. 3, we have

$$\begin{aligned} SR = \gamma &+ (\alpha_1 + \alpha_2 + \ldots + \alpha_K)s_1 + (2\alpha_1 + 2^2\alpha_2 + \ldots + 2^K\alpha_K)s_2 \\ &+ \ldots + (N\alpha_1 + N^2\alpha_2 + \ldots + N^K\alpha_K)s_N \end{aligned} \tag{5}$$

Factoring α_j, we have

$$\begin{aligned} SR = \gamma &+ \alpha_1(s_1 + 2s_2 + \ldots + Ns_N) \\ &+ \alpha_2(s_1 + 2^2 s_2 + \ldots + N^2 s_N) + \ldots \\ &+ \alpha_K(s_1 + 2^K s_2 + \ldots + N^K s_N) \end{aligned} \tag{6}$$

Or by defining the terms in s as z, we have

$$SR = \gamma + \alpha_1 z_1 + \alpha_2 z_2 + \ldots + \alpha_K z_K \tag{7}$$

Because we will choose $K \ll N$, parameter estimation by ordinary multiple regression will not be nearly so subject to multicollinearity problems in Eq. 7 as in Eq. 1. Therefore, we can estimate γ_j conventionally and by virtue of Eq. 4 estimate β in turn.

Two problems remain.

1. The order of the polynomial chosen to govern β is arbitrary. Or, in other words, How large should K be to ensure faithful representation of the population of β? For most applications, we might be satisfied with K = 3 or 4; however, unless we have considerable information about β, we can never be sure that important peaks and valleys in the β function are blurred by polynomials of low order. One course of action would be to let the selection procedures such as stepwise multiple regression determine K. For example, one could compute the various z_j in Eq. 7 for, say, K = 10. If all the z_j were regressed on SR, $\hat{\beta}$ would follow a tenth-order polynomial. This would be excessive for most applications; however, stepwise regression could statistically select those z_j that proved important enough to significantly reduce the residuals. The α_j corresponding to the z_j selected would then estimate the β_i by virtue of Eq. 4. Because we do not care which z_j are selected (unlike the case with the s_i), many combinations of z_j would probably suffice to estimate the function. We must not

be too permissive in the stepwise variable rejection procedure—too high an order of polynomial will tend to give the same unreliable results as an ordinary multiple regression on Eq. 1.

2. Not all the information governing the β_i distribution is used. It can be fairly assumed that no β_i should be negative. If this were not the case, the implication would be that power in these wavelengths improves ride. There are several ways in which this constraint on the β_i can be incorporated into the estimation procedure. One is to specify the β_i exponentially:

$$\beta_i = i\epsilon^{\sum_{k=1}^{K} \alpha_k i^k} \tag{8}$$

for K = 1, 2, ... This formulation forces the β distribution through 0 and requires all $\hat{\beta}_i$ to be positive. Moreover, the polynomial in the exponent can be of any desired order. Unfortunately, stepwise procedures cannot be used to determine this order because ordinary linear least squares procedures are not applicable. However, the α_k can be estimated by nonlinear computer search procedures.

EXAMPLE WITH FIELD DATA

As an illustration of the problems encountered with multicollinearity, consider the following example using the SR data and PSD described in detail by Holbrook in an earlier report (4). Fourteen test roads rated on roughness at 30 to 50 mph by a panel of 96 subjects using graphic rating scales were profiled with the General Motors rapid travel profilometer. This allowed the computation of frequency spectra for the range 0.02 to 0.50 cycle/ft. The degree of sample correlation found between pairs of PSD ordinates is shown in Figure 2 for the case of the 0.22 frequency. Correlation with adjacent ordinates is extremely high: +0.9990 and 0.9819. Throughout most of the frequency range, correlations with the 0.02 ordinate are 0.9000 or higher. With the multicollinearity problem as acute as this, ordinary multiple regression should provide very poor estimates of the relative importance of the respective frequencies. That this is so is shown by the $\hat{\beta}_i$ coefficients for regressions of SR on even and odd frequencies in Figure 3. Interpretation of these weights is difficult particularly in view of the large number of negative signs and the fact that the weights from the even frequency analysis are considerably different from those of the odd weight analysis. It would seem unlikely that negative weights are realistic when one considers that they imply that high amplitudes in the associated frequencies induce a better ride! Clearly we cannot depend on this traditional procedure to detect the important frequency ranges. Because the polynomial lag procedure might provide a better estimate of the β_i weight distribution, it was applied to the same data by using the stepwise procedure with Eq. 4. A $\hat{\beta}_i$ distribution was found that peaked at about 7-ft waves. However, for shorter waves, the curve became unstable and actually went negative. This was due to poorer correlations of PSD ordinates with SR in this wavelength region—possibly due to tape deck vibration in the test vehicle.

Equation 8 was then used because it disallows negative $\hat{\beta}_i$. Polynomials of orders 1 through 4 were used as shown in Figure 4. It appears that at least a second-order polynomial is necessary, although little change in the $\hat{\beta}_i$ distribution resulted from increasing the order beyond 2 (see inset of Fig. 4). One would infer from Figure 4 that 5- to 10-ft waves are of special importance in the determination of riding quality if vehicle speed were held constant throughout the test series. This was not true for these data (vehicle speed ranged from 30 to 50 mph); therefore, these results should be augmented with more extensive and better controlled experimental data. Notice also that no information concerning important wavelength ranges can be obtained from conventional multiple regression (Fig. 3).

Problems with this particular set of experimental data notwithstanding, if these results are taken as valid, the importance of this wavelength range can be rationalized as follows: Shake table tests of a typical vehicle resulted in maximum reactive force from tires when input frequencies were near 15 cps (14, 15, 16). This is the frequency range generated by 6- to 8-ft waves in a vehicle traveling at typical highway speeds

Figure 1. Kth degree polynomial.

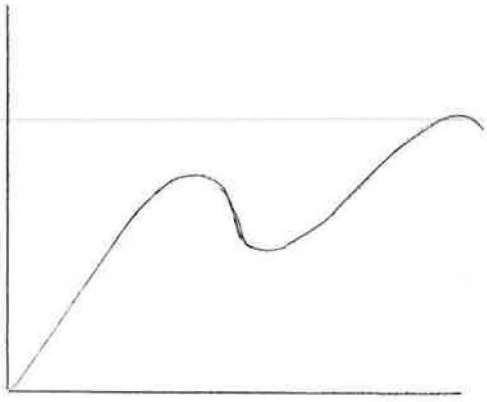

Figure 2. Correlation of frequency 0.22 with neighboring frequencies.

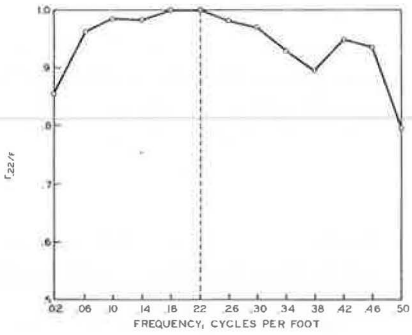

Figure 3. Frequency weights determined by using Eq. 1.

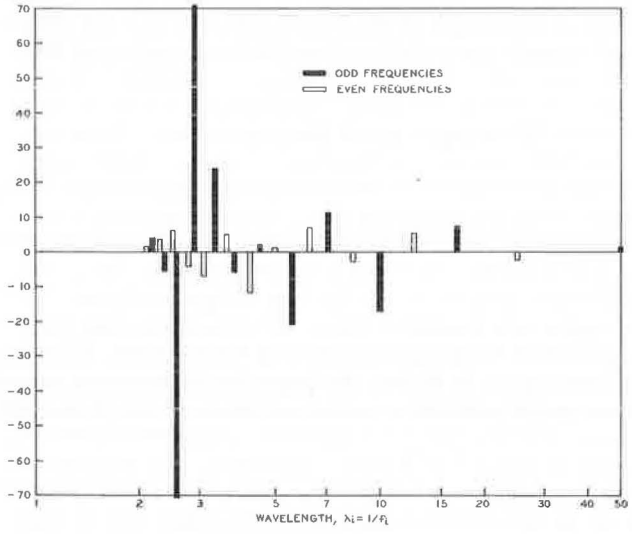

Figure 4. Frequency weights determined by using Eq. 8.

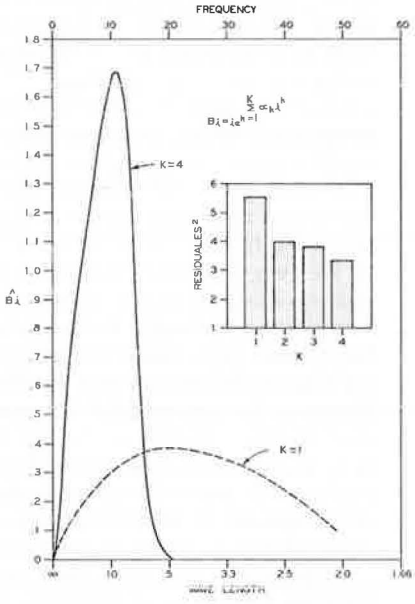

near 70 mph. Moreover, it is reasonable to assume that most automobiles have a similar response function despite differences in weight or suspension system. This is because the major determinant of vehicle response, the ratio of suspension spring constant to vehicle mass, remains generally constant over a wide range of vehicles. In addition, the 6- to 8-ft wavelength band is of sufficient width to accommodate some change in the mass to spring constant ratio.

An important implication of these findings concerns the design of a standardized ride-quality measuring system. The 6- to 8-ft wavelength band or even the 2- to 8-ft band can be easily measured by uncomplicated instruments. Such a device would be much simpler than the GM profilometer and would involve a single accelerometer and simple processing circuits. The statistic returned would be a single number representing average power in the 5- to 10-ft band. It would be possible to continuously display this statistic during a profile run to locate areas of excessive roughness. Although details of this system are not presented here, the authors will supply information on its design.

CONCLUSION

Because of high intercorrelations among amplitudes or road profile spectra, conventional multiple regression techniques should not be used to correlate frequency bands with subjective response to pavement roughness. In particular, one would get misleading estimates of the relative importance of the various bands as far as human response to road roughness is concerned. It would, therefore, become very unlikely that one would be able to separate the effects of the several frequencies on subjective response. Stepwise regression procedures merely exacerbate the problem because the statistics such as partial F-tests and partial correlation coefficients used in these procedures will reject important frequencies highly correlated with frequencies already included as independent variables. Consequently, these procedures discriminate against frequencies less correlated with subjective response than those frequencies selected earlier because of only slightly higher correlation. In short, with conventional regression analysis, one would expect to get drastically different estimates of the frequency coefficients from sample to sample. The method of overcoming the problem put forth in this paper is to impose restrictions on the frequency coefficients. An obvious restriction is the requirement that the coefficients must lie on a polynomial of specified order. The order can be arbitrarily set by the investigator (particularly if he has some prior knowledge of the coefficient distribution), or it can be determined by a selection procedure such as stepwise multiple regression. The coefficients of the polynomial are considerably fewer in number than those of the conventional regression and are, therefore, more reliably estimated. These parameters are then used with the specified polynomial to estimate the frequency coefficients originally sought.

Sample data provide an example that shows how conventional multiple regression fails to produce a reasonable distribution of the frequency coefficients. Application of the polynomial procedures to these same data provides an initial coefficient distribution that peaks at about 8 cycles/ft. Further studies based on more and better data are needed to establish the validity of this distribution.

REFERENCES

1. Spangler, E. B., and Kelly, W. J. GMR Road Profilometer—A Method for Measuring Road Profile. Highway Research Record 121, 1965, pp. 27-54.
2. Darlington, J. R. Evaluation and Application Study of the General Motors Corporation Rapid Travel Profilometer. Michigan Department of State Highways, Rept. R-731.
3. Walker, R. S., and Hudson, W. R. Practical Uses of Spectral Analysis With Surface Dynamics Road Profilometer. Highway Research Record 362, 1971, p. 113.
4. Holbrook, L. F. Prediction of Subjective Response to Road Roughness by Use of the Rapid Travel Profilometer. Highway Research Record 291, 1969, pp. 212-226.
5. Hutchinson, G. B. Principles of Subjective Rating Scale Construction. Highway Research Record 46, 1964.

6. Blackman, R. B. Data Smoothing and Prediction. Addison-Wesley, 1965, pp. 136-152.
7. Goldberger, A. S. Econometric Theory. John Wiley and Sons, 1964, pp. 192-194.
8. Goldberger, A. S. Topics in Regression Analysis. Macmillan, 1968, pp. 132-133.
9. Johnston, J. Econometric Methods. McGraw-Hill, 1963, pp. 201-207.
10. Draper, N., and Smith, H. Applied Regression Analysis. John Wiley and Sons, 1966, pp. 163-173.
11. Wonnacott, R. J., and Wonnacott, T. H. Econometrics. John Wiley and Sons, 1970, pp. 309-312.
12. Almon, S. The Distributed Lag Between Capital Appropriations and Expenditures. Econometrica, Vol. 33, Jan. 1965, pp. 178-197.
13. Kmenta, J. Elements of Econometrics. Macmillan, 1971, pp. 441-495.
14. Quinn, B. E., and DeVries, T. W. Highway Characteristics as Related to Vehicle Performance. HRB Bull. 250, 1960, pp. 20-36.
15. Quinn, B. E., and DeVries, T. W. Effects of Pavement Condition on Dynamic Vehicle Reactions. HRB Bull. 328, 1962, pp. 24-31.
16. Quinn, B. E., and VanWyk, R. A Method for Introducing Dynamic Vehicle Loads Into Design of Highways. Highway Research Record 40, 1961, pp. 18-20.

EFFECT OF SERVICEABILITY AND ROUGHNESS AT TRANSVERSE JOINTS ON PERFORMANCE AND DESIGN OF PLAIN CONCRETE PAVEMENT

M. P. Brokaw, Portland Cement Association

This paper covers the author's activities during the past 16 years in plain pavement evaluation. The studies include measurement of faulting by hand method, conversion of these data to slope variance, appraisal of highway user reaction to faulting roughness, measurement of cracking and patching, and survey of serviceability indexes by the PCA road meter. These performance features were related to wide spectra of pavement thicknesses, traffic, subgrade soil classification, joint spacing, and age of pavement in Minnesota, Wisconsin, North Dakota, and Iowa. Results have been expressed in a design model for the plain pavement system. Components are explained, data sources are cited, and suggestions are made for additional research and construction of test sections meeting the criteria established.

•CONCRETE pavements with closely spaced transverse joints, but without dowels and distributed reinforcement, have been in use for many years. Performance features have ranged from very good to very poor, yet the simplicity and economy of the system suggest that a method of design is needed so that the system can perform adequately in all situations.

The method finally adopted must account for the main weakness in the system, which is faulting or vertical dislocation of short pavement sections at transverse joints, and then for eventual serviceability indexes during an assigned analysis period.

Many field and laboratory studies have been reported. None has compared results of field measurements of faulting with highway user dissatisfaction, thickness of pavement, volume and weight of traffic loading, types of subgrade soil, transverse joint spacing, and age of pavement. None has attempted to relate findings to the concept of present serviceability index (PSI) developed at the AASHO Road Test.

In 1955, the Minnesota Department of Highways initiated a comprehensive, statewide survey of transverse joint faulting and pavement cracking in 74 projects having 15- and 20-ft joint spacing and 2 levels of pavement thickness. The survey was repeated in 1961 and 1967 for the purpose of establishing trends in faulting related to time and traffic loading (2).

Analysis of the 1955 data by the Portland Cement Association disclosed that faulting of Minnesota pavements was a function of average daily traffic of tractor semitrailer and combination vehicles and the square of the age of the pavement. In addition, ratings of pavement riding comfort suggested that the magnitude of tolerable faulting could be represented by statistics such as 100 percent of joints faulted 0.15 in. and more, or an average fault of about $^{6}/_{32}$ in. These factors were combined in an expression that enabled determination of the traffic level requiring joint reinforcement (3).

In 1960, the Portland Cement Association prepared a report setting forth methods of design for both plain and reinforced pavements in Minnesota (3). Pavement thicknesses were designed by load-stress analysis and by the additional requirement of joint and crack reinforcement when traffic exceeded 300 tractor semitrailer and combination

Publication of this paper sponsored by Committee on Pavement Condition Evaluation.

vehicles per day during a 35-year life to first resurfacing. The 35-year period was justified by concrete pavement survivor analysis. The method was subsequently adopted by the Minnesota Department of Highways and is contained in current concrete pavement design standards.

Research of the performance characteristics of plain pavements has continued in Minnesota and has been extended to Wisconsin, North Dakota, and Iowa to include the serviceability index concept developed at the AASHO Road Test (6, 7, 8, 9). Results were combined in a report (1) presented at a 7-state highway conference sponsored by the Minnesota Department of Highways in 1971.

The 1971 report showed that 5- and 6-in. plain pavements have greater capacity for load than previously expected and that the system can be designed for traffic levels greater than 300 tractor semitrailer and combination vehicles per day during a 35-year analysis period, but pavement thicknesses must be greater than those established for reinforced pavements by load-stress analysis. The reports also indicated that the pavements resting on subgrade soils having excellent internal drainage have substantially greater capacity for traffic load than can be attributed to customary increases in subgrade reaction (k).

PERFORMANCE MODEL

Plain pavements have a very short transverse joint spacing, usually 15 to 20 ft. Traffic and age effects are represented by deterioration (faulting and hinging) at joints. Additional breaks at intermediate points are limited if the joint spacing does not exceed about 20 ft. Therefore, the main source of pavement roughness is at joints, but with some addition from slopes in uncracked slabs between joints.

The additional slopes occur with and without faulting and contribute to total pavement roughness, depending mostly on frost effects and recovery, volume changes in subgrade, consolidation in subgrades and subbases, and time.

This hypothesis suggested that total pavement roughness (slope variance) might be the sum of uncorrelated parts such as initial constructed roughness, roughness at joints, and roughness between joints. In that event, PSI of a plain concrete pavement could be expressed by a modified AASHO equation (6), as follows:

$$PSI = 5.41 - 1.80 \log (SVC + SVF + SVO + 1) - 0.09 (C + P)^{0.05}$$

where

PSI = present serviceability index,
SVC = part of slope variance due to construction,
SVF = part of slope variance due to displacement at joints,
SVO = part of slope variance between joints, and
C, P = cracking and patching according to AASHO definition.

EVALUATION OF SERVICEABILITY COMPONENTS

Constructed Roughness

Initial serviceability indexes of the 138 projects included in the study were not measured in situ. However, time-related components of pavement roughness and serviceability were extrapolated to give reasonable estimates of probable initial serviceability (1).

Errors from this method are of little consequence when pavements reach maturity and approach serviceabilities that indicate need for resurfacing. For example, a pavement constructed to an initial PSI of 4.50 might serve for a number of years before reaching a PSI of 2.50. If the same pavement was constructed to an initial PSI of 4.00 and was subjected to the same traffic loading for the same number of years, the small increase in initial slope variance reduces the terminal PSI to 2.42. This disparity in PSI numbers is a result of the unique AASHO Road Test semilogarithmic equation dealing with slope variance that tends to exaggerate serviceability indexes when roughness inputs are low. However, the disparity rapidly diminishes when initial serviceability drops below 4.0, and this points to the need for vigilant construction controls.

Once the initial serviceability index has been selected, the corresponding constructed roughness can be computed, as follows:

$$SVC = 1{,}014/10^{0.56P_o} - 1$$

where P_o = initial serviceability index.

Roughness at Transverse Joints

Eventual roughness at transverse joints has been the main deterrent to greater use of the plain pavement system. When joints are placed at a constant spacing (say, 15 or 20 ft), faulting causes a cyclical roughness input to some vehicles that creates an adverse highway user reaction that was not recognized or measured in the AASHO Road Test. In effect, this means that customary terminal serviceability indexes might not be applicable and that design should also be a function of some limitation on joint roughness.

The portion of total slope variance attributable to joint roughness was computed for each project in the study by converting manual measurements of joint faulting to slope variance at joints only (1). These, in turn, were related to traffic of tractor semitrailer and combination vehicles, age of pavement, thickness of pavement, and 2 levels of subgrade soil classification. The relations are as follows: For A-1, A-2, and A-3 subgrade soils,

$$SVF = 1.94\ TA^2/D^{5.47}$$

and for A-4, A-5, A-6, and A-7 subgrade soils,

$$SVF = 1.11\ TA^2/D^{4.60}$$

where

T = average 2-way ADT of tractor semitrailer and combination vehicles;
A = age of pavement, years; and
D = thickness of pavement, in.

Studies of terminal serviceability indexes and limitations on slope variance at transverse joints are also given in an earlier report (1). It appears that faulting creates an incipient stage of highway user dissatisfaction when SVF is greater than 12 and joints are spaced at constant 15- to 20-ft intervals. If joints are spaced at random intervals (say, 13, 19, 18, and 12 ft) and are skewed, adverse roughness input to susceptible vehicles is reduced. In that case, the terminal limit of SVF might be increased to 14. It then becomes a design factor equal in importance to terminal serviceability index.

Roughness Between Joints

In a plain pavement system, roughness between joints is caused by slopes in uncracked panels. Although some transverse cracking may develop, it is usually at long intervals if the basic joint spacing does not exceed about 20 ft. The magnitude of slopes in the panels is small if the only source of roughness is faulting at transverse joints. For example, a $\frac{1}{4}$-in. fault in a 15-ft panel could account for about $\frac{1}{80}$-in. deviation in a profilometer 9-in. gauge length. Surface texturing for skid resistance can exceed this amount. Therefore, meaningful roughness between joints must be spatial in character, probably erratic, and related mostly to profile distortions from frost effects, volume changes in subgrade, consolidation in subgrades and subbases, and exposure time.

Pavement roughness between joints ought to be influenced by pavement thickness and traffic weight and frequency of application, especially when pavement thickness is grossly inadequate for the imposed loads. In fact, this situation was observed at the AASHO Road Test where pavements less than 8-in. thick were rapidly destroyed when subjected

to extreme overload. In these cases, pavement slabs were eventually shattered and slope measurements were increased by tilting and vertical displacement of segmented parts. Serviceability indexes also reached an unusual level of 1.5.

Analysis of data in 138 projects in Minnesota, Wisconsin, and North Dakota showed that roughness between joints had great variability and was not related to pavement thickness and rate of loading as long as the thickness was reasonably adequate for the rates imposed and serviceability index remained above 2.5. However, SVO did increase with time, but at a diminishing rate, for all levels of thickness regardless of the rates of loading. The analysis was extended to pavements with thicknesses of 8 to 12½ in. in the AASHO Road Test and to 6 in. in the Iowa county road system (10). The same phenomenon was observed (1), and this led to a general equation for slope variance between joints, as follows: For A-1, A-2, and A-3 subgrade soils,

$$SVO = (A + 1)^{0.58} - 1$$

and for A-4, A-5, A-6, and A-7 subgrade soils,

$$SVO = (A + 1)^{0.70} - 1$$

where A = age of pavement in years.

The idea that pavements can develop significant roughness without traffic, but at increased age, is a distinct departure from most design models. However, those familiar with the gradual increase in roughness of minor structures such as sidewalks and residential driveways or segments of heavy-duty pavement occasionally transferred to local traffic are aware of age effects alone.

Cracking and Patching

The plain pavement system is basically designed to minimize reductions in serviceability index caused by cracking of pavement slabs between transverse joints. To accomplish the objective, joint spacings have to be limited to a maximum of about 20 ft.

Pavements included in this report had both 15- and 20-ft transverse joint spacings, but both spacings were not equally represented in all variables of thickness, traffic, subgrade class, and age. Therefore, joint spacing was not differentiated in the analysis.

Composite data showed that cracking and patching increased with age of pavement and decreased with thickness of pavement. Departures from the design model indicate that projects with 15-ft joint spacing had an average serviceability index about 5.5 percent higher than those with 20-ft joint spacing.

Reduction of serviceability index for cracking and patching is

$$0.09 (C + P)^{0.5} = 0.62 + 0.01 A - 0.65 \log D$$

where

A = age of pavement, years; and
D = thickness of pavement, in.

DESIGN MODEL AND STATISTICAL SIGNIFICANCE

Design Model

The design model for plain concrete pavement is the summation of performance components developed in previous sections of the paper. Limitations are as follows: Faulting slope variance should not exceed 14; terminal serviceability index should not be lower than ordinary values, such as 2.0 to 2.2 for residential streets, 2.2 to 2.4 for county roads or lightly traveled secondary state routes, and 2.4 to 2.6 for important Interstate and primary highways; pavements should be constructed with random spacing and skewed joints; subgrade and subbase material should meet established criteria for resistance to pumping; and time, represented by age of pavement, should be the interval between construction and first resurfacing.

The design model is as follows: For A-1, A-2, and A-3 subgrade soils,

$$PSI = 5.41 - 1.8 \log \left[1{,}014/10^{0.56P_o} + 1.94\ TA^2/D^{5.47} + (A + 1)^{0.58} - 1 \right] - 0.01A + 0.65 \log D - 0.62$$

and for A-4, A-5, A-6, and A-7 subgrade soils,

$$PSI = 5.41 - 1.8 \log \left[1{,}014/10^{0.56P_o} + 1.11\ TA^2/D^{4.60} + (A + 1)^{0.70} - 1 \right] - 0.1A + 0.65 \log D - 0.62$$

where

PSI = serviceability index following years of service A after construction;
P_o = serviceability index constructed;
T = 2-way average ADT of tractor semitrailer and combination vehicles during years of service A;
A = years of service after construction and to reaching PSI; and
D = thickness of pavement, in.

Sample solutions of the model for a wide range of conditions are given in Table 1.

Statistical Significance

Measures of statistical significance are made possible by comparing observed serviceability indexes with those computed by use of the design model. Two methods were used. The first involved transformation of differences to a percentage increase or decrease from model serviceability index. This method simplifies comparisons among the various levels of thickness, joint spacing, traffic, subgrades, and age and also facilitated graphical representation of the data (4). A summary of percentage differences between observed and model serviceability indexes is given in Table 2.

Average differences and standard deviations of the averages were computed and subjected to null hypothesis to determine whether the differences were a result of sample variation or whether the model did not fully account for variations in each level. The following conclusions were drawn.

1. For 138 projects, including 2 levels of joint spacing, 4 levels of pavement thickness, 2 levels of subgrade soils, combination traffic ranging from 0 to 1,000 vehicles per day, ages ranging from 10 to 21 years, and serviceability indexes ranging from 2.51 to 3.91, the model is able to predict serviceability indexes with a mean error of +0.9 percent. Standard deviation of the differences amounts to 7.2 percent, and the standard error of the group mean is 0.6 percent. Null hypothesis indicates that the mean error of 0.9 percent can be attributed to sample variation and that the model equation is dependable.
2. Effects of the 2 levels of joint spacing are important. When these are analyzed separately, pavements with 15-ft joint spacing showed a mean serviceability index 3.7 percent greater than the model and those with 20-ft spacing had a mean serviceability 1.8 percent lower than the model. Null hypothesis indicates that the differences are greater than sample error, and the model does not account for either extreme in the best possible way. The discrepancy was expected because all joint spacings were pooled. Furthermore, the data point out superior performance of joints spaced at 15-ft intervals, and they do not preclude use of the model in a plain pavement system having random joint spacings ranging from about 12 to 20 ft.
3. Other items, tested by null hypothesis, showed differences beyond sample error when joint spacings were not equally divided. For example, 8-in. pavements performed significantly better than the model, and 10-in. pavements were lower than the model. In these cases, 8-in. pavements were represented by 62 percent of projects with 15-ft spacing, and 10-in. pavements all had 20-ft spacing. The same disparity to 15-ft joint spacing appeared in analysis of 105 projects carrying less than 300 combinations per day and in the group of projects that were more than 16 years of age.

Table 1. Design for plain pavement based on random-spaced and skewed joints, terminal SVF of 14, and initial PSI of 4.5 to 4.0.

Subgrade Soil[a]	Pavement Thickness (in.)	Design Life (years)	Final PSI	Initial TST-ADT and Growth/Year[b]			
				0 Percent	1 Percent	3 Percent	5 Percent
A-1, A-2, A-3	6	25	2.6 to 2.4	200	175	145	120
		30	2.5 to 2.3	140	120	95	80
		35	2.5 to 2.3	105	90	70	55
	7	20	2.8 to 2.7	750	680	575	500
		25	2.7 to 2.6	480	425	350	295
		30	2.6 to 2.5	335	290	230	190
		35	2.6 to 2.5	245	210	160	130
	8	20	2.8 to 2.7	1,450	1,320	1,190	965
		25	2.8 to 2.7	925	820	670	570
		30	2.7 to 2.6	690	600	475	395
		35	2.7 to 2.6	510	435	335	270
	9	20	2.9 to 2.8	2,960	2,690	2,290	1,970
		25	2.8 to 2.7	1,900	1,690	1,380	1,170
		30	2.7 to 2.6	1,320	1,150	910	755
		35	2.7 to 2.6	970	825	635	515
	10	20	2.9 to 2.8	5,290	4,800	4,060	3,520
		25	2.8 to 2.7	3,390	3,020	2,460	2,090
		30	2.7 to 2.6	2,340	2,040	1,610	1,340
		35	2.7 to 2.6	1,730	1,470	1,135	925
A-4, A-5, A-6, A-7	6	25	2.6 to 2.4	75	65	55	45
		30	2.5 to 2.3	50	45	35	30
		35	2.5 to 2.3	40	35	25	20
	7	20	2.7 to 2.6	245	225	190	165
		25	2.6 to 2.5	155	140	115	95
		30	2.5 to 2.4	110	95	75	65
		35	2.5 to 2.4	80	70	50	45
	8	20	2.7 to 2.6	450	410	345	300
		25	2.6 to 2.5	290	260	210	180
		30	2.6 to 2.5	200	175	140	115
		35	2.6 to 2.5	150	130	100	80
	9	20	2.8 to 2.7	775	705	595	515
		25	2.7 to 2.6	500	445	365	310
		30	2.6 to 2.5	345	300	240	195
		35	2.6 to 2.5	255	220	165	135
	10	20	2.8 to 2.7	1,260	1,145	970	840
		25	2.7 to 2.6	805	715	585	495
		30	2.6 to 2.5	555	480	385	320
		35	2.6 to 2.5	415	355	270	220
	11	20	2.8 to 2.7	1,960	1,780	1,370	1,310
		25	2.7 to 2.6	1,240	1,100	900	765
		30	2.6 to 2.5	860	745	595	490
		35	2.6 to 2.5	640	545	420	340
	12	20	2.8 to 2.7	2,910	2,640	2,240	1,940
		25	2.7 to 2.6	1,820	1,620	1,325	1,120
		30	2.7 to 2.6	1,300	1,130	895	740
		35	2.7 to 2.6	955	810	625	510
	13	20	2.8 to 2.7	4,220	3,840	3,250	2,820
		25	2.7 to 2.6	2,700	2,400	1,960	1,660
		30	2.7 to 2.6	1,880	1,640	1,300	1,070
		35	2.7 to 2.6	1,385	1,180	910	740

[a]Classes according to AASHO M 145.

[b]Initial TST-ADT is the maximum permissible volume of tractor semitrailer and combination vehicles at the beginning of the analysis period, which corresponds to design life. These amounts have been adjusted to account for 3 exemplary rates of annual growth during the analysis period.

Table 2. Statistical summary.

Item	Compare	Projects	Mean Difference Between Observed and Model PSI (percent)	Standard Deviation of Group Mean	Null Hypothesis t
All	All	138	+0.9	0.6	1.5
Joint space, ft	15	69	+3.7	0.9	4.1[a]
	20	69	-1.8	0.7	2.6[a]
Pavement thickness, in.	7	29	-1.1	1.4	0.8
	8	95	+2.1	0.7	3.0[a]
	9	7	-1.2	1.5	0.8
	10	7	-3.6	1.4	2.6[a]
Subgrade soil	A-1, A-2, A-3	42	+0.5	1.0	0.5
	A-4, A-5, A-6, A-7	96	-1.1	0.8	1.4
TST-ADT	0 to 300	105	+1.6	0.7	2.3[a]
	300 to 600	15	+0.5	1.4	0.4
	600 to 1,000	18	-1.6	1.2	1.3
Age, years	10 to 15	51	-0.6	0.8	0.7
	16 to 21	87	+2.3	0.8	2.9[a]

[a]Exceed sample error at 5 percent level of statistical significance.

The second method of statistical analysis was a simple linear regression relating observed and model serviceability indexes. The degree of correlation was influenced considerably by lack of initial data for all projects. However, the nature of the model equation is such that initial observed serviceability is that obtained by road meter measurement, which is affected by within-test variability. Initial model serviceability is additionally increased by variance related to SVF and SVO as time approaches or equals 0. Combination of all variances (those estimated at P_o and those measured at P_t) resulted in a correlation coefficient of 0.91 and standard error of 0.22, of which 0.08 can be attributed to measurement variation.

CONCLUSIONS

The performance equations provide a new approach to evaluation and design of plain pavements. Both serviceability index and a limit to transverse joint faulting are recognized. The method is unique in that it relates component parts of roughness slope variance to pavement thickness, joint spacing, traffic, subgrade soils, and age of pavement.

Weaknesses in the analysis are mostly a result of unequal partition of projects among model variables, restriction of project samples to a northern climatic environment, lack of data from projects where subgrade soils or granular subbases or both are specially treated with a variety of additives, and limitation of pavement thickness to 10 in. Strength of the analysis rests in the range of pavement ages and the fact that a high percentage of projects are still in service in 1973, with ages ranging to 27 years in both Minnesota and Wisconsin.

Companion studies of field performance are now under way in Georgia and California. These should give direction to the influences exerted by special subbases and benign climate. Recent construction (1972-1973) of 14-in. plain pavement, with random-spaced and skewed joints but without subbase on native silty-clay subgrade soil, in the western extension of the Illinois Tollway will offer another opportunity to evaluate performance features at an early age.

Continued use of and observation of excellent performance of 6-in. pavements on the Iowa county road system show that experimentation is no longer needed in this category. It is hoped that highway departments and the Federal Highway Administration will initiate and construct additional sections of thick plain pavement that meets the requirements set forth in this paper.

ACKNOWLEDGMENTS

Collection and interpretation of pavement performance data during a 16-year period were made possible by the cooperation and assistance provided by many people. Officials and engineers of the Minnesota, Wisconsin, North Dakota, and Iowa highway and transportation departments afforded sites for survey and project data essential for the report. The author wishes to thank each of these, and especially John Swanberg, formerly chief engineer of the Minnesota Department of Highways, who immediately recognized the value and authorized the continuing surveys of plain pavement performance in 1956.

REFERENCES

1. Performance and Design of Concrete Pavements Without Dowels and Distributed Reinforcement. Portland Cement Association, Nov. 1971.
2. Pavement Performance Survey—Final Report. Minnesota Department of Highways, 1968.
3. Concrete Pavement Designed for Minnesota Traffic. Portland Cement Association, Sept. 1960.
4. Plain Concrete Pavement Designed for Minnesota Traffic. Portland Cement Association, June 1972.
5. Plain Concrete Pavement Designed for Minnesota Traffic on Secondary Roads and City Streets. Portland Cement Association, Nov. 1972.

6. The AASHO Road Test: Report 5—Pavement Research. HRB Spec. Rept. 61E, 1962.
7. Carey, W. N., Jr., Huckins, H. C., and Leathers, R. C. Slope Variance as a Measure of Roughness and the CHLOE Profilometer. HRB Spec. Rept. 73, 1962, pp. 126-137.
8. Brokaw, M. P. Development of the PCA Road Meter: A Rapid Method for Measuring Slope Variance. Highway Research Record 189, 1967, pp. 137-149.
9. Brokaw, M. P. A 5-Year Report on Evaluation of Pavement Serviceability With Several Road Meters. HRB Spec. Rept. 116, 1971, pp. 80-91.
10. Bester, W. G. Performance of Concrete Pavements on County Roads in Iowa. HRB Spec. 116, 1971, pp. 174-178.
11. California Pavement Faulting Study. California Division of Highways, Jan. 1970.
12. Pavement Faulting Study: Extent and Severity of Pavement Faulting in Georgia. Georgia Department of Transportation, May 1972.

INSTRUMENT SYSTEM FOR MEASURING PAVEMENT DEFLECTIONS PRODUCED BY MOVING TRAFFIC LOADS

Gilbert Swift, Texas Transportation Institute, Texas A&M University

This paper describes a feasibility study that has led to the development of a first-generation instrument system for measuring transient pavement deflections. Accelerometers embedded in the pavement structure are used to sense the basic motion. Dual analog integration is used to obtain and record output indications proportional to displacement. The circuit characteristics are such that dynamic vertical movements as small as 0.002 in. or horizontal movements as small as 0.0005 in. occurring within less than 2 seconds can be recorded. These characteristics allow the system to be used for vehicle speeds of more than 25 mph and for any normal pavement structure. These performance characteristics could be altered, if desired, to accommodate the larger, longer movements that occur on bridge decks.

•THIS PAPER covers an investigation of the feasibility of developing an instrument system for measuring the dynamic transient deflections that occur in pavement structures under normal traffic loading conditions.

Measurements of pavement deflections have heretofore been limited to observation of rebound on removal of a previously stationary heavy vehicle (Benkelman beam testing) or to measurements, such as those obtained with the Dynaflect, of cyclic loads of 1,000 lb applied 8 times per second or to tests, such as the plate bearing test, of static loads.

Direct observation of the deflections induced by moving traffic loads has, so far as is known, not been possible for lack of suitable instrumentation. The principal hindrance to the development of instrumentation for this purpose is unavailability of a reference location that is sufficiently fixed in position and sufficiently near the point where deflections are to be measured. Accordingly, the present study undertook to determine the feasibility of a measuring system that employs inertial sensors and therefore requires no external fixed reference point.

BACKGROUND

This research began with a proposal in response to the U.S. Department of Transportation's prospectus regarding the development of transducers capable of measuring the recoverable vertical deflections on and beneath the pavement surface. The desired measurement range was from 0 to 0.05 in., with precision of measurement to 0.0001 in., and the flat frequency response was from 0 to 100 Hz.

Consideration of these requirements in the light of present technology of motion sensing devices and of existing techniques for applying them led to the conclusion that an inertial reference should be used and that accelerometers were available having the requisite characteristics for measuring such displacements at frequencies above 1.0 or possibly 0.1 Hz.

A paramount consideration underlying this plan was the fact that one aspect of the objective is believed to be unattainable. Specifically it is not deemed feasible to mea-

Publication of this paper sponsored by Committee on Pavement Condition Evaluation.

sure this wide span of small displacements over the entire frequency range down to and including 0 frequency. Any displacement measurement requires a reference point. If a physical tangible reference point is to be used, it must be sufficiently remote to remain undisturbed during the measurement to the extent set by the specified accuracy. In a pavement structure subject to normal traffic loading, suitable physical reference points are quite remote—at least as far as 50 ft distant on the surface and as deep as 20 ft or more from the load application point. The use of such reference points is considered incompatible with the specified performance, especially over a wide range of frequencies as great as 100 Hz or greater.

Accordingly, an inertial reference point, which may be regarded as the average position of the measuring point during the recent past, is believed to provide the most practical alternative. Displacements relative to an inertial reference point may be measured with great accuracy over wide ranges of amplitude and frequency by integrating the response of vertical (velocity or acceleration) transducers, such as geophones or accelerometers (1). The principal limitation introduced by the inertial reference is that displacement response down to 0 frequency (static response) is not attainable. However, it appears fully feasible to obtain flat displacement response from below 1.0 Hz to above 100 Hz and with the desired displacement ranges by using this approach.

Accordingly, the basic measuring system was originally proposed in 1969, but that proposal was abandoned when the prospectus was canceled in 1970. In the belief that a need exists for instrumentation that can record the deflections within a pavement structure under the transient loading provided by passing vehicles, a new but similar proposal was made to the Texas Highway Department in March 1971 to initiate the 1-year feasibility study described here. Such instrumentation should permit the study of pavement deflection behavior with respect to loads varying in magnitude and distribution and in speed.

CHRONOLOGICAL ACCOUNT

This study began in September 1971 with preparation of purchase specifications for the critical components. Accelerometers were purchased in accordance with the specifications given in Table 1.

Early in the circuit development phase it became apparent that, in a system of 2 integrators in cascade, it is extremely difficult to obtain long-term stability. If 2 integrators are directly coupled, an offset in the first necessarily produces the integral of this offset, which is a steady drift, at the input of the second. The output of the second integrator thereupon drifts at an ever accelerating rate. The stability was substantially improved by coupling 1 integrator to the other through a suitable capacitor that provides infinite attenuation at 0 frequency while passing all frequencies of interest (those above approximately 0.03 Hz in the present apparatus).

The first field installation of the system was made at the Texas A&M Research Annex. One accelerometer was buried in a typical flexible pavement roadway, and the vertical deflections produced by 1 passenger car and 1 truck were recorded. Dynaflect measurements (2) were also made on this site. However, before any horizontal displacements could be recorded, the opportunity arose to install the equipment in the vicinity of Fairfield, Texas, where vertical deflections were recorded on a private haul-road under specialized vehicles carrying loads as heavy as 240,000 lb. At this location approximately 100 recordings were made of the passage of these 3-axle vehicles, some fully loaded, others empty, at approximately 25 selected sites. Although most of these recordings were satisfactory, it was learned during this series of measurements that the accelerometers must be implanted firmly and relatively deep in the pavement system to avoid initial shifts of position upon application of the first few loadings after installation.

Suddenly shifting the sensitive axis of an accelerometer from the vertical to a slightly off-vertical position, at which it then remains fixed, produces an effect identical to that of introducing a continuous upward acceleration. This occurs because the accelerometer no longer has the earth's gravitational field directed along its sensitive axis, but instead

is acted on by the component of gravity in the direction of its axis. Such a shift of the axis produces a change in the apparent acceleration expressed by the following relation:

$$a = g\ (\cos\theta - 1) \tag{1}$$

where

a = apparent change in acceleration,
g = acceleration due to gravity, and
θ = angle between the sensitive axis and the vertical.

If the accelerometer were initially placed with its axis vertical, a quick nonrecoverable rotation through 1 deg would thus produce an apparent upward acceleration of 0.0002 g, which is approximately 0.08 in./s^2. The second integral of this acceleration corresponds to a displacement that reaches 0.040 in. (40 mils) at the end of 1 s and 160 mils at 2 s and continues to increase at an ever faster rate. The corresponding effect of rotation on a horizontally placed accelerometer is substantially less tolerable for 2 reasons. First, the apparent change in acceleration is given by

$$a = g \sin\theta \tag{2}$$

instead of by Eq. 1. Thus, it is nearly 100 times larger, or 0.018 g, for a 1-deg tilt. Second, the expected horizontal displacements in a pavement structure are generally on the order of 4 to 10 times smaller than the vertical displacements.

Accordingly, placement of accelerometers within the pavement structure, especially a horizontal accelerometer, must be done in such a way as to minimize the likelihood of incurring appreciable tilting movement after installation. This appears to be best accomplished by installation at an adequate depth, such as 6 or 8 in., and by surrounding the accelerometer with a rather rigid material, such as plaster of paris, before filling the remainder of the hole. The tendency for a tilting movement to occur during the measurement interval can be further diminished by application of repeated vehicular loadings to the emplacement area before the transient displacements are measured. That the final positions of the accelerometers be truly vertical or truly horizontal is relatively unimportant because the errors incurred by a permanent misalignment of a few degrees will be relatively small.

After the sensors were re-implanted in a second flexible pavement at the A&M Research Annex, a series of recordings was made by using a variety of vehicle speeds and loadings. That activity, the data analysis, and the preparation of this report represent the final phases of this 1-year feasibility study.

APPARATUS

Accelerometers

The Kistler model 305T servoaccelerometer used in this study meets the most exacting specifications of any commercially available accelerometer known to the author (Table 1). Almost unique among instruments of any kind is its ability to respond throughout a range of 10 million to 1, that is, from 5 μg to 50 g. However, for this application it would be preferable if its response ranged instead from 0.5 μg to 5 g.

The operating principle of a force-balance servoaccelerometer is shown by Figure 1, which has been taken from the Kistler Company's literature. The seismic mass of a few grams is nonpendulously suspended by 3 pairs of flexible arms that constrain it to move only axially. Movement of this mass is sensed by a capacitive displacement sensor, which, through its associated amplifier, produces a current in the forcer coil such as to restore the mass to its original position. The servo constraint is sufficiently "tight" that almost no appreciable movement ever occurs. Thus, the current in the forcer coil, to which the output signal is proportional, continuously corresponds to the force acting on the seismic mass. Inasmuch as force is equal to mass times acceleration, this current constitutes an accurate measure of the instantaneous acceleration acting along the sensitive axis.

The overall dimensions of the basic accelerometer are 1.125 in. diameter by 2 in. long. However, for use in this study the accelerometers were placed in slightly larger waterproof housings, as shown in Figure 2. Each accelerometer was equipped with a 40-ft shielded multiconductor cable terminated in a plug that fits a receptacle on the panel of the dual integrator unit.

Dual Integrator Unit

This unit, shown in Figure 3, provides 2 channels that may be used separately or simultaneously. Each channel accepts the output signal from an accelerometer, provides an adjustable nulling current to oppose the effect of gravity, and performs a dual analog integration on the accelerometer signals. Thus, it provides output signals proportional to displacement.

The instrument is equipped with meters that monitor the output of each integrator. The gravity-null control serves to center the pointer of the lower meter, and the bias control of the second integrator serves to center the upper meter. A push button below these controls restores the second integrator to 0. The circuit diagram of this unit is shown in Figure 4.

In the case of pavement deflections caused by moving traffic loads, it can be presumed that, for normal vehicle velocities above, say, 20 mph, the duration of the appreciable vertical deflections will not exceed about 2.0 s and that the duration of the appreciable horizontal displacements will be somewhat shorter. To reproduce such displacements faithfully by twice integrating the corresponding accelerations requires that the integration time be extended substantially beyond the actual duration of the signals. This requirement occurs because of unavoidable phase shift associated with the truncation of the integrator response at a finite frequency (or time) limit.

The present apparatus has been constructed with an integration time of 6.0 s for the vertical signal channel and 1.2 s for the horizontal channel. Phase shift effects are less serious in the horizontal channel, despite its shorter integration time, because the horizontal motions are inherently bidirectional and the vertical displacements are always downward.

The response characteristics of each 2 dual-integration channels are shown in Figures 5 and 6. Figure 5 shows the overall response in the frequency domain and may be regarded as indicating the system response to sinusoidal input signals of equal magnitude with respect to their frequency. The upper portion of Figure 5 shows that the frequency range over which the gain diminishes at the rate of 100:1 per decade of frequency (the slope that corresponds to dual integration) extends from 0.05 to beyond 1,000 Hz for the vertical channel and that the maximum gain (2 integrators in cascade) is 100,000 for each channel. This gain is in addition to the gain of the internal amplifiers within the accelerometers. The response with respect to displacements is shown in the lower portion of Figure 5.

In a channel having these characteristics, a change within the first integrating amplifier equal to 1 μV, or an equal change at the output of the accelerometer, necessarily results in an output signal that rises at the rate of 1 V/s. Should a change of this magnitude occur, while the system is being used to record pavement displacements, the pavement would falsely appear to have suddenly begun to move at the rate of several mils per second. Accordingly, for satisfactory operation of the system, the stability of the first amplifier and of the accelerometer is required to be substantially better than 1 μV. In practice in the field, it has been found feasible to set the compensating controls of the integrators such that the output does not drift appreciably during a period as long as 2 hours, provided the accelerometers are disconnected. However, random changes that occur in the accelerometer output signals make it impossible to maintain freedom from drift, except for brief periods ranging as high as perhaps 30 s. This effect, which would appear to require a major accelerometer-development effort to overcome, sets the attainable limits with respect to measuring small transient displacements that occupy a finite period of time.

The limits, with the present accelerometers, have been found to be in the vicinity of 2.0 mils minimum for vertical displacements occupying 2.0 s and 0.5 mil minimum for

Table 1. Specifications for accelerometer.

Item	Specification
Range, g max	±50
Dynamic range, g min	5,000,000
Resolution, g	0.000005
Sensitivity, A/g	0.00002
Damping factor	0.6 to 0.7
Output impedance, MΩ min	1.0
Frequency range	
dc, Hz	to 500
Flat, percent	±5
Power supply voltage, V dc	±15
Linearity (independent), percent full scale	0.01
Output at 0 g, A max	0.000001
Temperature, percent/F max	
Coefficient of sensitivity	0.03
Zero shift	0.05
Shock limit, any axis, g (ms)	100(5)
Suspension	Nonpendulous
Weight, oz	3.4
Length, in. max	$2^{1}/_{16}$
Diameter, in. max	
Body	1
Mounting flange	1.125
Estimated cost each, dollars	750

Note: Must be interchangeable with Kistler Instrument Company model 305T and equipped with isolated self-test coil and terminals and 40-ft long shielded cable.

Figure 1. Working elements of a force-balance servoaccelerometer.

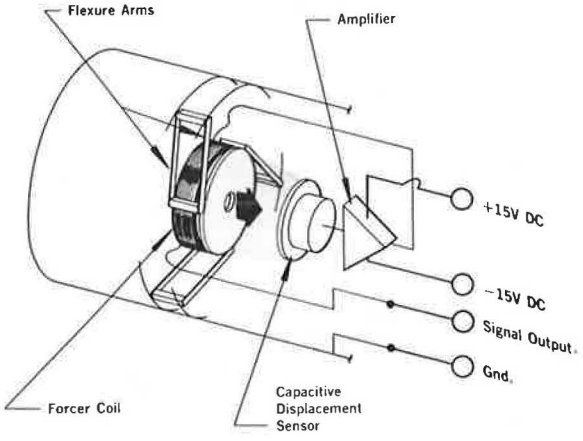

Figure 2. Accelerometer mounted in waterproof housing.

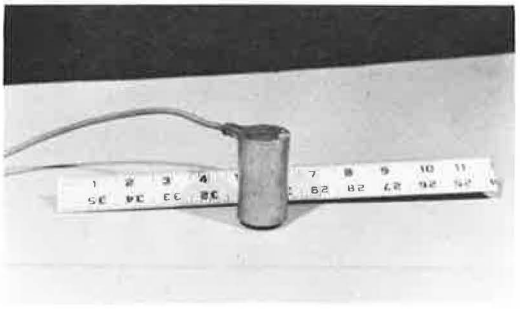

Figure 3. Pavement displacement measuring system.

Figure 4. Circuitry of 2-channel dual integrator.

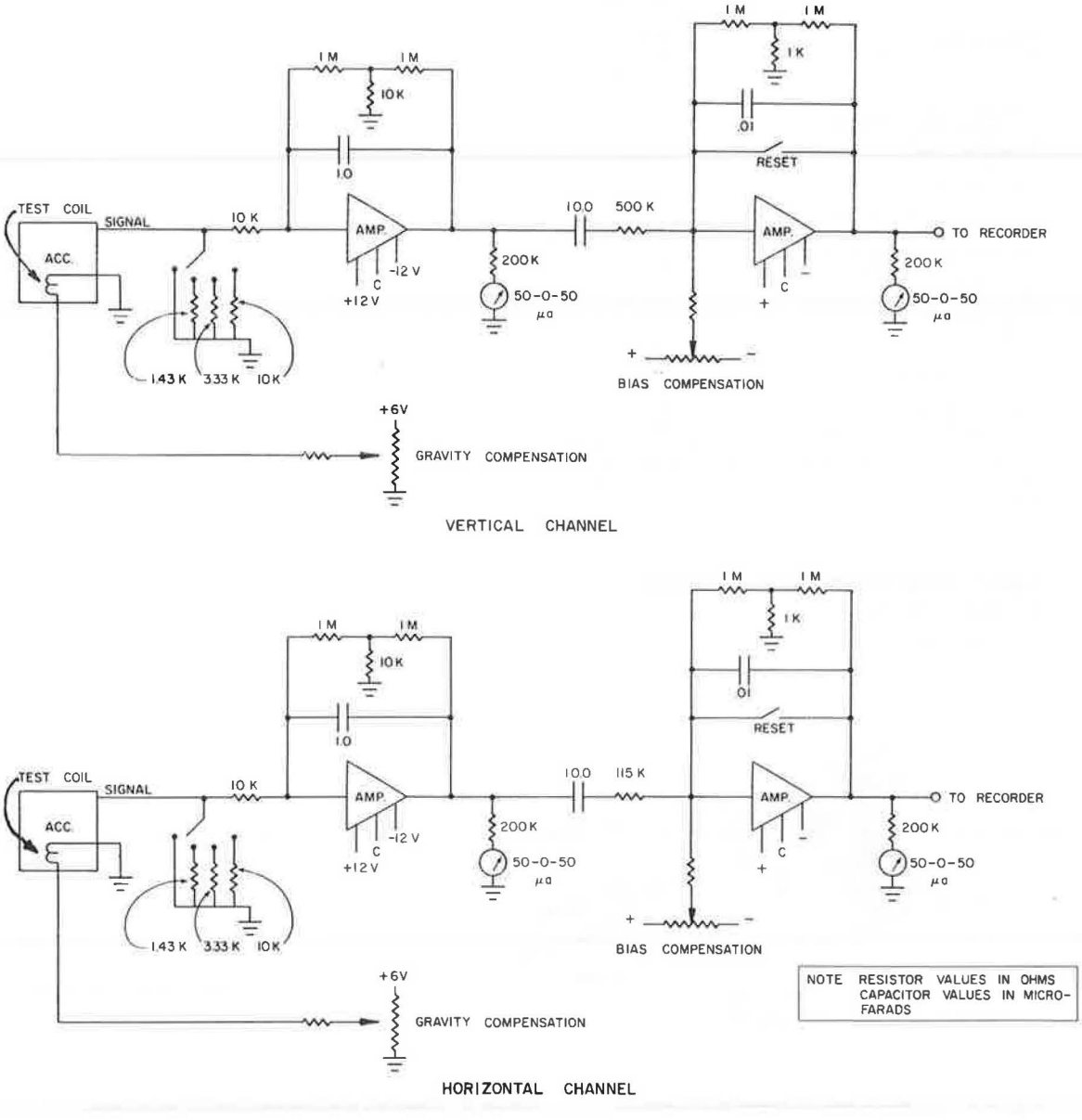

horizontal displacements occupying 0.5 s. However, repetitive sinusoidal displacements, within the frequency range 0.5 to 400 Hz, can be measured down to the order of millionths of an inch. Simple alterations of the circuitry can accommodate slower transient displacements, provided their magnitudes are correspondingly greater, and vice versa.

The impulse response of the vertical channel is shown in Figure 6 to indicate the type of distortion that is introduced by truncating the frequency response. (The response shown is that of the vertical channel of the dual integrator unit. The response of the horizontal channel would appear the same if drawn to a time scale approximately one-fourth as long.) Distortion of the signal is substantially negligible for impulses that are short compared with 1.0 s but becomes substantial as the impulse duration approaches or exceeds 5.0 s. Phase correction networks that diminish this effect during the initial 1- or 2-s interval were installed, but were removed from the circuit because of their deleterious effects on the longer period behavior. This effect is more severe for the rectangular impulses shown in the figure than for the rounded shapes represented by pavement deflections. Figure 7 shows typical pavement behavior. The upper curve depicts the variation of acceleration versus time, the central curve indicates the first integral of the acceleration, which is the velocity, and the lower curve shows the second integral, which is the displacement, produced by the passage of a 2-axle vehicle.

Recorder

A recorder found to be suitable for use in the field with the displacement measuring system is that shown in Figure 3. It is basically an Astro-Med model 102C modified to operate from batteries. A 2-channel recorder would make it possible to record from both channels of the integrator unit simultaneously.

System Configuration

Power for operating the accelerometers and the integrator unit is obtained in the field from a pair of 12-V lantern batteries. The recorder requires, in addition, the use of a 12-V storage battery.

The entire system is readily transported and operated in the rear seat of a passenger car and may be connected to the car battery. A convenient procedure consists of implanting the horizontal and vertical accelerometers at equal depths in separate holes drilled into the pavement structure, with known spacing of a few feet along the wheelpath.

SYSTEM CALIBRATION

Calibration of the overall displacement measuring system, comprising an accelerometer and dual integrator, cannot be done statically because the system response does not extend to 0 frequency. Accordingly, calibration is best accomplished by application of a periodically repetitive displacement having a known amplitude. A very convenient device for this purpose is the Dynaflect calibrator unit, which can provide cam-actuated movements having double amplitudes from 0.005 to 0.020 in. at frequencies within the range 1 to 10 Hz. The actual movements of the Dynaflect calibrator were verified and compared with "static" displacements by using the optical displacement tracker (4), as shown in Figure 8, to measure the dynamic as well as the static displacements of the calibration platform. The calibration factors for the system thus determined are as follows:

Gain Step	Vertical Channel (V/mil)	Horizontal Channel (V/mil)
1	0.1	0.460
1/2	0.0495	0.235
1/4	0.0255	0.119
1/8	0.0130	0.0595

Figure 5. Integrator response in frequency domain.

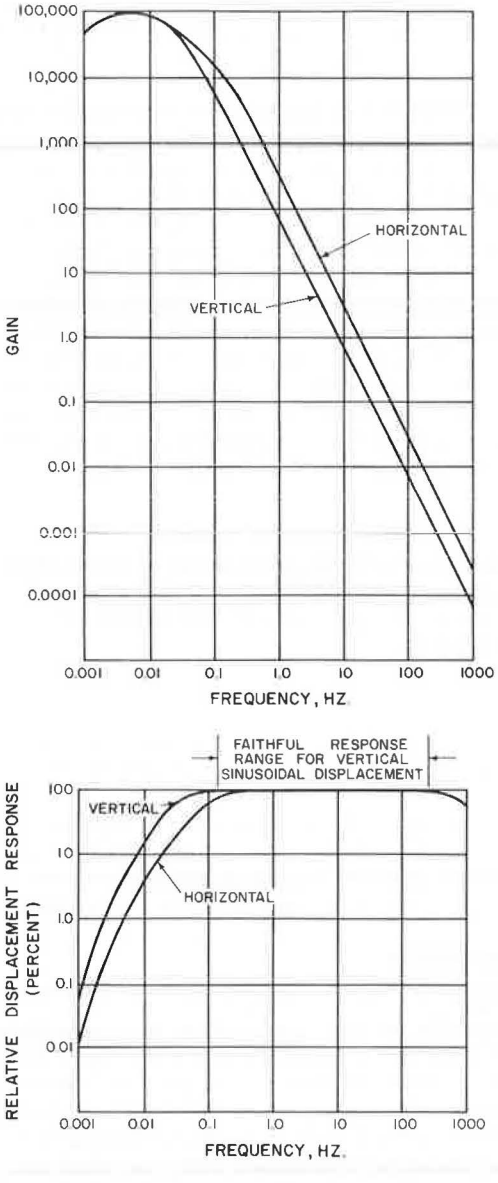

Figure 6. Integrator response in time domain.

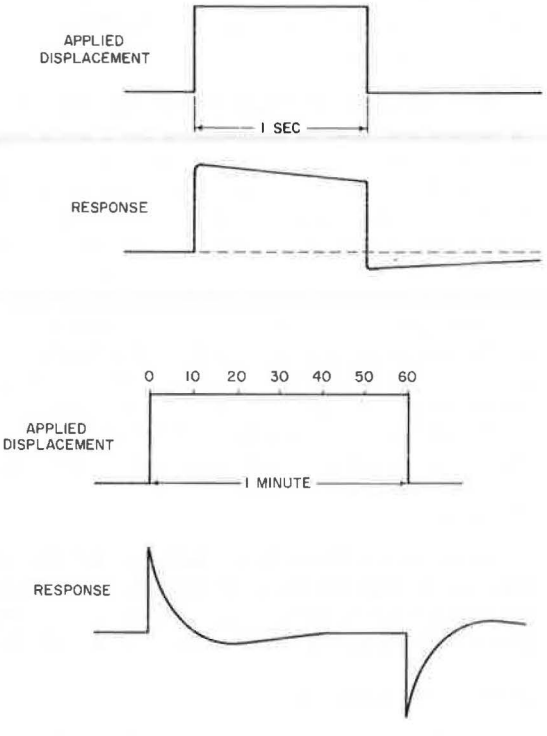

Figure 7. Shapes of dynamic vertical acceleration, velocity, and displacement versus time in a typical pavement on which a 2-axle vehicle passed.

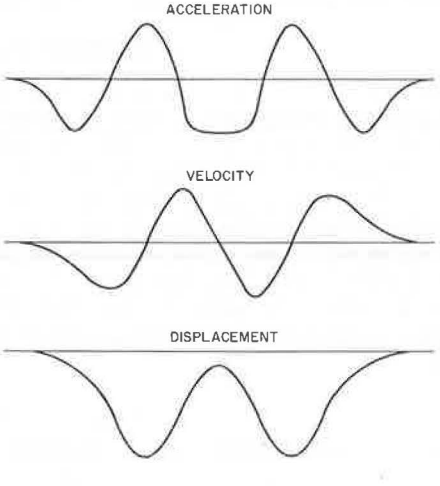

The strip-chart recorder, as used with the system, has a sensitivity as great as 1,000 (chart divisions) mm/V. Thus the overall system recording capability extends as follows: 1-mm chart deflection = 0.1 mil (0.0001 in.) pavement deflections for the vertical channel, and 1-mm chart deflection = 0.02 mil (0.00002 in.) for the horizontal channel. The chart-paper drive speed is 10 cm/s; each 1-mm division along the record thus represents 0.01 s.

MEASUREMENTS

A typical record of the vertical deflection produced by a passenger car is shown in Figure 9a. The deflection basin, as measured by Dynaflect at the same location, is shown plotted to the same scale in Figure 9b.

Figure 10 shows 3 recordings obtained on a private haul-road during the passage of an exceptionally large heavy vehicle. These observations were later used in another study to evaluate the elastic constants of the pavement structure by comparison with deflections computed from elastic theory. When ⅔ loaded, this vehicle applies wheel loads of 26,500, 72,000, and 78,000 lb respectively at its front, drive, and rear wheels. Its overall wheelbase, 52 ft long, requires nearly 1.8 s to pass the measuring location at a speed of 20 mph. The recorded deflections necessarily occupy a slightly longer period. Two of the recordings are satisfactory, and the magnitude and shape of the deflection basins can be readily determined from these records. The upper record, however, illustrates the effect of a drift that began shortly after the passage of the second wheel over the sensor. A repetition will usually have better than a 50/50 chance of producing a satisfactory record. This chance is further improved if the deflections are of shorter duration, such as from a faster vehicle or a shorter wheelbase or both.

Two recordings of the vertical deflections produced by a lightly loaded conventional truck are shown in Figure 11. The lower record shows the effects of rough surface conditions located approximately 50 ft away from the measuring point. The vehicle is still bouncing as it passes the sensor. The upper record is from a location of the same road, more remote from the rough area.

CONCLUSIONS

1. An instrument system has been developed that demonstrates the feasibility of the original approach and that is capable of recording pavement deflections under moving traffic loads.

2. It appears that, in its present form, this measuring system can be used in a field test program to obtain useful information concerning the deflection behavior of various pavement structures under controlled vehicular and random traffic loadings. It also appears that measurements of this behavior have not heretofore been obtainable. [Since completion of this work, a brief description of a similar instrument developed in Denmark has appeared in the appendix to a paper by Bohn et al. (5).]

3. With minor modification, the present apparatus could be adapted to record the larger but longer duration movements of bridge decks subjected to traffic loading.

4. Limitations of the system have been noted as follows:

a. Only one channel, either the vertical or the horizontal, may be recorded at a time. Purchase of a dual-channel recorder would remove this limitation.

b. The present circuit configuration, chosen to accommodate deflections on the order of 0.001 in., requires that, to be faithfully recorded, the transient deflections not exceed 1- or 2-s duration. With vehicles of conventional wheelbase, this necessitates travel at speeds of 20 mph or greater. Response to smaller and slower transient displacements requires accelerometers having characteristics beyond those known to be commercially obtainable.

c. Requirement for rigid implacement of the accelerometers has been found to be critical, but it is believed that the embedment technique developed during this study is adequate. Implantation of accelerometers at depths less than 6 in. in flexible pavement sections or less than 3 in. in rigid pavements is not recommended. Because the deflections at such depths are ordinarily not very different from the deflections closer to the surface, this limitation is not believed to impair the usefulness of the system.

Figure 8. Movement of Dynaflect calibrator unit, on which accelerometer has been mounted for calibration, verified by optical displacement tracker.

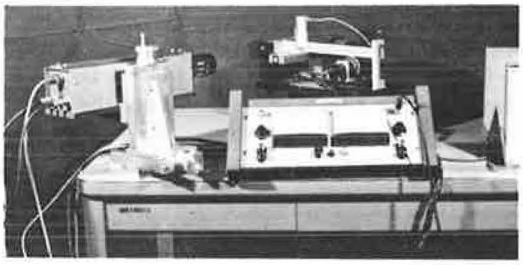

Figure 9. Deflection basins (a) produced by passenger car at 30 mph and 1,000-lb front 675-lb rear wheel loads and (b) measured by Dynaflect with 1,000-lb loading at 8 Hz.

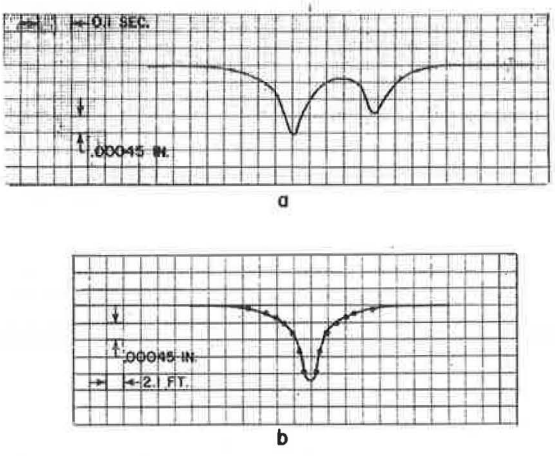

Figure 10. Records obtained on haul-road from passage of heavy vehicle.

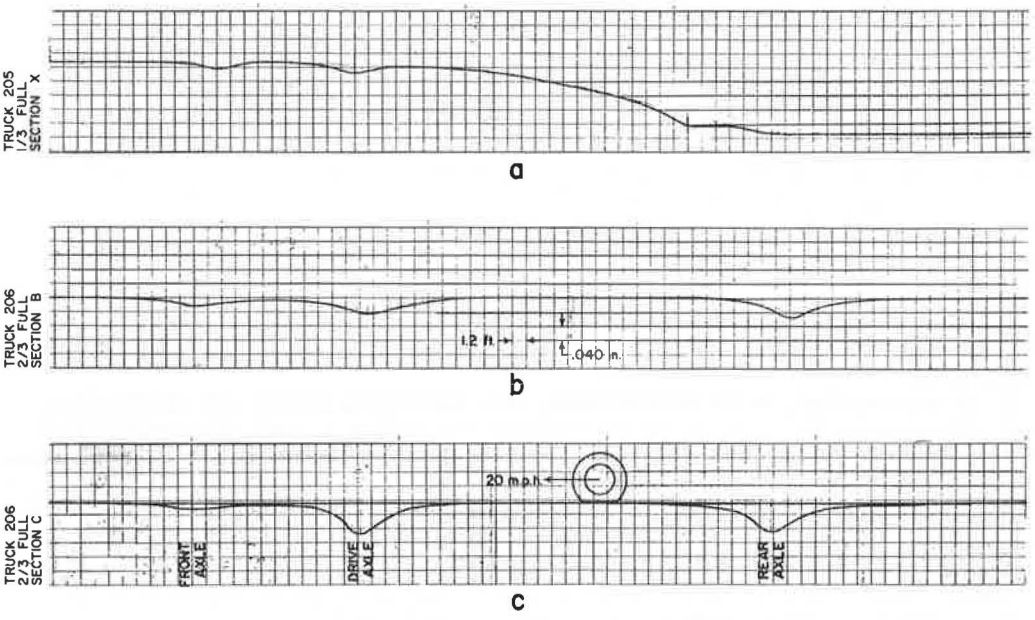

Figure 11. Deflection basin due to truck (a) traveling at 25 mph on relatively smooth pavement and (b) bouncing after passing over rough area 50 ft away.

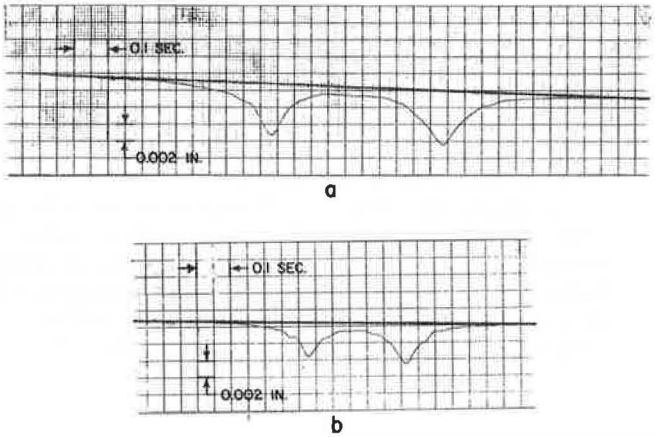

d. Imperfections (drifts) of the accelerometer output signals represent the principle limitation to the measurement of small slow displacements. Occasionally (less than 50 percent of the time), a drift spoils the record of a given vehicular traverse. Accordingly, to record the deflections produced by a specific vehicle sometimes requires the vehicle to repeat its traverse.

ACKNOWLEDGMENT

This 1-year feasibility study was conducted by the Texas Transportation Institute as part of the cooperative research program with the Texas Highway Department and the Federal Highway Administration. The author wishes to thank all members of the institute who assisted in the work leading to the present paper. The author is grateful to the Texas Highway Department for its interest and cooperation, especially to James L. Brown and L. J. Buttler of the Highway Design Division for their support of this research. The contents of this paper reflect the views of the author, who is responsible for the facts and the accuracy of the data. The contents do not necessarily reflect the official views or policies of the Federal Highway Administration. This report does not constitute a standard, specification, or regulation.

REFERENCES

1. Slater, J. M. Inertial Guidance Systems. Reinhold Publishing Co., New York, 1964, pp. 145-194.
2. Scrivner, F. H., Swift, G., and Moore, W. M. A New Research Tool for Measuring Pavement Deflection. Highway Research Record 129, 1966, pp. 1-11.
3. Graeme, J. G., Tobey, G. E., and Huelsman, L. P. Operational Amplifiers. McGraw-Hill, New York, 1971, pp. 213-218.
4. Moore, W. M., Swift, G., and Milberger, L. J. Deformation Measuring System for Repetitively Loaded, Large-Diameter Specimens of Granular Material. Highway Research Record 301, 1970, pp. 28-39.
5. Bohn, A., Ullidtz, P., Stubstad, R., and Sorensen, A. Danish Experiments With the French Falling Weight Deflectometer. Proc., 3rd Int. Conf. on Structural Design of Asphalt Pavements, Univ. of Michigan, Ann Arbor, Vol. 1, 1972, pp. 1119-1128.

USE OF PROFILE WAVE AMPLITUDE ESTIMATES FOR PAVEMENT SERVICEABILITY MEASURES

Roger S. Walker and W. Ronald Hudson, Center for Highway Research, University of Texas at Austin

For a number of years, engineers were interested in developing objective criteria for designing and maintaining highways on the basis of pavement performance, i.e., riding quality. The development of the serviceability performance concept by Carey and Irick provided a method for developing such criteria. Although this method may seem rather crude to some, it is still the best method available of those that consider the subjective riding-quality measurements of highway users. Several classes of instruments have been used for obtaining the objective measurements required for this concept; one is the slope-variance measuring device. Serviceability index models were developed based on slope variance of road profile data obtained with the surface dynamics profilometer. Subsequently, a serviceability index model was developed based on profile wave amplitude estimates of the road profile data. This latter model has been found to be superior to the slope variance model and has now been used extensively for providing measurements in Texas. This paper describes this model and some of the results of its uses in field operations.

•FOR A number of years, engineers have sought an objective measure of the riding quality of highways in order to establish better highway design and maintenance procedures. Various measuring devices have been proposed and tried in attempts to provide objective data to indicate a pavement's riding quality. The problem was further complicated in these initial attempts because there were no means of calibrating these roughness data when they were obtained; e.g., How rough is rough, or how smooth is smooth? Finally, during the planning for the AASHO Road Test, Carey and Irick (4) developed a serviceability concept that serves as a basis for most current pavement rating systems and is based on a subjective evaluation of the road user's opinion of the pavement at any given time.

Because this concept requires correlation between objective physical measurements of pavement characteristics and subjective measurements of the pavement, the development of reliable serviceability index (SI) prediction models is not a trivial task, for it requires some type of an adequate statistically designed highway rating experiment for the subjective measurements and some type of roughness measuring device for the objective measurements.

The availability of the surface dynamics profilometer (SDP) provided a profile-measuring device with which roughness characteristics could be obtained. The Texas Highway Department purchased the first such profilometer (15). In subsequent research (12), a large-scale pavement rating experiment was conducted in which a panel of typical road users riding in typical American automobiles expressed their opinions on the riding quality of a group of pavements. The sites selected for the rating sessions represented different topographical areas of Texas. The road profiles of these test site pavements were measured with the SD profilometer, and pavement deterioration (con-

Publication of this paper sponsored by Committee on Pavement Condition Evaluation.

dition survey) information was obtained. Roughness index and slope variance statistics computed from those data were then used for characterizing the pavement sections.

The roughness statistics and the condition survey information were correlated to the mean panel present serviceability rating (PSR) to get pavement SI prediction models (12, 16).

Because of the complexities of a road profile, a much better possibility of characterizing a pavement section appears to be by its power spectrum or wavelength components than by a single statistic such as slope variance. With wavelength information, various problems such as profilometer sensor wheel bounces can be isolated or accounted for to provide more accurate pavement characterizations.

It would also appear that a predictor of riding quality at least as good and probably better could be obtained by correlating the effects of individual frequencies with PSR through multiple regression analysis techniques. By this method, only those frequencies that are found to be highly correlated with PSR could be included, and the rest could be discarded.

SI MODEL DEVELOPMENT USING PROFILE WAVE AMPLITUDE ESTIMATES

To predict a pavement serviceability index as a function of profile wavelength, the following linear model is considered:

$$SI = \beta_0 + \beta_1 X_1 + \beta_2 X_2 + \beta_3 X_3 + \ldots + \beta_N X_N + \epsilon \quad (1)$$

where

β_i = linear model parameters, and
X_i = average wavelength amplitude.

Average wavelength amplitudes are considered the independent variable, for these values obviously affect the riding quality or roughness of a pavement and are more easily realized physically by the highway engineer than are, say, the power spectrum estimates. Such amplitudes may be obtained from the power spectrum estimate from

$$X_i = \sqrt{2Q_i \Delta f} \quad (2)$$

where Q_i represents the 2-sided power or variance spectrum component for the ith frequency band, and Δf is the frequency containing this variance.

In the development of the model, the original rating session data (12) were reexamined by using the mean panel ratings from 86 representative test sections throughout Texas. The power or variance spectrum estimates for each of the road profiles of these 1,200-ft sections were then obtained. [Walker and Hudson (18) discuss the assumptions necessary for power spectrum estimates of road profile data obtained with the SDP.] The power spectrum estimates for the right and left wheelpaths and the cross power were computed for each profile section.

Figure 1 shows the relation between PSR and road profile power spectrum estimates. The power spectrum estimates for several frequencies or wavelength bands were computed and are shown for various road roughness classes, as indicated by PSR. That is, the 86 pavement sections covering the gamut of pavement roughness were grouped as shown (PSR intervals from 4.5 to 5.0, 4.0 to 4.5, and so on), and their average spectrum amplitudes were obtained. In general, the rougher the road is, the greater the spectrum amplitude is. This figure thus indicates that there should be some appropriate equation that relates SI to power spectrum estimates and thus wave amplitudes. The problem then is to determine which wavelengths or bands to include in this function or model.

A stepwise regression procedure (8) was used. The PSR values from the original rating session experiment were the dependent variables, and the logs of the wavelength amplitudes were the independent variables. Regression analysis assumes that the dependent variable is the only random variable. Because there are errors in these in-

dependent variables and these errors are not symmetrically distributed [power spectrum or variance estimates are distributed according to the chi-square distribution (2)], they would tend to bias the results unless these errors were symmetrically distributed. Thus, the log transformation on these values was used. The use of the log transformation in this case is rather intuitive but is supported by Scheffe (13) when the analysis of variance on variance estimates is used. (It should be noted that, after the log transformation is performed, only a constant separates the power spectrum amplitudes from the profile wave amplitudes. Thus, similar results can be obtained by using power spectrum estimates as the independent variables rather than wave amplitudes.) In addition, the independent variables were centered before the regression was performed.

An ideal model for riding quality is characterized by realistic and relatable terms. However, an extensive search revealed no such ideal model. Some of the problems in modeling procedures that could have prevented obtaining such a model are presented here.

First, the linear scale rating method that was used and is similar to the one used at the AASHO Road Test has been criticized as not giving an adequate subjective representation. Thus, if not all pavement classes are properly distinguished by the raters, it becomes difficult if not impossible to obtain an appropriate model.

Second, for the higher frequencies (or shorter wavelengths), adjacent power spectrum estimates are highly correlated. For the lower frequencies (or longer wavelengths), this correlation drops significantly. For example, the correlation coefficient R between the first and second bands (0.0116 and 0.0231 cpf) was 0.599. For bands above 0.231, these values increased to above 0.9. These upper frequencies, however, were not highly correlated with PSR. Also, when the values were examined, average amplitude levels for frequencies of 0.231 cpf and higher were much less than 0.01 ft for the smoother roads; that is well beyond the measuring accuracies of the vehicle. As roads get rougher, these levels increase in the same proportion. Because these frequencies probably affect roughness for some of the classes of rougher roads, a better technique should be used for including their effect in the equation. Because of their high interrelations and their unreliability for the smooth roads, these values were omitted. A satisfactory prediction model, however, was obtained by including the longer wavelengths (or lower frequencies). These values, as noted, were not very interrelated and were found suitably correlated to PSR. Thus, the model does seem to indicate that these wavelengths are important in riding quality.

Initially a 32-band model was developed (52 deg of freedom) that included 3 amplitude terms centered at 0.023, 0.046, and 0.069 cpf, 3 amplitude interaction terms, 2 cross-amplitude terms, and 1 pavement type term, or a total of 9 deg of freedom for the regression and 76 for the residual. The correlation coefficient was only 0.9 (R^2 = 0.81), and there was some lack of fit. This model is as follows:

$$\begin{aligned} SI = {} & 3.24 - 1.47X_1 - 0.133X_2 \\ & - 0.54X_3 + 1.08XC_1 - 0.25XC_2 \\ & + 0.08X_2X_3 - 0.91X_3X_4 + 0.67X_6X_{10} \\ & + 0.49T \end{aligned} \tag{3}$$

where

$X_1 = \log A_{0.023} + 2.881$;
$X_2 = \log A_{0.046} + 4.065$;
$X_3 = \log A_{0.069} + 4.544$;
$X_4 = \log A_{0.093} + 4.811$;
$X_6 = \log A_{0.139} + 5.113$;
$X_{10} = \log A_{0.231} + 5.467$;
$XC_1 = \log C_{0.023} + 3.053$;
$XC_5 = \log C_{0.116} + 5.659$;
A_i = average right and left wavelength amplitude, in in.;
C_i = cross-amplitude, in in.;

i = frequency band, in cycles/ft; and
T = 1 for rigid pavements and 0 for flexible pavements.

The regression analysis results are as follows:

Source	Degrees of Freedom	Sum of Squares	Mean Square	F Ratio
Regression	9	47.68	5.297	37.46
Residual	76	10.75	0.1414	

Correlation coefficient R = 0.90, and standard error for residuals = 0.38.

An attempt was made to obtain a better model by rerunning the same regression procedure on 64-band power spectrum estimates (32 deg of freedom for each estimate) of the same data. The correlation coefficient for the model in this case increased to 0.94, and the standard error of residual decreased to 0.32 (no lack of fit). Although the same frequency band centers entered the model, more interaction terms were included. Repeat runs using both models revealed little difference; thus, the 32-band model is illustrated because of fewer terms, greater regression significance, and more reliable power spectrum estimates.

A desirable regression model should make sense physically, show suitable correlation between the dependent and independent variables, exhibit an acceptable lack of fit, and produce reasonable results in actual field use.

This model appears to make sense in that the greater the amplitude terms are, the less the SI readings are. The cross-amplitude term (which comes from cross power) is a little more difficult to define physically; however, it indicates the similarities between the 2 profile heights (cross roll or roughness effects). The interaction terms are useful in fitting the model.

The best practical test for the model is how well it performs in use. The performance of this model on more than 300 miles of pavements has been quite acceptable, and it is currently being used for all SI measurements involving the SDP. Table 1 gives a typical set of repeat data runs. That is, 3 different 1,200-ft pavement sections (none of which was included in the original rating sessions) were each run 5 times with the SDP. The data were digitized, and the power spectrum estimates were computed for each run. The appropriate terms were then computed, and the SI was obtained for each run.

USES OF THE SI MODEL

As indicated, the current model is being used for all SI measurements involving the SD profilometer. In addition, because of the stability of the model, primarily due to the internal calibration facilities of the SD profilometer, these measurements are also currently being used as a standard for SI measurements by the Mays road meter (MRM) (19). The relation found between the MRM cumulative roughness readings, in in./mile, and the SD profilometer SI measurements is

$$SI = 5e^{-\left(\frac{\log_e M}{\beta}\right)^{\alpha}} \quad (4)$$

where

M = MRM roughness readings, in./mile; and
β and α = MRM instrument coefficients (regression coefficients).

This equation was obtained by regressing the MRM readings onto the SI values and then solving for SI. A typical plot of this equation for one of the MRM devices calibrated to the SI standard is shown in Figure 2. Table 2 gives the results from different MRM calibrations during this past year.

Figure 1. Wavelength versus power spectrum estimates for rating session data.

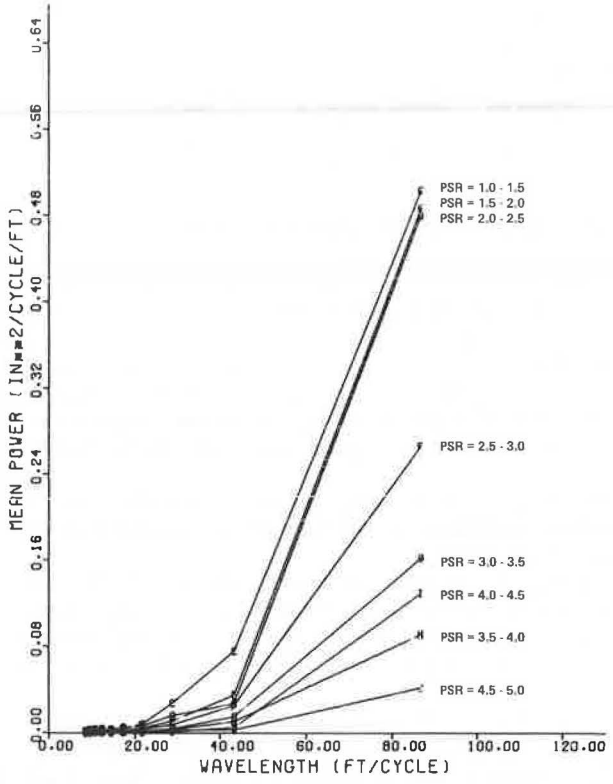

Table 1. SI replications.

Test	Run	SI
1	1	4.50
	2	4.53
	3	4.61
	4	4.57
	5	4.57
2	1	4.18
	2	3.70
	3	3.76
	4	3.98
	5	4.14
3	1	2.02
	2	1.69
	3	1.53
	4	1.92
	5	1.86

Table 2. MRM-SDP SI calibration results.

MRM	β	α	SI Model Error	R^2
1	5.679	5.1	0.327	0.998
2	5.343	4.6	0.314	0.997
3	5.192	4.0	0.292	0.994
4[a]	5.547	4.9	0.391	0.997
5	5.720	5.1	0.351	0.997
6	5.971	4.0	0.328	0.996
7	5.564	4.0	0.337	0.996
8	5.602	5.0	0.269	0.998

[a]Mechanical Mays road meter (the other results shown are for the new electronically controlled models manufactured by Rainhart Company).

Figure 2. SI values of SDP versus roughness readings of MRM.

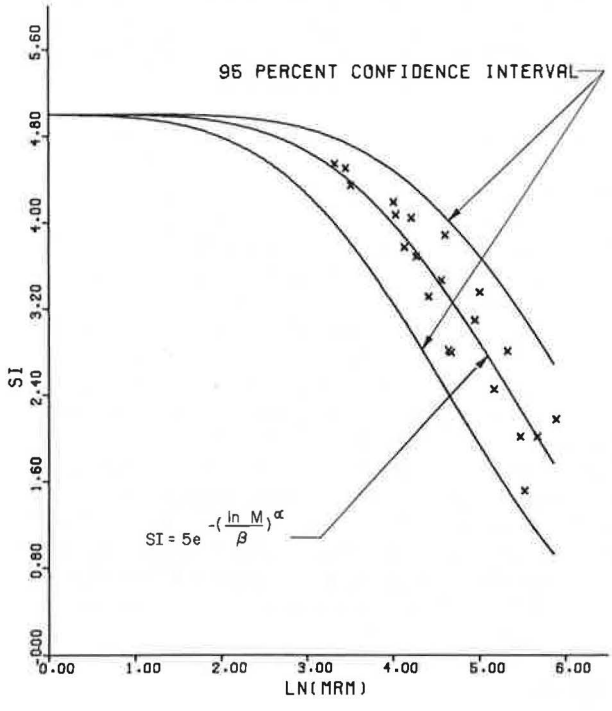

Table 3. Amplitudes for PSR intervals.

PSR Interval	Number of Sections	Frequency (cpf)	Power Mean ($in.^2$/cpf)	Amplitude of Upper 99 Percent (in.)
4.0 to 4.5	10	0.012	1.2945	1.4134
		0.023	0.0520	0.2833
		0.035	0.0159	0.1566
		0.046	0.0076	0.1085
		0.058	0.0044	0.0823
		0.069	0.0028	0.0661
		0.081	0.0025	0.0617
		0.092	0.0022	0.0580
		0.104	0.0018	0.0526
		0.116	0.0017	0.0516
2.0 to 2.5	10	0.012	2.6602	2.0262
		0.023	0.2538	0.6258
		0.035	0.0759	0.3422
		0.046	0.0307	0.2176
		0.058	0.0249	0.1960
		0.069	0.0174	0.1641
		0.081	0.0108	0.1291
		0.092	0.0087	0.1161
		0.104	0.0082	0.1127
		0.116	0.0084	0.1140

By using the SI measurements of the SDP as a standard, a general set of calibration, operation, and control procedures has been developed for all MRM devices purchased by the Texas Highway Department. These procedures provide a means of measuring roughness in standard roughness units for all MRM devices and thus enable 2 separate instruments, installed in separate vehicles, to get the same roughness readings for the same road section.

In addition to being used for SI measurements, this model can also provide useful information in regard to the importance of the various wavelength amplitudes. The original power spectrum estimates from the large-scale rating session might also be of interest. For instance, the average power spectrum estimates for various classes of roads can be obtained and used for computing the wave amplitudes (Fig. 1). Table 3 gives a summary of this information for the various road classes for the PSR intervals of 4.0 to 4.5 and 2.5 to 3.0. For each frequency band of these 2 intervals, the mean power and the corresponding upper 99 percent confidence band are given. This upper range for the individual amplitude term is also given. This upper band might be useful in construction control studies, for typically mean amplitude values should not exceed these upper ranges (control of such specifications is, of course, another matter). For example, roads in Texas are typically designed to allow deviations from a 10-ft straightedge to be no greater than $\frac{1}{8}$-in. As noted, roads in the roughness class 2.5 to 3.0 (frequency near 0.104) are near this upper range. The values given in this table however, should be viewed as rough estimates, for their accuracy depends on the statistical assumptions necessary for accurate power spectrum estimates (18), which are not exactly met. Another useful analysis method would be to examine the profile data with digital filtering techniques. With such techniques, the amplitudes within specific frequency bands can be examined as a function of distance.

SUMMARY

A model for measuring highway roughness or riding quality based on spectrum estimates of road profile data has been presented. The road profile data are obtained with the surface dynamics road profilometer. Through actual field use on several hundred miles of varied highway pavements, the model has been found to provide acceptable riding-quality measurements. The application of some of its uses in field operations has also been briefly described. This included the use of SI measurements obtained with this model as a measurement standard for Mays road meters.

ACKNOWLEDGMENTS

This investigation was conducted at the Center for Highway Research at the University of Texas at Austin. The authors wish to thank the sponsors, the Texas Highway Department and the Federal Highway Administration. The contents of this report reflect the views of the authors, who are responsible for the facts and the accuracy of the data presented. The contents do not necessarily reflect the official views or policies of the Federal Highway Administration. This report does not constitute a standard, specification, or regulation.

REFERENCES

1. Bergland, G. D. A Guided Tour of the Fast Fourier Transform. IEEE Spectrum, July 1969.
2. Blackman, R. B., and Tukey, J. W. The Measurement of Power Spectra. Dover Publications, New York, 1958.
3. Brigham, E. O., and Morrow, R. I. The Fast Fourier Transform. IEEE Spectrum, Vol. 4, Dec. 1967, pp. 63-70.
4. Carey, W. N., Jr., and Irick, P. E. The Pavement Serviceability-Performance Concept. HRB Bull. 250, 1960, pp. 40-58.
5. Cooley, J. W., Lewis, P. A. W., and Welch, P. D. Historical Notes on the Fast Fourier Transform. Audio and Electroacoustics, IEEE Trans., Vol. AU-15, June 1967.

6. Cooley, J. W., Lewis, P. A. W., and Welch, P. D. The Fast Fourier Transform Algorithm and Its Application. IBM, Res. Paper RC-1743, Feb. 1967.
7. Darlington, J. R. Evaluation and Application Study of the General Motors Corporation Rapid Travel Profilometer. Michigan Department of State Highways, Res. Rept. R-731, April 1970.
8. Draper, N. R., and Smith, H. Applied Regression Analysis, 1st Ed. John Wiley and Sons, 1967.
9. Kozuh, J. A. A New F-Test Strategy for Selecting the Best Regression Equation. Univ. of Texas at Austin, PhD dissertation, Aug. 1971.
10. Nakamura, V. F., and Michael, H. L. Serviceability Ratings of Highway Pavements. Highway Research Record 40, 1963, pp. 21-36.
11. Ostle, B. Statistics in Research, 2nd Ed. Iowa State Univ. Press, Ames, 1963.
12. Roberts, F. L., and Hudson, W. R. Pavement Serviceability Equations Using the Surface Dynamics Profilometer. Center for Highway Research, Univ. of Texas at Austin, Res. Rept. 73-3, April 1970.
13. Scheffe, H. The Analysis of Variance. John Wiley and Sons, 1959.
14. Spangler, E. B., and Kelly, W. J. GMR Road Profilometer—A Method for Measuring Road Profiles. Engineering Mechanics Department, General Motors Corp, Res. Publ. GMR-452, Dec. 1964.
15. Walker, R. S., Roberts, F. L., and Hudson, W. R. A Profile Measuring, Recording, and Processing System. Center for Highway Research, Univ. of Texas at Austin, Res. Rept. 73-2, April 1970.
16. Walker, R. S., Hudson, W. R., and Roberts, F. L. Development of a System for High-Speed Measurement of Pavement Roughness. Center for Highway Research, Univ. of Texas at Austin, Res. Rept. 73-5F, April 1970.
17. Walker, R. S., and Hudson, W. R. A Road Profile Data-Gathering and Analysis System. Highway Research Record 311, 1970, pp. 36-54.
18. Walker, R. S., and Hudson, W. R. Practical Uses of Spectral Analysis With Surface Dynamics Road Profilometer. Highway Research Record 362, 1971, pp. 104-119.
19. Walker, R. S., and Hudson, W. R. A Correlation Study of the Mays Road Meter With the Surface Dynamics Profilometer. Center for Highway Research, Univ. of Texas at Austin, Res. Rept. 156-1, Aug. 1972.

PROBABILITY MODEL FOR JOINT DETERIORATION

Lawrence Holbrook, Michigan Department of State Highways

Based on condition surveys at 5-, 10-, and 15-year intervals, joints from 43 post-World War II pavement construction projects in Michigan were grouped into 4 classes of deterioration depending on the extent of damage. These classes were then considered as states through which a joint could progress as it deteriorated in time. It was further assumed that the probability of a joint passing from a given state to the next higher state depended only on which state the joint was in and not on the previous deterioration history. This assumption allowed joint deterioration to be modeled as a continuous-time Markov process that specified the probability of a joint being in each state for any time during service life. A nonlinear least squares estimation technique was used to estimate 4 parameters governing the process for each of the 43 construction projects. The model's fit to field data for each of these projects was quite good, thereby suggesting that similar procedures might be used for a large variety of structural deterioration problems.

•BECAUSE joint deterioration is a serious problem from both a roughness and a maintenance point of view, to model the deterioration process for predictive purposes is desirable. A successful model would forecast problem occurrences such as blowups and thereby afford an opportunity for preventive maintenance. It is unlikely that the large number of variables that affect joint deterioration would be tractable enough to allow an extract (deterministic) formulation of the problem. Under such circumstances, one often resorts to the prediction of probabilities, provided one can reasonably define states for the process. This type of predictive model is called stochastic and often fits the real world quite well. For the case of joint deterioration, the first problem encountered in developing the model occurred in the measurement of deterioration. The general index approach to deterioration measurement is given in an earlier paper (1).

THE DATA

Because all post-World War II state trunk-line concrete pavement construction was examined in Michigan by condition survey, it was possible to record joint condition at survey intervals of 5, 10, and 15 years of service life (Fig. 1). Tabulation and analysis of these data were made possible through the financial support of the Federal Highway Administration. Deterioration, usually joint spalls and slab cracks, is visually recorded on survey sheets more or less to scale. One might suppose that a good measure of joint deterioration would be spall count. However, as the number of spalls increases, they tend to merge; hence, more advanced deterioration, namely the blowup, is qualitatively different from spalls and is therefore not amenable to this scaling procedure.

To measure all types of joint deterioration in proportion to their seriousness, a more comprehensive scaling method had to be developed. Consequently, it was decided to measure joint deterioration as the percentage of the total transverse joint length affected by all kinds of concrete failure. Mathematical modeling was facilitated by grouping these percentages into 4 categories or states as follows:

Publication of this paper sponsored by Committee on Pavement Condition Evaluation.

State Defined	Percentages
1	0 to 25
2	26 to 50
3	51 to 75
4	76 to 100

State 1 consists mostly of external corner spalls, and state 4 consists mostly of blowups—rarely would a joint be spalled 75 to 100 percent of its transverse length. Usually state 4 joints were seen by the investigator as full slab width patches that by their extent and character suggested that a blowup occurred. These definitions of joint deterioration were used to classify each joint and to chart its progression from state to state with each subsequent condition survey.

DEVELOPMENT OF THE MODEL

It seems reasonable to assume that the state of current joint deterioration essentially determines the probability of progression to the next higher state. This is tantamount to assuming that the time history of deterioration is irrelevant as far as future behavior is concerned and that all one needs to know is the present state and the probabilities of further deterioration associated with each state. From a stochastic process point of view, this assumption of lack of system memory is called the "Markov property" and, if applicable, suggests that the deterioration process may be considered as a Markov chain (2, 3, 4). Crucial to the concept of a Markov process are the following assumptions.

1. For each pair of state E_j, E_k, for $j \neq k$, there exists the continuous function $\lambda_{jk}(t)$ such that

$$\frac{P_{kk}(t,\ t+h)}{h} \to \lambda_k(t)$$

as $h \to 0$. Moreover, the above limit is uniform in t and uniform in j for fixed k. $\lambda_{jk}(t)$ defines the time rate of change that governs the passage from state E_j to state E_k (Fig. 2).

2. For each state E_k there exists a continuous function $\lambda_k(t) \geq 0$ such that

$$\frac{1 - P_{kk}(t,\ t+h)}{h} \to \lambda_{kk}(t)$$

uniformly in t, as $h \to 0$. $\lambda_k(t)$ defines the time rate of change that governs the passage out of state E_{jk} and must equal the sum of the particular passages, $\sum_{k \neq 1} \lambda_{kl}(t)$. Now the Markov assumption of the independence of past and future events allows the Chapman-Kolmogorov equation for continuous time.

$$P_{ik}(\tau,\ t+h) = \sum_j P_{ij}(\tau,\ t)\, P_{jk}(t,\ t+h)$$

where τ, t, and $h = 0$. This equation states that the probability of a transition from state i to state k during the time interval $(\tau,\ t+h)$ is equal to the probability of transition from state i to some intervening state j during the time interval $(\tau,\ t)$ multiplied by the probability of transition from state j to state k during the time interval $(t,\ t+h)$ summed over all intervening states j. This equation allows us to compose

$$\frac{P_{ik}(\tau,\ t+h) - P_{ik}(\tau,\ t)}{h} = -\frac{1}{h} P_{ik}(\tau,\ t) + \frac{1}{h} \sum_j P_{ij}(\tau,\ t)\, P_{ik}(t,\ t+h)$$

or by extracting the j = k term from the sum

$$\frac{P_{ik}(\tau,\ t+h) - P_{ik}(\tau,\ t)}{h} = -\frac{1}{h}P_{ik}(\tau,\ t) + \frac{1}{h}P_{ik}(\tau,\ t)\,P_{kk}(t,\ t+h)$$

$$+\frac{1}{h}\sum_{j\neq k} P_{ij}(\tau,\ t)\,P_{jk}(t,\ t+h) \qquad (1)$$

By assumptions 1 and 2, we have, by letting $h \to 0$ in Eq. 1,

$$\frac{\partial P_{ik}(\tau,\ t)}{\partial t} = -\,P_{ik}(\tau,\ t)\,\lambda_k(t) + \sum_{j\neq k} P_{ij}(\tau,\ t)\,\lambda_{jk}(t) \qquad (2)$$

Now, by definition, we have

$$\sum_{l} P_{kl}(\tau,\ t) = 1$$

and

$$\frac{\partial}{\partial t}\sum_{l} P_{kl}(\tau,\ t) = 0 = \sum_{l}\lambda_{kl}(t)$$

Further, noting Eq. 2, we have

$$\lambda_k(t) + \lambda_{kk}(t) = 0$$

or

$$\lambda_k(t) = -\,\lambda_{kk}(t)$$

If we let

$$P(\tau,\ t) = [P_{ij}(\tau,\ t)]_{ij}$$

and

$$\Lambda(t) = [\lambda_{ij}(t)]_{ij}$$

then Eq. 2 becomes

$$\frac{\partial}{\partial t}P(\tau,\ t) = P(\tau,\ t)\,\Lambda(t) \qquad (3)$$

If the $\{\lambda_{ij}(t)\}$ are constant for all time, the process is said to be time-homogeneous. If the $\{\lambda_{ij}(t)\}$ change over time, the process is said to be non-time-homogeneous. Because joints like other physical structures age, it seems unlikely that joint deterioration would be time-homogeneous. Notice also that it is impossible for joints to pass from a given state to a lower state. This requires that the matrices $P(\tau,\ t)$ and $\Lambda(t)$ be upper triangular—a feature that makes it possible to solve the system of differential equations generated by Eq. 3. Now let us require that in the case of joint deterioration it is reasonable to specify that a joint cannot progress to an advanced state of deterioration without passing through each intervening state. Consequently, all transition probability rates for which $j > i + 1$ must be 0. Thus $\Lambda(t)$ now becomes

$$\Lambda(t) = \begin{bmatrix} -\lambda_{12}(t) & \lambda_{12}(t) & 0 & \dots & 0 \\ 0 & -\lambda_{23}(t) & \lambda_{23}(t) & \dots & 0 \\ \dots & \dots & \dots & \dots & \dots \\ 0 & \dots & \dots & \dots & 0 \end{bmatrix} \tag{4}$$

because $\sum_k \lambda_{jk}(t) = 0$ as discussed earlier. It was decided to classify joint condition into 4 classes and thereby to limit Eq. 4 to a 4×4 matrix. All of these considerations define a special case of Eq. 3 that generates the system of differential equations:

$$\frac{\partial}{\partial t} P_{11}(\tau, t) = - P_{11}(\tau, t)\lambda_{12}(t)$$

$$\frac{\partial}{\partial t} P_{12}(\tau, t) = P_{11}(\tau, t)\lambda_{12}(t) - P_{12}(\tau, t)\lambda_{23}(t)$$

$$\frac{\partial}{\partial t} P_{22}(\tau, t) = - P_{22}(\tau, t)\lambda_{23}(t)$$

$$\frac{\partial}{\partial t} P_{23}(\tau, t) = P_{22}(\tau, t)\lambda_{23}(t) - P_{23}(\tau, t)\lambda_{34}(t)$$

$$\frac{\partial}{\partial t} P_{33}(\tau, t) = - P_{33}(\tau, t)\lambda_{34}(t)$$

$$\frac{\partial}{\partial t} P_{13}(\tau, t) = P_{12}(\tau, t)\lambda_{23}(t) - P_{13}(\tau, t)\lambda_{34}(t)$$

The $P_{j4}(\tau, t)$ are known because $\sum_k P_{jk} = 1$.

The preceding development does not specify the way in which the transition rates $\lambda_{t,t+1}(t)$ vary with time. As mentioned before, aging very likely increases the probability that a joint in a given state of deterioration will pass to a higher state for the same time interval. Therefore, it would seem plausible that the $\lambda_{t,t+1}(t)$ would increase in time. A simple formulation that fits graphical plots of the data is

$$\lambda_{12}(t) = \alpha t^{\phi} \tag{5a}$$

$$\lambda_{23}(t) = \beta t^{\phi} \tag{5b}$$

$$\lambda_{34}(t) = \gamma t^{\phi} \tag{5c}$$

where α, β, γ are scaling coefficients and ϕ is a parameter that indicates the degree of time nonhomogeneity. If $\phi = 0$, the process is time-homogeneous; if $\phi \neq 0$, the process is non-time-homogeneous. Furthermore, we would expect that $\alpha < \beta < \gamma$ because a joint already in a highly deteriorated state can be expected to decay more rapidly to the next higher state. This specification of $\lambda_{t,t+1}(t)$ together with the initial conditions, $P_{11}(\tau, \tau) = P_{22}(\tau, \tau) = P_{33}(\tau, \tau) = 1$, yields the following solutions to the system of equations:

$$P_{11}(\tau, t) = e^{-\theta_i \int_{\tau}^{t} x^{\phi} dx} = e^{-\theta_i \left(\frac{t^{\phi+1} - \tau^{\phi+1}}{\phi+1} \right)}$$

where

$\theta_1 = \alpha$,
$\theta_2 = \beta$, and
$\theta_3 = \gamma$.

Also,

$$P_{12}(\tau,\ t) = c_1(\tau)e^{-\beta\int_\tau^t x^\phi dx} + \text{particular solution}$$

$$\text{Particular solution} = \alpha e^{-\beta\int_\tau^t x^\phi dx} \int_\tau^t e^{\beta\int_\tau^y z^\phi dz}\, y^\phi P_{11}(\tau,\ y)\, dy$$

$$= \alpha e^{-\beta\left(\frac{t^{\phi+1}-\tau^{\phi+1}}{\phi+1}\right)} \int_\tau^t y^\phi e^{\frac{(\beta-\alpha)(y^{\phi+1}-\tau^{\phi+1})}{\phi+1}}\, dy$$

$$= \alpha e^{\frac{-\beta(t^{\phi+1}+\alpha\tau^{\phi+1})}{\phi+1}} \int_\tau^t y^\phi e^{\frac{(\beta-\alpha)y^{\phi+1}}{\phi+1}}\, dy$$

$$= \frac{\alpha}{\beta-\alpha}\left[e^{-\frac{\alpha(t^{\phi+1}-\tau^{\phi+1})}{\phi+1}} - e^{-\frac{\beta(t^{\phi+1}-\tau^{\phi+1})}{\phi+1}}\right]$$

Because the initial condition $P_{12}(\tau,\ \tau) = 0$, $c(\tau) = 0$. Therefore,

$$P_{12}(\tau,\ t) = \frac{\alpha}{\beta-\alpha}\left[e^{-\frac{\alpha(t^{\phi+1}-\tau^{\phi+1})}{\phi+1}} - e^{-\frac{\beta(t^{\phi+1}-\tau^{\phi+1})}{\phi+1}}\right]$$

where τ specifies the time at which the process starts. Similarly,

$$P_{23}(\tau,\ t) = \frac{\beta}{\gamma-\beta}\left[e^{-\frac{\beta(t^{\phi+1}-\tau^{\phi+1})}{\phi+1}} - e^{-\frac{\gamma(t^{\phi+1}-\tau^{\phi+1})}{\phi+1}}\right]$$

Now,

$$P_{13}(\tau,\ t) = c_2(\tau)e^{-\gamma\int_\tau^t x^\phi dx} + \text{particular solution}$$

$$\text{Particular solution} = e^{-\gamma\int_\tau^t x^\phi dx} \int_\tau^t e^{\gamma\int_\tau^t z^\phi dz}\, \beta y^\phi P_{12}(\tau,\ y)\, dy$$

$$= \frac{\alpha\beta}{(\beta-\gamma)(\alpha-\gamma)} e^{-\frac{\gamma(t^{\phi+1}-\tau^{\phi+1})}{\phi+1}} + \frac{\alpha\beta}{(\gamma-\beta)(\alpha-\beta)} e^{-\frac{\beta(t^{\phi+1}-\tau^{\phi+1})}{\phi+1}}$$

$$+ \frac{\alpha\beta}{(\beta-\alpha)(\gamma-\alpha)} e^{-\frac{\alpha(t^{\phi+1}-\tau^{\phi+1})}{\phi+1}}$$

Because the initial conditions are $P_{13}(\tau,\ \tau) = 0$, $c_2(\tau) = 0$. Therefore,

$$P_{13}(\tau,\ t) = \alpha\beta\left[\frac{e^{-\frac{\alpha(t^{\phi+1}-\tau^{\phi+1})}{\phi+1}}}{(\beta-\alpha)(\gamma-\alpha)} + \frac{e^{-\frac{\beta(t^{\phi+1}-\tau^{\phi+1})}{\phi+1}}}{(\gamma-\beta)(\alpha-\beta)} + \frac{e^{-\frac{\gamma(t^{\phi+1}-\tau^{\phi+1})}{\phi+1}}}{(\beta-\gamma)(\alpha-\gamma)}\right]$$

ESTIMATION OF PARAMETERS

The problem now arises as to how to estimate α, β, γ, and ϕ. Because the expressions for $P_{11}(\tau, t)$ and $P_{11}(\tau, t)$ are nonlinear, classical least squares techniques are not helpful. In the present case, a computer optimization procedure containing a modification of the steepest method was used (7, 8, 9). The procedure minimized the expression where the $P_{11}(\tau, t)$ were proportions computed directly from the survey data. In addition, each residual was weighted in proportion to the number of joints entering into the probability determination.

RESULTS WITH FIELD DATA

An attempt was made to estimate the model's 4 parameters by the nonlinear least squares procedure for all the 43 construction projects surveyed at 5-, 10-, and 15-year intervals. Except for a small number of extremely good projects for which there was no appreciable deterioration at 15 years, estimates for α, β, γ, and ϕ converge rapidly. In all cases, the model's fit was within ±0.10 for the 4 probabilities × 3 survey years × 43 projects = 516 data points (Figs. 3, 4, 5, and 6). Examples of state probability history curves for several particularly good and poor projects are shown in Figures 7 and 8. Shown in Figure 9 are the expected (average) state histories for the same 2 projects. The probabilities for states 2 and 3 of the poorly performing projects peak at about 11 and 13 years and then decline. This is because joints are not entering states 2 and 3 so fast as they are leaving these states for state 4. State 4 is a terminal or absorbing state and naturally captures more joints with time until all joints are finally in this state.

Also of interest is the finding that $\hat{\alpha} < \hat{\beta} < \hat{\gamma}$. Thus, a joint is more likely to deteriorate to the next highest state if it is already in a deteriorated condition. Distributions of $\hat{\beta}/\hat{\alpha}$ and $\hat{\gamma}/\hat{\alpha}$ are shown in Figure 10. Attempts were made to quantify these relations, thereby reducing the number of model parameters, but the models did not fit the data satisfactorily (residuals as high as ±0.30 were encountered). Because $\hat{\gamma}$ was generally greater than $\hat{\alpha}$ and $\hat{\beta}$, one would presume that state 3 joints would be the ones most likely to progress to state 4. Therefore, if state 4 (mostly blowups) prediction is desired, a good strategy would be to look for joints in state 3. Because the model will predict the probability of state 4, given state 3 for any elapsed time, one can compute state 4 probability curves once α, β, γ, and ϕ have been estimated from earlier performance data (or possibly environmental and materials variables).

Figure 11 shows for an arbitrary construction project the cumulative probability of state 4 occurring given that a joint was in state 3 at the selected τ times of 1, 11, and 15 years. Notice the rapid rate of increase in probability as τ increases. For example, if a joint is in state 3 at 1 year ($\tau = 1$), it takes just over 12 years before the potential occurrence of state 4 has reached a probability of 0.50. However, if the joint is in state 3 at 11 years ($\tau = 11$), it takes only 3 years for the probable occurrence of state 4 to reach 0.50. These curves will not give good forecasts of blowup probability unless α, β, γ, and ϕ are reliably estimated from early performance data for each project itself or from a group of relevant causal variables.

As discussed earlier, ϕ is a measure of the non-time-homogeneity of the process. Figure 12 shows the frequency distribution of $\hat{\phi}$ for the 40 projects for which ϕ could be estimated. $\hat{\phi}$ varies from about 0.20 to 5.83 with a median value of about 2.3. Thus, our hypothesis concerning non-time-homogeneity is tenable, particularly because most $\hat{\phi}$ are significantly greater than 0.0 (α level = 0.05, as tested by a linearized t test).

CONCLUSION

Condition survey data were used to define 4 joint conditions in terms of the percentage of transverse joint length deteriorated. Progressive deterioration of a joint was considered as the passage from a given state to the next higher state. This process over time appeared to embody the Markov assumption, which requires that only the current state determine the probability of passage to another state. The Markov assumption was used to design a continuous time, non-time-homogeneous Markov process

Figure 1. Survey data on joint condition.

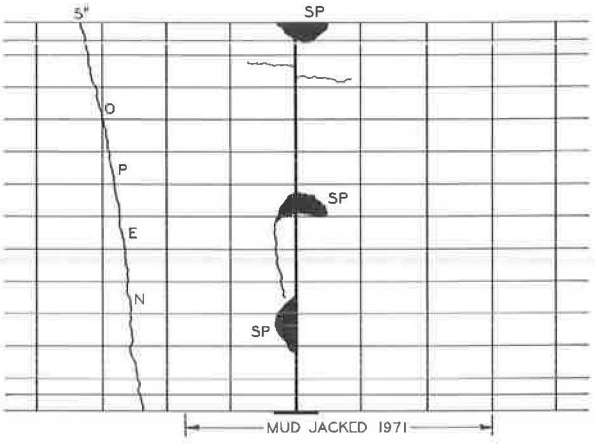

Figure 2. Probability transition from state i to state j as a function of time.

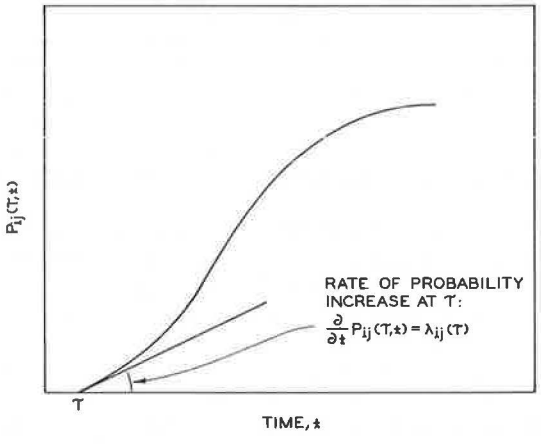

Figure 3. Estimated versus actual probability of a joint in state 1 for 5, 10, and 15 years.

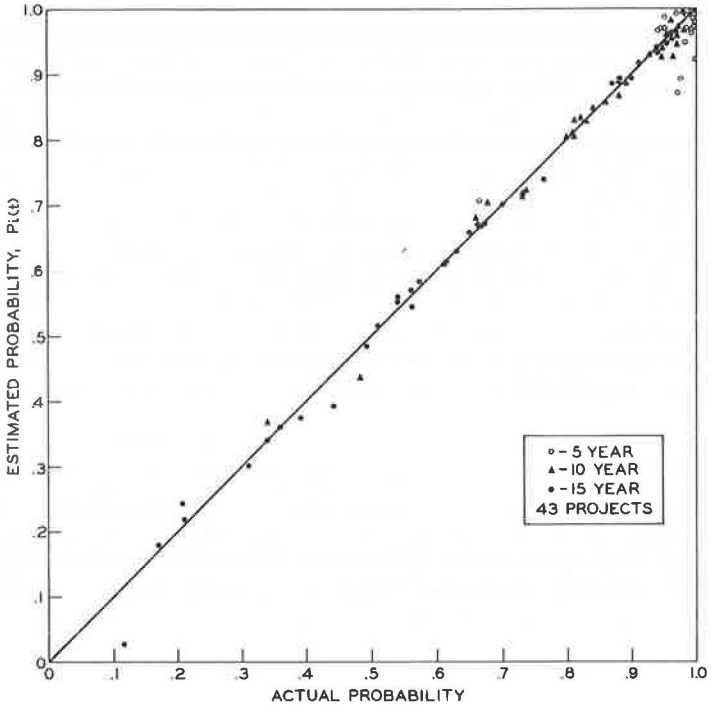

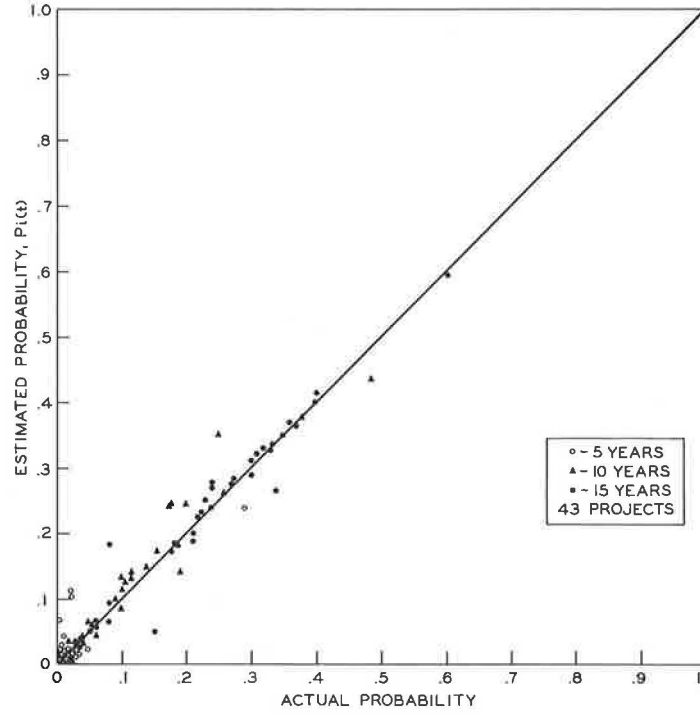

Figure 4. Estimated versus actual probability of a joint progressing from state 1 to state 2 within 5, 10, and 15 years.

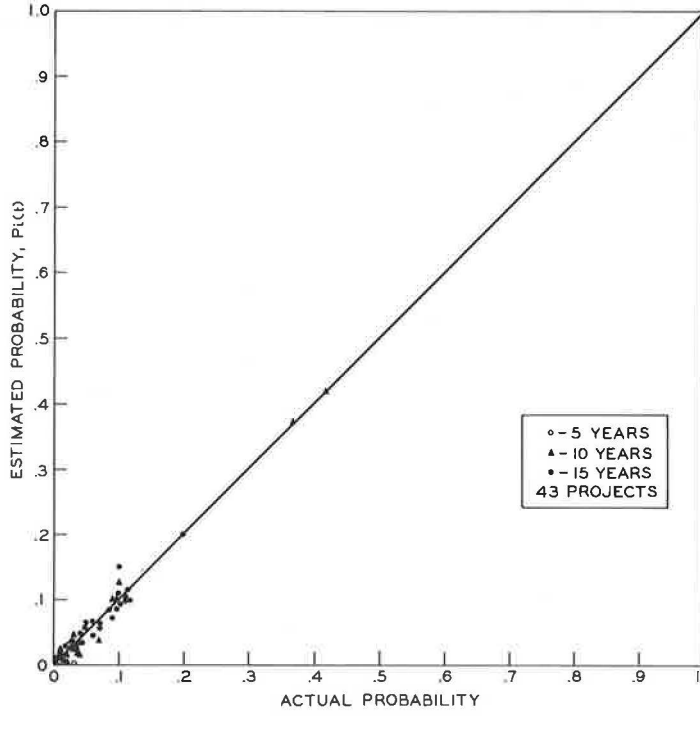

Figure 5. Estimated versus actual probability of a joint progressing from state 1 to state 3 within 5, 10, and 15 years.

Figure 6. Estimated versus actual probability of a joint progressing from state 1 to state 4 within 5, 10, and 15 years.

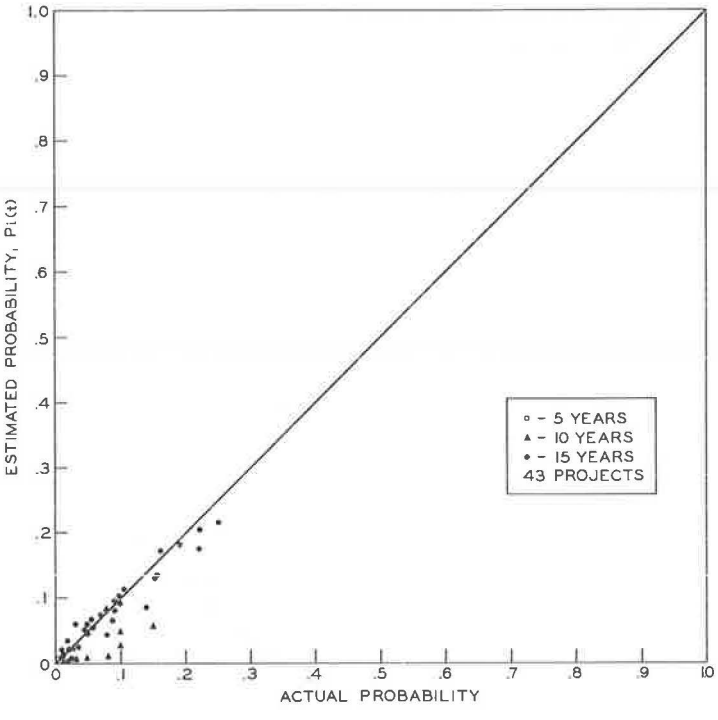

Figure 7. Estimated probability of a joint from a good project being in a state during a 15-year service life.

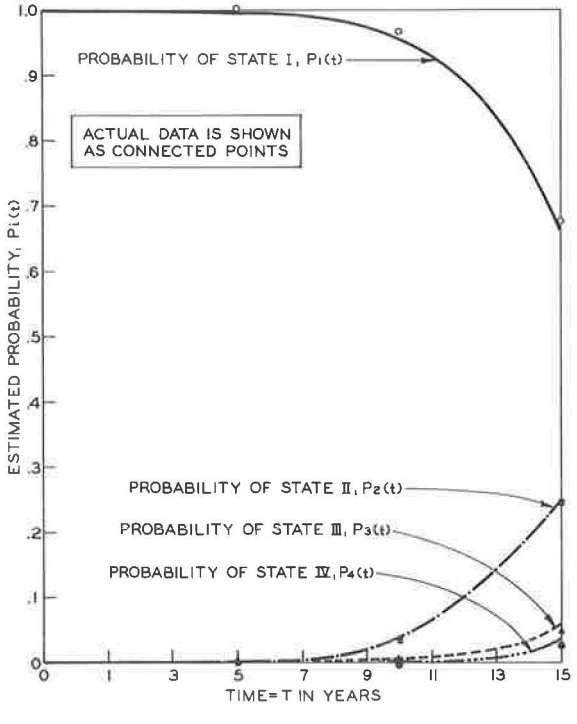

Figure 8. Estimated probability of a joint from a poor project being in a state during a 15-year service life.

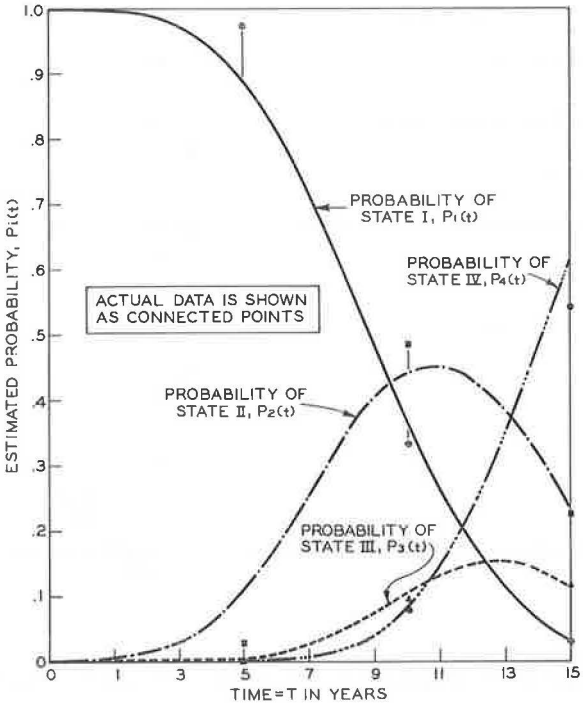

Figure 9. Estimated expected state for projects within 15-year service life.

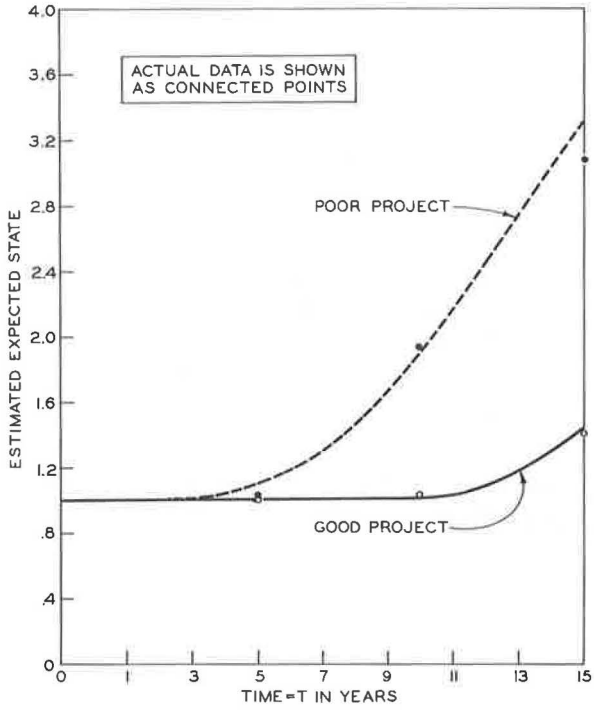

Figure 10. Cumulative ratios for coefficients plotted on normal probability paper.

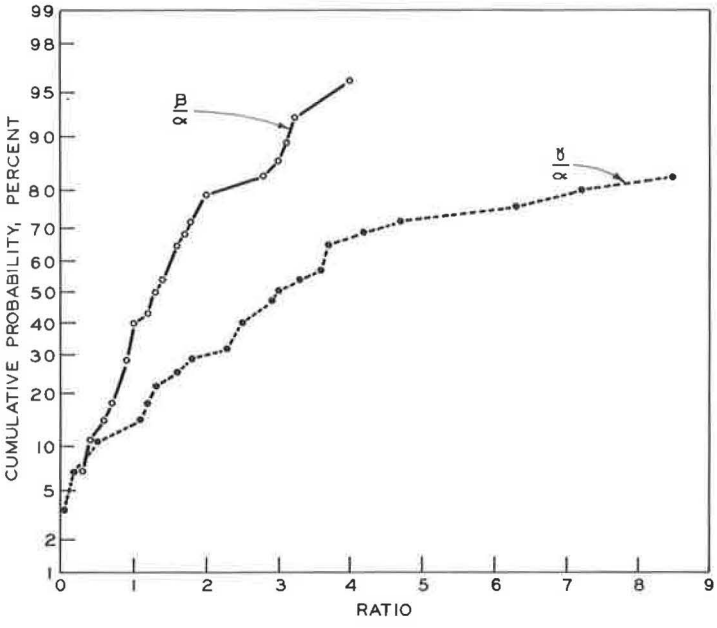

Figure 11. Cumulative probability of a joint progressing from state 3 at 1, 11, and 15 years to state 4 at t.

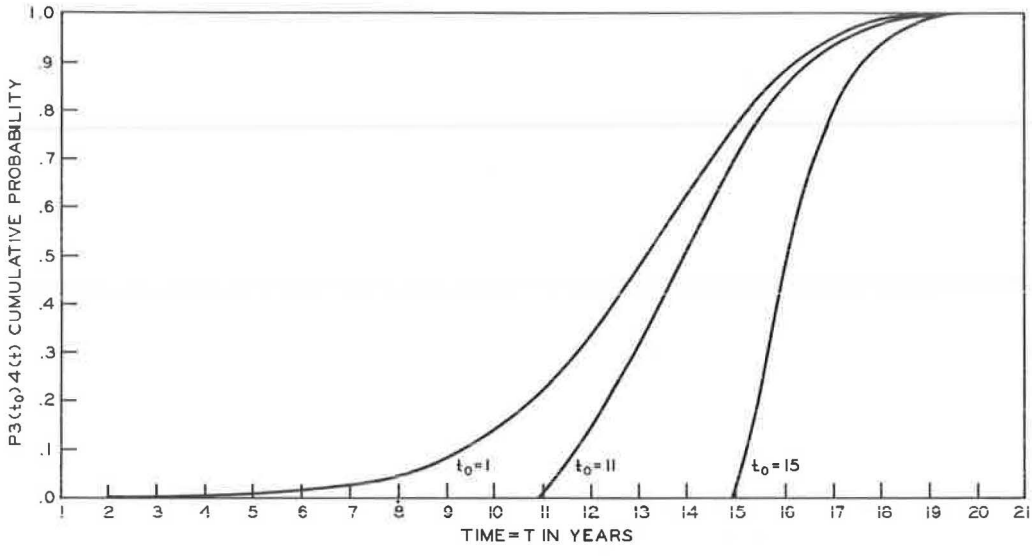

Figure 12. Cumulative distribution of ϕ.

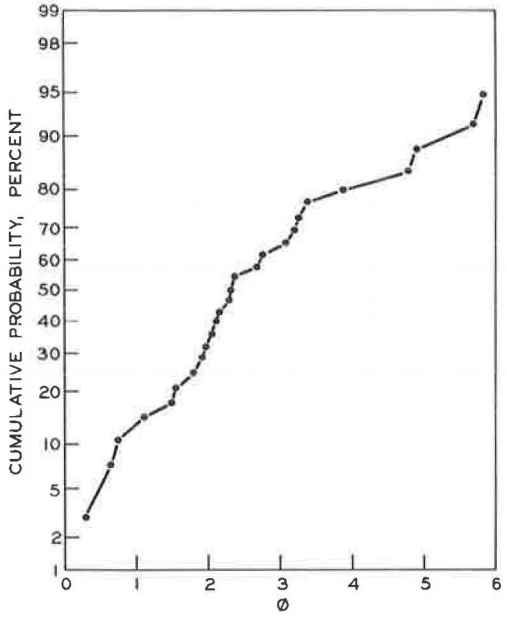

to model joint deterioration. The particular model chosen required the nonlinear estimation of 4 fitting parameters to predict 27 probabilities of joint condition measured at the 5-, 10-, and 15-year periods of service life. This procedure proved very satisfactory except for projects showing practically no deterioration, For these, parameter estimation was not possible because of computer overflow problems. Generally excellent fits of estimated and actual data were obtained for the 43 projects examined. Based on these results the procedure looks quite promising for structural deterioration modeling in general.

REFERENCES

1. Holbrook, L. F. An Examination of Concrete Pavement Structural Performance. Highway Research Record 311, 1970, pp. 55-67.
2. Clarke, B. A., and Disney, R. L. Probability and Random Processes for Engineers and Scientists. John Wiley and Sons, 1970.
3. Karlin, S. A First Course in Stochastic Processes. Academic Press, 1969.
4. Parzen, E. Stochastic Processes. Holden Day, 1962.
5. Koenig, H. E., Tokad, Y., Kesavan, H. K., and Hedges, H. G. Analysis of Discrete Physical Systems. McGraw-Hill, 1967.
6. Bronson, R. Matrix Methods. Academic Press, 1969.
7. Dye, J. L., and Nicely, V. A. A General Purpose Curve Fitting Program for Class and Research Use. Jour. of Chemical Education, Vol. 48, 1971, p. 443.
8. Draper, N., and Smith, H. Applied Regression Analysis. John Wiley and Sons, 1966.
9. Aoki, M. Introduction to Optimization Techniques. Macmillan, 1971.

SPONSORSHIP OF THIS RECORD

GROUP 2—DESIGN AND CONSTRUCTION OF TRANSPORTATION FACILITIES
John L. Beaton, California Division of Highways, chairman

PAVEMENT DESIGN SECTION
George B. Sherman, California Division of Highways, acting chairman

Committee on Surface Properties-Vehicle Interaction
W. E. Meyer, Pennsylvania State University, chairman
Malcolm D. Armstrong, Glenn G. Balmer, F. Cecil Brenner, Arthur D. Brickman, William F. R. Briscoe, William C. Burnett, A. Y. Casanova III, Blaine R. Englund, William Gartner, Jr., Ralph C. G. Haas, Douglas I. Hanson, Robert N. Janeway, David C. Mahone, B. F. McCullough, Robert B. McGough, Paul Milliman, Alexander B. Moore, E. W. Myers, F. William Petring, Bayard E. Quinn, John J. Quinn, Frederick A. Renninger, Rolands L. Rizenbergs, Hollis B. Rushing, Richard K. Shaffer, Elson B. Spangler, W. E. Teske, M. Lee Webster, Ross G. Wilcox, Dillard D. Woodson

Committee on Pavement Condition Evaluation
Karl H. Dunn, Wisconsin Department of Transportation, chairman
Frederick Roger Allen, Frederick E. Behn, W. B. Drake, Malcolm D. Graham, Leroy D. Graves, Ralph C. G. Haas, William S. Housel, W. Ronald Hudson, C. S. Hughes III, J. W. Lyon, Jr., Alfred W. Maner, K. H. McGhee, Phillip L. Melville, Alfred B. Moe, Bayard E. Quinn, G. Y. Sebastyan, Foster A. Smiley, Lawrence L. Smith, Elson B. Spangler, W. E. Teske, Allen P. Whittemore, Eldon J. Yoder

Lawrence F. Spaine, Highway Research Board staff

Sponsorship is indicated by a footnote on the first page of each report. The organizational units and the chairmen and members are as of December 31, 1972.